NATIONAL BUREAU OF STANDARDS REPORT

10 814

A STUDY OF DYNAMIC AIR INFILTRATION THROUGH OFFICE BUILDING WINDOWS

U.S. DEPARTMENT OF COMMERCE
NATIONAL BUREAU OF STANDARDS

NATIONAL BUREAU OF STANDARDS

The National Bureau of Standards [1] was established by an act of Congress March 3, 1901. Today, in addition to serving as the Nation's central measurement laboratory, the Bureau is a principal focal point in the Federal Government for assuring maximum application of the physical and engineering sciences to the advancement of technology in industry and commerce. To this end the Bureau conducts research and provides central national services in four broad program areas. These are: (1) basic measurements and standards, (2) materials measurements and standards, (3) technological measurements and standards, and (4) transfer of technology.

The Bureau comprises the Institute for Basic Standards, the Institute for Materials Research, the Institute for Applied Technology, the Center for Radiation Research, the Center for Computer Sciences and Technology, and the Office for Information Programs.

THE INSTITUTE FOR BASIC STANDARDS provides the central basis within the United States of a complete and consistent system of physical measurement; coordinates that system with measurement systems of other nations; and furnishes essential services leading to accurate and uniform physical measurements throughout the Nation's scientific community, industry, and commerce. The Institute consists of an Office of Measurement Services and the following technical divisions:

Applied Mathematics—Electricity—Metrology—Mechanics—Heat—Atomic and Molecular Physics—Radio Physics [2]—Radio Engineering [2]—Time and Frequency [2]—Astrophysics [2]—Cryogenics.[2]

THE INSTITUTE FOR MATERIALS RESEARCH conducts materials research leading to improved methods of measurement standards, and data on the properties of well-characterized materials needed by industry, commerce, educational institutions, and Government; develops, produces, and distributes standard reference materials; relates the physical and chemical properties of materials to their behavior and their interaction with their environments; and provides advisory and research services to other Government agencies. The Institute consists of an Office of Standard Reference Materials and the following divisions:

Analytical Chemistry—Polymers—Metallurgy—Inorganic Materials—Physical Chemistry.

THE INSTITUTE FOR APPLIED TECHNOLOGY provides technical services to promote the use of available technology and to facilitate technological innovation in industry and Government; cooperates with public and private organizations in the development of technological standards, and test methodologies; and provides advisory and research services for Federal, state, and local government agencies. The Institute consists of the following technical divisions and offices:

Engineering Standards—Weights and Measures — Invention and Innovation — Vehicle Systems Research—Product Evaluation—Building Research—Instrument Shops—Measurement Engineering—Electronic Technology—Technical Analysis.

THE CENTER FOR RADIATION RESEARCH engages in research, measurement, and application of radiation to the solution of Bureau mission problems and the problems of other agencies and institutions. The Center consists of the following divisions:

Reactor Radiation—Linac Radiation—Nuclear Radiation—Applied Radiation.

THE CENTER FOR COMPUTER SCIENCES AND TECHNOLOGY conducts research and provides technical services designed to aid Government agencies in the selection, acquisition, and effective use of automatic data processing equipment; and serves as the principal focus for the development of Federal standards for automatic data processing equipment, techniques, and computer languages. The Center consists of the following offices and divisions:

Information Processing Standards—Computer Information — Computer Services — Systems Development—Information Processing Technology.

THE OFFICE FOR INFORMATION PROGRAMS promotes optimum dissemination and accessibility of scientific information generated within NBS and other agencies of the Federal government; promotes the development of the National Standard Reference Data System and a system of information analysis centers dealing with the broader aspects of the National Measurement System, and provides appropriate services to ensure that the NBS staff has optimum accessibility to the scientific information of the world. The Office consists of the following organizational units:

Office of Standard Reference Data—Clearinghouse for Federal Scientific and Technical Information [3]—Office of Technical Information and Publications—Library—Office of Public Information—Office of International Relations.

---

[1] Headquarters and Laboratories at Gaithersburg, Maryland, unless otherwise noted; mailing address Washington, D.C. 20234.
[2] Located at Boulder, Colorado 80302.
[3] Located at 5285 Port Royal Road, Springfield, Virginia 22151.

NATIONAL BUREAU OF STANDARDS REPORT

NBS PROJECT		NBS REPORT
4214102	February 1, 1972	10 814

A STUDY OF DYNAMIC AIR INFILTRATION THROUGH OFFICE BUILDING WINDOWS

by
James E. Hill
Svein Myklebost
Takao Tsuchiya
Tamami Kusuda
Environmental Engineering Section
Building Research Division
Institute for Applied Technology
National Bureau of Standards
Washington, D. C. 20234

U.S. DEPARTMENT OF COMMERCE
NATIONAL BUREAU OF STANDARDS

A Study of Dynamic Air Infiltration Through Office Building Windows

by

J. E. Hill[1/], S. Myklebost[2/], T. Tsuchiya[3/] and T. Kusuda[4/]

Abstract

Currently available methodology for estimating air leakage of buildings does not take into account the fluctuating nature of the outdoor wind conditions. Studied in this report is the air leakage of two office rooms with reference to dynamic profiles of wind velocities and pressure differentials across the windows. It has been found that the air leakage measured was generally quite different from that calculated using the recommended ASHRAE procedure. The reason for this discrepancy is postulated to be due to a complex process caused by the dynamically varying differential pressure across the window as well as flow occurring through the window in both directions simultaneously.

Key Words: Air leakage of buildings, wind velocity, dynamic differential pressure

1/ University of Maryland, College Park, Maryland

2/ Norwegian Building Research Institute, Forskningsveien 3B, Blindern, Oslo 3, Norway

3/ Building Research Institute, Tokyo, Japan

4/ Environmental Engineering Section, Building Research Division, National Bureau of Standards

Table of Contents

Figure Captions

Tables

1. Introduction

In the design of a building, the heating and cooling load must be estimated rather accurately in order to properly size the heating and cooling system as well as to make a suitable prediction of the seasonal energy requirements. Energy is added to or taken from a structure in a variety of ways. Among these are: conduction and convection of heat through the solid portion of the structure; thermal radiation through transparent surfaces such as windows; the addition of energy from people and equipment inside; and finally the energy associated with the air that is continually infiltrating into and exfiltrating out of the structure. Of all these factors, the infiltration is perhaps the most difficult to predict and can be as much as 1/3 of the heating load and even more for a cooling load.

The ASHRAE Handbook of Fundamentals (1967) describes the two basic techniques used in predicting air infiltration rates. One method known as the air change method consists simply of assuming a certain number of air changes per hour for each room. The number depends upon the relative location of the room inside the structure, as well as the number of windows and doors in the room. The second method is based upon measured leakage characteristics of the building structure. Since cracks around windows and doors are usually the main source of air infiltration, it is known as the crack method. It is usually regarded as more accurate as long as the leakage characteristics can be evaluated properly. The air flow can be expressed by the equation:

$$Q = C \Delta P^n \qquad (1)$$

where

Q = volumetric flow rate of air

C = proportionality constant

n = exponent between 1/2 and 1

ΔP = pressure difference across the window.

C and n must be determined for the structure component in question and of course the pressure difference must be evaluated. This pressure difference exerted on an enclosure is the result of wind blowing over and around the building. In addition, infiltration can result from a difference in density between the inside and outside air.

Much research has been done to refine the design calculations of heating and cooling loads, and in particular the infiltration portion as it applies to complex buildings and structures. Among some of the recent contributions are papers by Svetlov (1966), Jackman and den Ouden (1968), and Gabrielsson and Porra (1968). In all of the cases, some form of equation (1) has been applied to all of the rooms within the structure, with a pressure difference used that is calculated from assumed velocity and temperature profiles both inside and out. This general approach has been used for some time and is present in the latest ASHRAE publication Procedure for Determining Heating and Cooling Loads for Computerized Energy Calculations (1971). Of course since all of these procedures are based on the crack method and equation (1), they

assume a steady flow situation with a constant pressure drop across the crack, thus implying a constant wind velocity on the outside of the building. This rarely if ever happens. The purpose of this present research effort is to determine experimentally if meaningful infiltration data can be determined from observing the fluctuating wind and pressure difference exerted on an enclosure. In addition an attempt will be made to evaluate the precise correlation between these two dynamic variables.

2. Experimental Investigation

The Building Research Division office building located on the grounds of the Bureau of Standards in Gaithersburg, Maryland is Building 226, shown in Figure 1. Two separate offices (A331 and B322) approximately 10' high by 10' wide by 16' long were renovated and used as test rooms for this study. As shown, one of the rooms was on the north side of the building (prevailing wind is out of the north) and the other was on the south. Both were on the third floor and each contained one window approximately 5' wide x 8' high and one door facing a corridor. The normal office windows were removed and replaced with experimental plastic windows containing adjustable cracks as shown in Figure 2 and Figure 3. The adjustable braces could be loosened so that the two center pieces would slide about, thus changing the width of the test crack.

Before putting the test windows in place they were calibrated in a temporary structure as shown in Figure 4. A blower (Western Electric Model KS 5856, 475 cubic feet per minute, powered by a 1/8 hp, 1725 rpm, electric motor)* was used to pull air through the test crack, then into a polyethylene enclosure around the blower that pumped the air back into the room for recirculation. An adjustable damper was used to obtain several flow rates through the window. A pitot tube mounted in the 3 inch suction pipe was used to determine the air flow rate. The pressures were measured with a Hook gage manometer (NBS #95804). The manometer was also used to measure the pressure drop across the window by opening one side to the room, and connecting the other to the inside of the enclosure using 1/4 inch inside diameter (1/8 inch wall thickness) plastic tubing. The two windows were calibrated at crack widths of .05" and .025"**. Several different damper positions were used to determine the calibration curve at steady flow conditions as shown in Figure 5.

---

* Certain commercial equipment, instruments, or materials are identified in this paper in order to adequately specify the experimental procedure. In no case does such identification imply recommendation or endorsement by the National Bureau of Standards, nor does it imply that the material or equipment identified is necessarily the best available for the purpose.

** A hack saw blade was used as a convenient device for setting the gap since its thickness was precisely .025".

Once the test windows were placed in the offices, the test equipment was arranged as shown in Figure 6. A differential pressure transducer (Statham Model PM 197, measuring $\pm$ 0.01 psi difference with 10 volt maximum output and 15 psi gage maximum line pressure) was located in each room, one side connected to the outside through a small hole in the test window and the other side open to the room. Three transducers are shown on the chair in Figure 7. The transducers would thus measure the instantaneous pressure drop across the windows. The transducer outputs were fed by way of shielded cable down the hall to an amplifier in the instrumentation room. The amplified signals were in turn sent to a two pen chart recorder (Varian Associates, Instrument Division, Model G-22, variable speed, maximum scales .01 to 100 volts, NBS #99818) and an analog tape recorder located on the first floor of the building (Honeywell FM, 14 channel instrumentation recorder, Model 7600, NBS #175641). An air pump (Universal Electric Company, Model LR 12645, 3000 rpm) circulated air through 1/4 inch inside diameter (1/8 inch wall thickness) plastic tubing from one or the other of the test rooms (depending on the position of the two-way valve) through the CO_2 analyzer and back into the rooms. In order to insure the proper flow rate of air through the analyzer (approximately 1 liter per minute), a flow rotameter was inserted in the line (Brooks Rotameter, tube size 2-15-3). The analyzer used was a Lira Infrared Analyzer Model 300 (NBS #175830). Its principle of operation is basically as follows: Two indentical infrared beams are passed through two parallel stainless steel gas cells housed in a solid aluminum block. One cell contains a gas of known composition and the other the sample gas (in this case air and CO_2).

After the radiation beams pass through the gas cells they are directed into a single detector unit. Upon comparison of the two radiation beams the detector puts out a signal proportional to the amount of component of interest (in this case CO_2) in the sample gas.

The purpose of releasing CO_2 into the test rooms and continually analyzing the CO_2 content of the air was to determine the air change rate for the rooms. This air change rate is defined as the ratio of the hourly rate at which air enters (or leaves) the enclosure to the volume of the enclosure. The amount of decay in CO_2 concentration in the test space per unit time is numerically equal to the amount of CO_2 leaving the space with the outlet air in the same unit time. This can be expressed by the equation:

$$-VdC = NVCdt \qquad (2)$$

where

V = volume of the space, ft^3

C = concentration of CO_2 at time t

N = number of air changes per hour

t = time, hours

With $C = C_o$ at time $t = o$, the solution to equation (2) is:

$$N = \ln[C_o/C]/t \qquad (3)$$

Equation (3) states that the number of air changes occurring during time t is equal to the natural logarithm of the ratio of the initial CO_2 concentration to the concentration at the end of the time interval.

A meter reading calibration curve was supplied with the Lira analyzer and is shown in Figure 8. The analyzer output was also displayed and recorded as a function of time on the #2 pen chart recorder (Honeywell Electronik 19, NBS #164602). The recorder, along with the Lira Analyzer and the two pen chart recorder are shown mounted in a movable rack in Figure 9. During all tests, the initial concentration of CO_2 in the test rooms was 1% or less. Since the output of the analyzer was linear in this range, the voltage readings displayed on the pen chart recorder could be used directly for calculation of the air change rate. A typical test recording of CO_2 decay is shown in Figure 10. Since the slope of the curve on this semi-logarithmic scale is the air change rate, the method of least squares was used to determine the equation of the straight line passing through the data with the "least error" and the slope or air change rate was thus determined.

This technique of infiltration measurement was selected as the result of the work done by Albright, et. al. (1963). They investigated several ways of determining air change rate experimentally, among these the "tracer gas technique" used in this investigation. Their conclusion was that the technique was suitable and accurate as long as the air change rate was below 3 or 4 per hour. As will be shown in the Experimental Results Section, this limitation was satisfied in the present work.

The wind velocity and direction were determined by anemometers located on a tower 300 ft directly north of the building. They were approximately 30 ft above the ground. The total wind velocity was measured by a cup-type anemometer (U. S. Weather Bureau Model F420) which is essentially a d-c permanent magnet generator, where the output voltage is directly proportional to the speed of rotation of the 3-cup rotor attached to its shaft. Two propeller-type anemometers (Gill Model 27100) were also mounted on the tower to measure the north-south and east-west component of the wind velocity. These also were minature d-c generators providing an analog voltage output proportional to the wind speed. They respond only to that component of the wind which is parallel to the axis of rotation and in addition indicate forward and reverse air flow by a reversal of signal polarity at the generator. All three indicators were calibrated so that 100 mv output represented 10 miles per hour of wind speed. These voltage signals were recorded simultaneously with the two pressure difference signals on 5 channels of the analog tape recorder located in Room B150 of the building.

Fifteen copper-constantan thermocouples were placed in each test room as described in Table 1. Their signals were recorded on the Hewlett-Packard data acquisition system (NBS #165622) located in Room A134. The purpose of recording the temperatures was to ascertain if any thermal driving force existed that might affect the infiltration.

Table 1 Description of Temperature Measurements

Thermocouple	Location
1	Outside surface of the test window
2, 3	Inside surface of the test window; one at the top, the other near the bottom
4, 5, 6	Suspended in the air 2 feet from the test window (on the inside) and approximately parallel to the bottom of the window
7	Suspended in the air 2 feet from the test window (on the inside) and located at a height comparable to the center of the window
8, 9, 10	Suspended in the air 2 feet from the test window (on the inside) and approximately parallel to the top of the window
11, 12, 13	Suspended vertically in the center of the test room and equally spaced between the floor and ceiling
14	Secured to one inside wall approximately half-way between the floor and ceiling
15	Located in the corridor outside the test room

The following steps were taken during any individual test:

1. The power to all instruments was turned on approximately an hour before starting the test. If time permitted, the amplifier was allowed to warm up several hours.
2. The Lira analyzer meter reading was adjusted to zero while the air pump was circulating normal room air through the instrument. The #1 pen chart reading was zeroed simultaneously.
3. The pressure transducers were calibrated in the following way: With both sides of the transducer open to the room, the amplifier output was read on a digital voltmeter (DYMEC Corporation, Model 2401 C, NBS #159210) and adjusted to zero. A plastic tubing, stopcock, Hook-gage manometer arrangement was then connected across the transducer such that a specified pressure difference could be imposed on the transducer. A pressure difference of 0.1 inch water gage was always used and the amplifier was adjusted to give 200 millivolts of output as measured on the voltmeter. As each transducer output was adjusted, the corresponding pen on the #2 pen chart recorder was also adjusted to the zero and 200 mv position.
4. The pressure transducers were then connected to measure the pressure difference across the window. One side was left open to the room and the other side was connected to the outside by plastic tubing through a small hole in the upper center of the test window.

5. The magnetic tape was mounted on the analog tape recorder and the speed was set at 3 and 3/4 inches per second. All anemometer and pressure difference leads were connected to the proper channel imputs on the recorder.
6. The air pump was started and the air flow rate through each room was checked to insure that approximately 1 liter per minute was flowing.
7. The ice bath used for the thermocouple reference junction was filled with ice.
8. The data acquisition system was set for one scan of the thirty thermocouples every ten minutes and then started.
9. Masking tape that was normally kept over the test cracks was removed.
10. CO_2 was released from tanks into the test rooms until an initial concentration of approximately 1 and 1/2 to 2% was obtained. The CO_2 was mixed thoroughly with the room air by use of small fans.
11. The doors to the rooms were then shut and the entire opening sealed with polyethylene and masking tape.
12. After the room air motion, room air temperatures, and decay rate of CO_2 were stabilized (usually 30 to 45 minutes after the rooms had been sealed), the tape recorder was started.

13. The duration of the test was one hour, after which all recording was stopped, rooms opened, and test cracks re-sealed.

14. At the completion of the test, all data was directly accessible for analysis except the wind velocity and pressure difference data recorded on the analog tape. It was obtained in the following way: The tape was played back through an analog to digital converter (Adage, Inc., Model VR 16AD, Serial #613, 50-1000 cycles per second) where all channels were scanned 5 times per second. The data was punched on paper tape as it was read (Teletype punch, code BRPE11, NBS #157361). The paper tape was in turn read by a paper tape to magnetic tape converter (Digidata Corporation, Model #1430) and written on digital magnetic tape compatible with the National Bureau of Standards' Univac 1108 Computer.

3. Discussion and Analysis of Experimental Results

The results of the experimental research effort to date are shown in Figures 11 through 45. For nine separate tests run during the summer of 1970, data is shown for the wind velocity, wind direction, and the fluctuating pressure drop across the windows in both rooms. Room A and Room B on the pressure difference plots signify data for Room A331 and Room B322 respectively. In addition, the wind velocity components were combined to compute a wind direction as shown. Zero degrees represents wind out of the north; + 90 degrees, out of the west; - 90 degrees, out of the east; + or - 180 degrees, out of the south. As noted previously, this data was taken from aenomometers located approximately 300 feet north of the building and 30 feet above ground. Therefore, they represent "free-stream" conditions and most likely would be different from what is occurring at the building surface. However, they should be indicative of the surface conditions, particularly on the north side of the building.

By observing the plots, it can be seen that the wind velocity and pressure differences are far from steady. A comment should be made about the rather extreme wind direction changes indicated by Figures 23, 31 and 39. A wind direction that is oscillating close to due south could indicate a direction change of approximately 180 degrees as a result of the computation scheme. This should be kept in mind when observing the results of Tests 4, 6, and 8. Table 2 shows a summary of

the infiltration studies. Indicated in this table are the observed wind data at the NBS site together with similar data obtained at Dulles International Airport, approximately 20 miles southwest of NBS. Columns 9 and 15 show the actual air change rate as measured by the CO_2 decay technique. Preliminary tests were run on each of the test rooms completely sealed with window cracks closed. A small amount of leakage still occurred so that the uncertainty associated with the actual air change rates is approximately 0.05 per hour. The steady flow characteristics of the two test windows as displayed in Figure 5 were analyzed by use of the Method of Least Squares to give the coefficient C and exponent n tabulated in columns 6, 7, 12, and 13. An air change rate was calculated for each test using these constants and the time average of the measured pressure fluctuations (columns 8 and 14) in conjunction with equation (1). A third air change rate is tabulated in columns 11 and 17 and is labeled Q_{ASHRAE} to signify a calculation done according to recommended procedures in the ASHRAE Handbook of Fundamentals.

As mentioned in the Introduction, there are two driving forces that could cause air movement into or out of a structure; a pressure difference due to the wind forces and a pressure difference due to a difference in air density between the inside and outside air. The latter one is usually only important in multistory buildings where for example, if the inside temperature is higher than the outside, there is a lower inside pressure and inward flow of air at lower levels and a corresponding higher inside pressure and outward flow at the higher levels. Of course the reverse occurs when the inside temperature is lower than the outside.

In the present study, the only significant air flow occurring in and out of the room was at the cracks themselves. Consequently there was no "through flow" and the "stack-effect" was non-existent.

ASHRAE does recommend the use of equation (1) for calculating infiltration rates as a result of wind forces provided that the leakage characteristics of the window (C and n) are known. The only difficulty arises in the choice of a ΔP. The velocity head equivalent to a given wind speed is expressed by

$$P_v = 0.000482\ V_w^2 \qquad (2)$$

where

P_v = velocity head, inches of H_2O

and

V_w = wind velocity, miles per hour

It is very difficult to determine in an actual situation the values of static pressure around a building to use in the calculations. For example, pressures may vary from $+0.5\ P_v$ to $+0.9\ P_v$ on the windward side and from -0.3 to $-0.6\ P_v$ on the leeward side for simple square or rectangular shaped buildings. Pressures on the other sides, parallel to, or at slight angles to the wind direction, may range from -0.1 to $-0.9\ P_v$.

Of course the pressure difference across the walls of the building and not just the external static pressure is required. The amount of pressure buildup inside due to the wind action will depend on the resistance of cracks and openings and their location with respect to the wind direction. If the openings are uniformly distributed around the walls of the building, inside pressures will usually be within plus or minus 0.2 P_v. If openings on the windward side predominate, inside pressures up to +0.8 P_v may occur. Conversely, if openings on the leeward side predominate, inside pressures may have negative values of 0.2 to 0.4 P_v or greater.

All of the above discussion from the Handbook of Fundamentals simply points out the extreme complexity of the problem. About the only definitive statement made in regards to the choice of a ΔP for equation (1) is: "To account for the buildup of pressure inside the building, it is common practice to take 0.64 P_v as the pressure difference across the windward wall". Consequently, the air change rates tabulated in columns 11 and 17 were determined precisely by using equation (1) with

$$\Delta P = .000308\ V_w^2 \qquad (3)$$

and V_w taken as the wind velocity measured at the NBS site averaged over the duration of the test. Strictly speaking, one should only expect good agreement between the ASHRAE calculation and the actual air change rate during test no. 6 for room A331 and test no. 2 for room B322 since in both of these tests the predominate "free-stream" wind direction was

normal to the respective windows. By observing the values, the first case shows a design calculation 117% high and in the second, 37% low.

The various air change rates of Table 2 are plotted in Figures 46 through 50. As can be seen from Figure 46 for room A331 and a crack width of 0.05 inches, there is very little correlation among the three differently determined rates. For room B322 and a crack width of 0.05 inches (Figure 47), there is relatively good correlation between the measured and steady flow calculation (using the average of the measured ΔP's) at the higher wind velocities. For all tests involving the smaller crack (.025 inches wide), the correlation between the actual rate and steady state calculation is moderate to good (see Figures 48 and 49). For all tests where the average wind velocity was larger than about 5 miles per hour, the ASHRAE calculation gave a much higher air change rate than actually occurred. This can be explained in part by the fact that the wind direction was very seldom perpendicular to the window in question and consequently the static pressure at the outside of the window was perhaps never as large as indicated by equation (2). In addition, since little or no "through-flow" was allowed, the pressure buildup inside the room was such that the ΔP at any instant was considerably less than $0.64\ P_v$. It is not implied that at air velocities lower than 5 miles per hour the above observations are not valid; however, it will be postulated below that there are other factors present that cause the ASHRAE calculation and measured rates to be of the same order at these low velocities.

TABLE 2 Infiltration Results

1	2	3	4	5	6	7	8	9	10	11	12	13	14	15	16	17
					Room A331						Room B322					
Test No.	Crack Width inches	Average Wind Direction	Average Wind Velocity mph	Average Wind Velocity at Dulles mph	C ft^3/min	n	Average ΔP in. H_2O	AC_{act} #/hr	AC_{sf} #/hr	AC_{ASHRAE} #/hr	C ft^3/min	n	Average ΔP in. H_2O	AC_{act} #/hr	AC_{sf} #/hr	AC ASHRAE #/hr
1	0.05	W	9.5	10.0	369.5	.603	--	0.26	--	1.34	298.5	.537	-.0065	0.54	0.51	1.10
2	0.05	N	4.0	6.0	369.5	.603	-.0052	0.15	0.37	0.47	298.5	.537	-.0002	0.70	0.08	0.44
3	0.05	WNW	13.1	10.0	369.5	.603	.0029	0.62	0.26	1.96	298.5	.537	.0102	0.79	0.65	1.58
4	0.05	SW	2.5	6.0	369.5	.603	-.0008	0.12	0.12	0.27	298.5	.537	-.0024	0.15	0.30	0.27
5	0.05	SE	5.2	9.0	369.5	.603	-.0014	0.32	0.17	0.64	298.5	.537	-.0003	0.22	0.10	0.59
6	0.05	S	6.0	6.0	369.5	.603	.0000	0.36	0.0	0.78	298.5	.537	-.0066	0.63	0.51	0.68
7	0.025	NE	3.3	5.0	198.3	.620	-.0025	0.069	0.12	0.18	176.2	.615	.0005	0.10	0.044	0.14
8	0.025	SSW	5.4	7.0	198.3	.620	.0043	0.15	0.16	0.33	176.2	.615	-.0128	0.20	0.31	0.25
9	0.025	ENE	9.3	11.5	198.3	.620	-.0038	0.18	0.15	0.66	176.2	.615	.0027	0.08	0.12	0.49

Figure 50 shows the relationship between the average wind velocities measured at the NBS site and those reported at surrounding weather stations at the same time. Friendship Airport is 35 miles east, National Airport is 25 miles southeast and Dulles Airport is approximately 20 miles southwest of NBS. As one might expect, readings from aenomometers mounted on airport towers indicate velocities generally larger than measured locally.

Elkins and Wensman (1971) recently reported on an air infiltration study in which two residences in Canton, Ohio were instrumented to measure infiltration rates. Measurements were taken for a period of almost one year. Since these were single story dwellings, the results indicated infiltration rates almost solely a function of wind velocity and direction.

It is postulated and has been verified by many tests that the infiltration rate is a linear function of wind velocity. This linearity arises because the infiltration rate is proportional to the wind pressure to approximately the one-half power while the wind pressure is proportional to the square of the wind velocity. Observing this, Elkins and Wensman divided their experimentally measured infiltration rates by the wind velocity and plotted the new factor against wind direction. The resulting curve had a clearly defined peak thus showing the separate effect of wind velocity and direction. A similar plot was attempted for the data of this study and is shown in Figure 51. As can be seen, there is no definite trend in the data indicating perhaps localized processes at the windows unrelated to the wind velocity and direction measured 300 ft. north of the building.

In attempting to further analyze or explain the results of this investigation, it is natural to observe the analysis of recent investigations of pulsating flow through orifices. This is particularly so due to the type of crack studied during this investigation and the fact that steady orifice flow is described by essentially the same equation as that for steady infiltration through windows (Equation 1). The exponent n has a fixed value of 1/2 for orifice flow.

The essential problem to be solved in both of these situations is to relate the mean flow rate to the mean pressure drop across the opening. If the steady flow equation is used, most authors agree that a substantial portion of the error* in the calculation is due to the so-called "square-root effect", i.e., the average of the square root of the pressure drop does not equal the square root of the average pressure drop. In addition, McCloy (1966) points out three other reasons why the steady flow equation may not be applicable to the pulsating process: a) a certain amount of the pressure difference is used to accelerate or decelerate the flow (inertia effects), b) the contraction or discharge coefficient may change under dynamic conditions, and c) the friction losses may be entirely different in unsteady flow compared to steady flow. He derives the basic equations for unsteady one-dimensional flow through an orifice subjected to a sinusoidal pressure oscillation of a single frequency. Assuming that the discharge coefficient is constant

---

* By an error, it is meant that the steady-state discharge coefficient multiplied by the square root of the time average pressure drop does not equal the actual net flow rate through the opening.

and considering single direction flow as well as flow reversal, the net flow rate is shown to be always less than the amount calculated using the average pressure drop and the basic square root relationship. It is evident from his analysis that the amplitude as well as the frequency of the pressure is important in determining the flow rate.

Earles and Zarek (1963) use the basic tool of dimensional analysis coupled with a substantial number of experiments on two different orifice geometries to obtain a correlation for the net flow rate during pulsative flow. The correlation was essentially a correction factor or multiplying factor to be inserted into the steady flow equation (using average pressure drop) to give the actual flow rate. This correction factor was a function of the frequency of the pulsations, orifice and pipe diameters, amplitude and waveform of the pulsations, and pressure drop across the orifice. As with the analysis of McCloy, the factor was found to be always less than one.

The results of the above studies indicate that if the infiltration-exfiltration process occurring through the test windows is indeed the same as that which occurs in pulsating orifice flow, the air change rates calculated using the steady flow equation and time average pressure drop should give a value larger than actually occurred. However, in over 60% of the tests the measured infiltration rate exceeded that calculated using the steady flow equation. It is interesting to note however that for test no. 3, each individual pressure difference was raised to the proper exponent and the time average of ΔP^n was obtained. Consistent with the above discussion concerning the square root error the following results were obtained:

Room A331 $$ACR = \frac{C\ \overline{\Delta P^n} \cdot 60}{V_A} = 0.26$$

$$ACR = \frac{C\ \overline{\Delta P^n} \cdot 60}{V_A} = 0.104$$

Room B322 $$ACR = \frac{C\ \overline{\Delta P^n} \cdot 60}{V_B} = 0.65$$

$$ACR = \frac{C\ \overline{\Delta P^n} \cdot 60}{V_B} = 0.543$$

where V_A = volume of room A331, ft^3

V_B = volume of room B322, ft^3

$\overline{\ \ }$ = denotes time average

Very recently H. K. Malinowski (1971) presented a discussion of the wind effect on the air movement inside buildings. His observations are that the air exchange is a result of four factors:

1. air flow through a space
2. pulsating flow
3. the penetration of eddies (turbulence)
4. static or molecular diffusion

The air exchange by through-flow is depicted in A of Figure 52 and occurs when openings are located in areas of different pressure. As noted previously, this type of flow was practically eliminated in the present study as a result of completely sealing the room except for the test window.

Pulsating flow occurs when all the openings are located in an area of the same external pressure, or when the pressure difference is very small, but the variation of the pressure in time predominates. This process is demonstrated in B of Figure 52 and as already noted was perhaps the predominate factor in the experiments conducted in this study. Another type of pulsation flow exists when the external pressure changes between two or more openings in such a way that the flow periodically changes direction (C of Figure 52). Because of the basic configuration of the test cracks, this latter process could very well have occurred during the tests and would help explain why the infiltration rate calculated using the steady flow equation and measured ΔP would give values smaller rather than larger than actually measured during 60% of the tests. Unfortunately only one location in the center of the window was chosen for a pressure difference measurement and no quantitative data exists to verify the occurrence of this phenomena.

If the external flow is turbulent, or potential turbulence is created in the vicinity of the opening then eddies, by penetration into the building are carrier vehicles for the conveyance of external air into the building and for the removal of the internal mixture of air to the outside. This process is illustrated in D of Figure 52. It is felt that openings much larger than existed in the present tests would be required before this process becomes significant.

Finally static or molecular diffusion is always accompanying the other modes but is an extremely slow process and its relative contribution to total air exchange through openings is very small. However, for the porous wall with low permeability to air, the contribution of molecular diffusion is of the same order as the external velocity effect and should not be neglected.

4. Spectrum Analysis

If any meaningful simulation is to be made of the dynamic infiltration process, then the frequency of the wind and/or pressure difference oscillations must be known. The range of frequencies that are predominant have been determined by a spectrum analysis of the data that was taken.

Consider, for example, one of the velocity components of the wind. Over a certain length of time the average value of this component can be determined. The instantaneous value is then assumed to be composed of the time average value plus some time dependent fluctuation.

$$U_1 = \bar{U}_1 + u_1 \tag{4}$$

where U_1 = instantaneous velocity component

$\bar{U}_1$ = time average value

u_1 = instantaneous value of the fluctuating component

The kinetic energy of the turbulent fluctuations can be considered to consist of the sum of the contributions of all the frequencies n.

Let $E(n)\,dn$

be the contribution to u_1 of the frequencies between n and n + dn; the distribution function E (n) then has to satisfy the condition

$$\int_0^\infty E(n)\,dn = \overline{u_1^2} \tag{5}$$

E (n) is called the power spectrum.

In the field of statistics, there are many types of correlation function that have been defined. One such function involves the correlation between values of a fluctuating quantity at a fixed point in a flow field at two different instants t' and t'-t or t'+t. For the experiment being analyzed here, the quantity of interest is the fluctuating velocity component u_1. The correlation desired is then

$$\overline{u_1(t')\,u_1(t'-t)}$$

or in terms of a coefficient

$$R(t) = \frac{\overline{u_1(t')\,u_1(t'-t)}}{\overline{u_1'^2}} \tag{6}$$

where the average is taken with respect to time t.

It was shown originally by Taylor (1938) and more recently by Hinze (1959) in his book Turbulence, that the time correlation coefficient defined above and the power spectrum are Fourier cosine transforms.

$$R(t) = \frac{1}{\overline{u_1^2}} \int_0^\infty dn\ E\ (n) \cos 2\pi nt \tag{7}$$

and

$$E\ (N) = 4\ \overline{u_1^2} \int_0^\infty dt\ R(t) \cos 2\pi nt \tag{8}$$

Consequently the power spectrum can be obtained by first computing the correlation coefficient and then obtaining the power spectrum. In the analysis of the discrete data obtained from this experiment, the following sequence of calculations were used:

$$\overline{X} = \frac{1}{N} \sum_{n=1}^{N} X\ (t_n) \tag{9}$$

$$X'\ (t_n) = X\ (t_n) - \overline{X} \tag{10}$$

$$\sigma^2 = \frac{1}{N} \sum_{n=1}^{N} (X'\ (t_n))^2 \tag{11}$$

$$R(k) = \frac{1}{N-k} \sum_{n=1}^{N-k} X'\ (t_n)\ X'\ (t_{n+k}) \tag{12}$$

for $k = 0, 1, \ldots m$

$$P\left(\frac{\nu}{m}\frac{1}{2\Delta t}\right) = \Delta t \left\{R(0) + 2\sum_{k=1}^{m-1} R(k) \cos 2\pi \frac{\nu}{2m} k + (-1)^{\nu} R(m)\right\} \tag{13}$$

for $\nu = 0, 1, \ldots m$

$$P\left(\frac{-\nu}{m}\ \frac{1}{2\Delta t}\right) = P\left(\frac{\nu}{m}\ \frac{1}{2\Delta t}\right)$$

$$\bar{P}\left(\frac{\nu}{m}\ \frac{1}{2\Delta t}\right) = \sum_{n=-i}^{i} a_n P\left(\frac{\nu-n}{m}\ \frac{1}{2\Delta t}\right) \tag{14}$$

where

$X(t_n)$ = value of the variable of interest at time t_n

σ^2 = variance

Δt = time increment between discrete data values

N = no. of data values chosen for the analysis

a_n = smoothing window

The purpose of the window is to smooth the distortion caused by the finite and discrete data.

The above sequence of calculations were applied to a 400 length segment of north-south and east-west velocity components of test no. 3 and the results are shown in Figure 53. The ordinate is a normalized power (normalized by R(0)) and the abscissa is the frequency in cps. The time increment between data points was 0.5 seconds which limits the highest possible frequency detectable by the analysis to 1 cycle per second. The smoothing window chosen was:

$$\begin{aligned} a_0 &= 0.6398 \\ a_1 &= -a_1 = 0.2401 \\ a_2 &= -a_2 = -0.061 \\ a_4 &= -a_4 = 0.00 \end{aligned} \tag{15}$$

As can be seen, the highest significant frequency is on the order of 0.1 cps with the maximum "power" occurring at frequencies in the range of 0.01 cps. The data of other tests were analyzed and similar results were obtained.

Turbulence in a flow field is called isotropic if its statistical features have no preference for any direction. This condition simultaneously requires no average shear stress and no velocity gradient in the field. Even though it is a hypothetical situation, the majority of theoretical analysis on turbulence has been in this area and a knowledge of its characteristics have formed a fundamental basis for the study of actual turbulent flows. One of the ranges of frequencies where an equation for the power spectrum has been derived on a theoretical basis assuming isotropic turbulence is the so-called "inertial subrange". It can be shown that the "power" is equal to a constant times the frequency

to the minus 5/3 power. It is interesting to note in Figure 53 that the spectrum obtained indeed has this kind of dependence over a large portion of the range.

Figure 54 shows the results of a similar analysis that was done on the pressure differences across the test windows during test no. 3. As with the velocity components, the significant frequencies lie below 0.1 cps with the maximum "power" occurring at frequencies below 0.01 cps. Again the increment of time between discrete data points was 0.5 seconds, the number of data points chosen was 400, and the Akaike-W_2 smoothing window was used (equation (15)). The dependence of "power" on frequency raised to the minus 17/3 power over much of the frequency range also agrees with the theory of isotropic turbulence applied to a scaler quantity such as pressure in the inertial subrange. Perhaps the most significant observation is that the meaningful pressure fluctuations are so low in frequency that the use of a steady flow equation for air flow rate can almost be justified.

5. Conclusions and Recommendations

The most obvious conclusion to be drawn from the present study is that the infiltration process that actually occurs in and around window cracks is an extremely complex one. It was postulated that the air change was primarily a result of a pulsation process at the window crack and was complicated by the fact that air flow could occur into and out of the room simultaneously.

The design calculation as recommended by ASHRAE gave air change rates larger than those measured, particularly when the average wind velocity was higher than approximately 5 miles per hour. The correlation between actual air change rates and ones calculated using the steady flow equation and a measured ΔP that was averaged over the duration of the test was moderate to good. The agreement was better at higher average wind velocities. The concept that the steady flow calculation may give valid results was further substantiated by a spectrum analysis showing pressure differences across the test windows at significant frequencies of 0.1 cps and lower. The major reason that the agreement between the actual flow rates and those calculated using the steady-flow assumption was not better was assumed to be the simultaneous forward and reverse flow already mentioned.

The investigators of this study recommend that additional experiments be conducted. Perhaps the most important thing would be to isolate the relative importance of pulsation, pulsation with simultaneous two-directional flow, and through-flow. Relatively simple experiments could be constructed in the laboratory to provide pulsating flow, with and without simultaneous through-flow. The frequency of the pulsations could be varied from zero down to 0.1 cps and it could be determined at precisely what frequency the steady flow equation "breaks down" or predicts a flow rate too far from the measured value. Naturally it would also be possible in such controlled experiments to determine the effect of velocity and direction on the infiltration. The results could then be extrapolated to determine the relative importance of "two-directional" flow in a realistic infiltration process.

6. Acknowledgments

The authors would like to acknowledge the assistance of Mr. Jim Raines of the Structures Section, Building Research Division. His help in processing the data recorded on the analog tapes was greatly appreciated. Also, the assistance of Mr. James D. Allen of the Environmental Engineering Section, Building Research Division, for calibrating and installing the instrumentation and for logging and processing the large amounts of data was much appreciated.

7. References

1. ASHRAE Handbook of Fundamentals, American Society of Heating, Refrigerating, and Air-Conditioning Engineers, Inc., 1967.
2. Procedure for Determining Heating and Cooling Loads for Computerized Energy Calculations, American Society of Heating, Refrigerating, and Air-Conditioning Engineers, Inc., 1971.
3. Svetlov, K. S., "Calculation of Air Exchange in Multi-Storey Buildings Using Electronic Computers", Vodosnabzenie i sanitarna tekhnika, Vol. 11, pp. 28-31, 1966.
4. Jackman, P. J. and H. Ph. L. den Ouden, "The Natural Ventilation of Tall Office Buildings", 1968.
5. Gabrielsson, J. and P. Porre, "Calculation of Infiltration and Transmission Heat Loss in Residential Buildings by Digital Computer", J.I.H.V.E., pp. 357-368, March 1968.
6. Albright, G. H., Isenberg, M. W., McLaughlin, E. R. and E. R. Queer, Measurement of Natural Draft, prepared under Contract No. OCD-OS-62-64 to the Office of Civil Defense, 1963.
7. Elkins, R. H. and C. E. Wensman, "Natural Ventilation of Modern Tightly Constructed Homes", Paper presented at the American Gas Association - Institute of Gas Technology Conference on Natural Gas Research and Technology, Chicago, Illinois, February 28 - March 3, 1971.

8. McCloy, D., "Effects of Fluid Inertia and Compressibility on the Performance of Valves and Flow Meters Operating Under Unsteady Conditions", Journal Mechanical Engineering Science, Vol. 8, No. 1, pp. 52-61, 1966.

9. Earles, J. W. E. and J. M. Zarek, "Use of Sharp-Edged Orifices for Metering Pulsating Flow", Proceedings of the Institute of Mechanical Engineers, Vol. 177, No. 37, pp. 997-1024, 1963.

10. Malinowski, H. K., "Wind Effect on the Air Movement Inside Buildings", Paper presented at Tokyo Conference on Wind Loads, Tokyo, Japan, September 6, 1971.

11. Jenkins, G. M. and D. G. Watts, Spectral Analysis and Its Application, Holden-Day Publishing Company, 1968.

12. Hinze, J. O., Turbulence, McGraw-Hill Book Company, 1959.

13. Taylor, G. I., Proceedings of the Royal Society of London, 164A, 476, 1938.

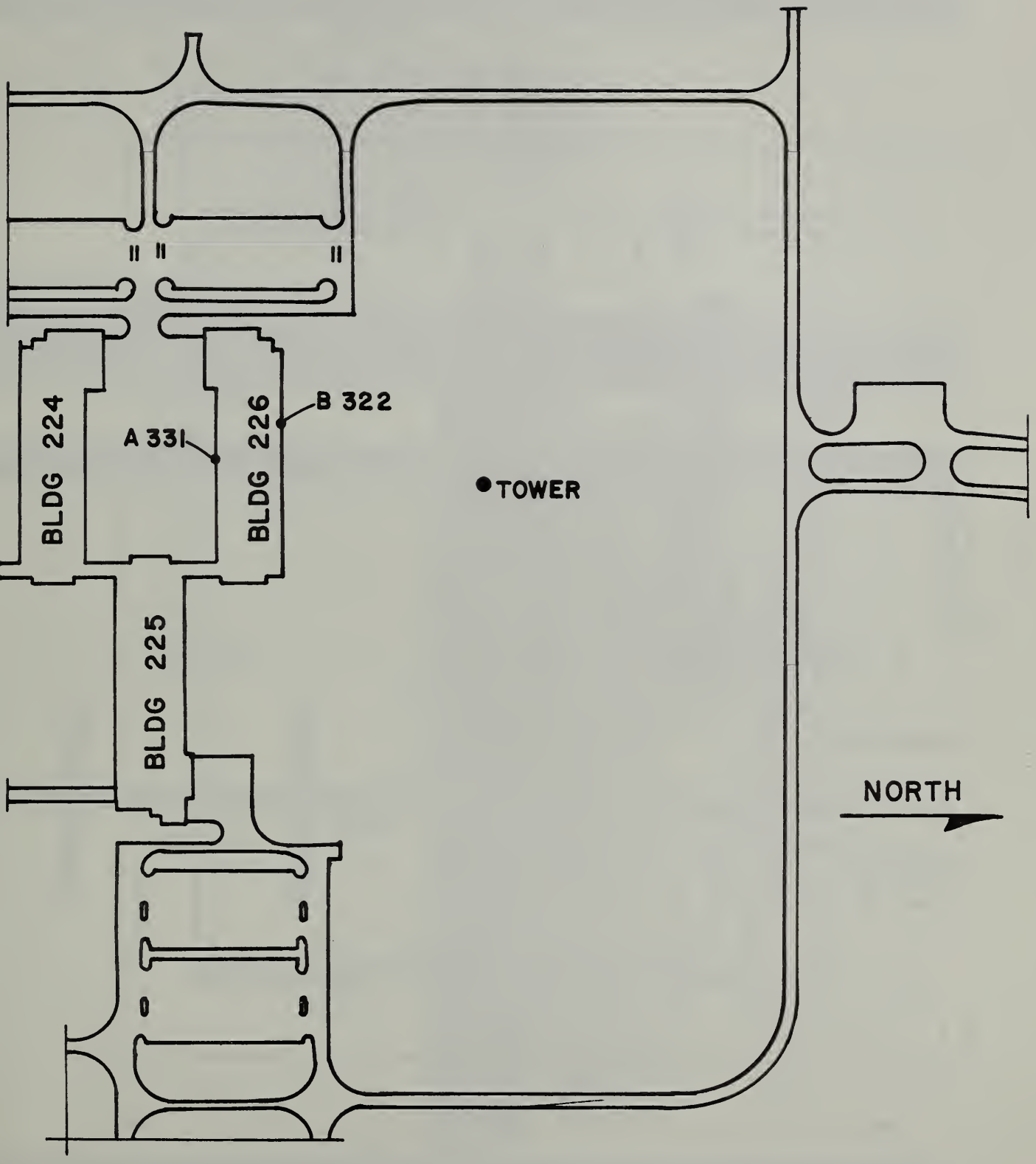

Scale 1" = 250'

Figure 1

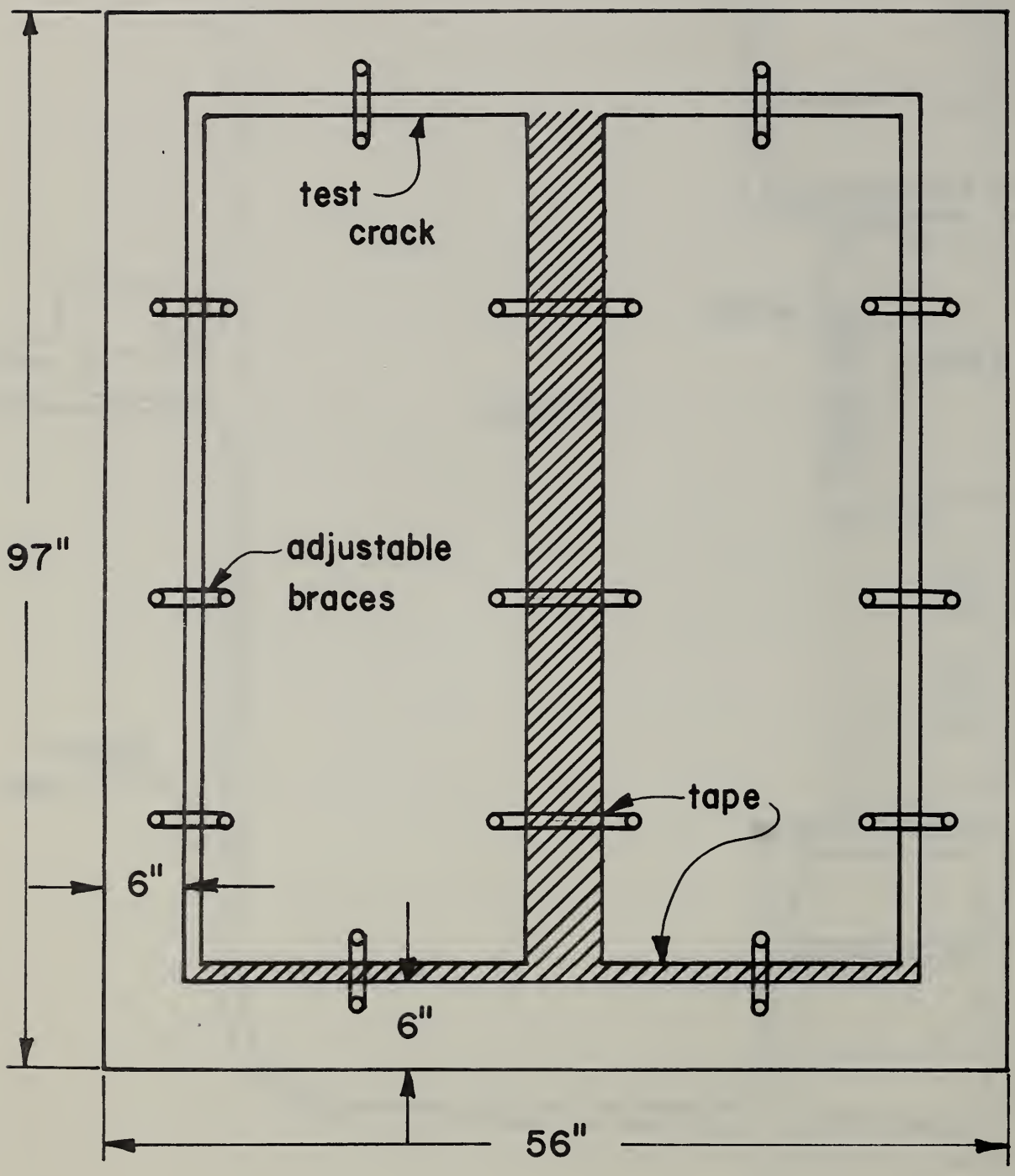

Figure 2

Figure 3

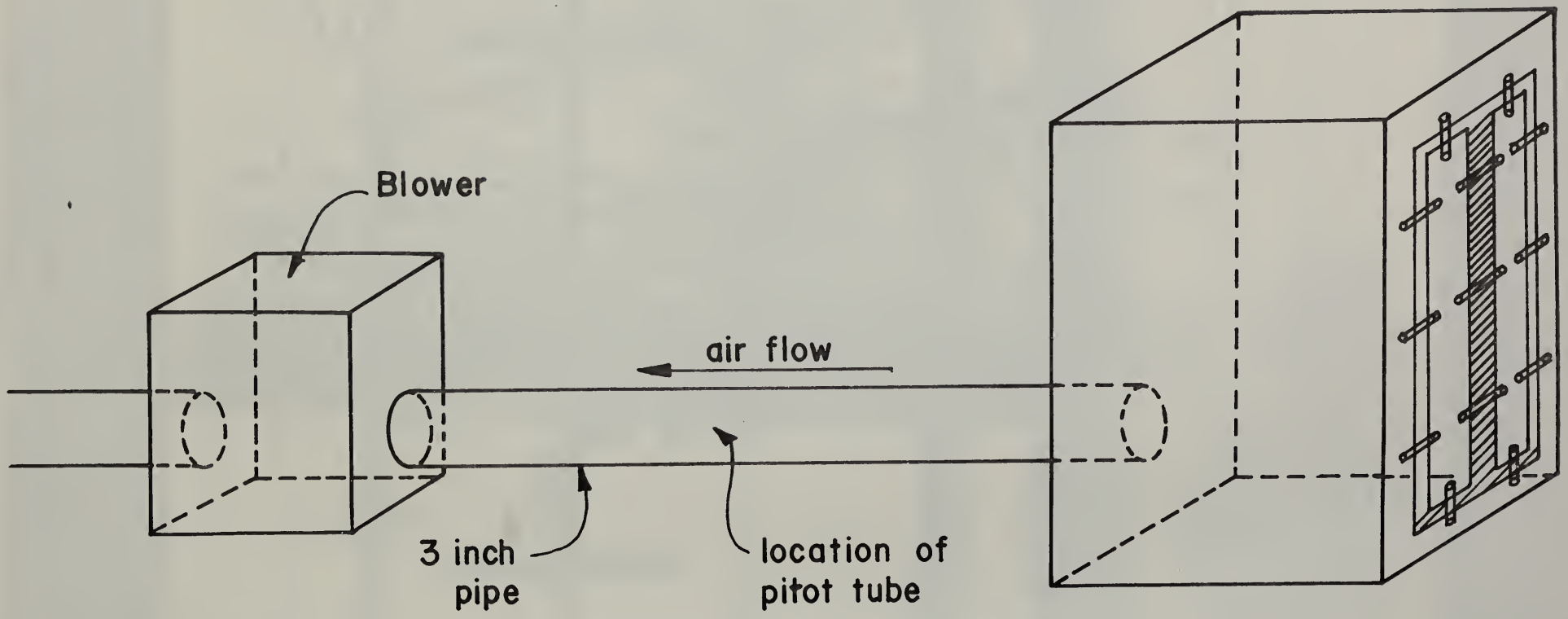

Figure 4

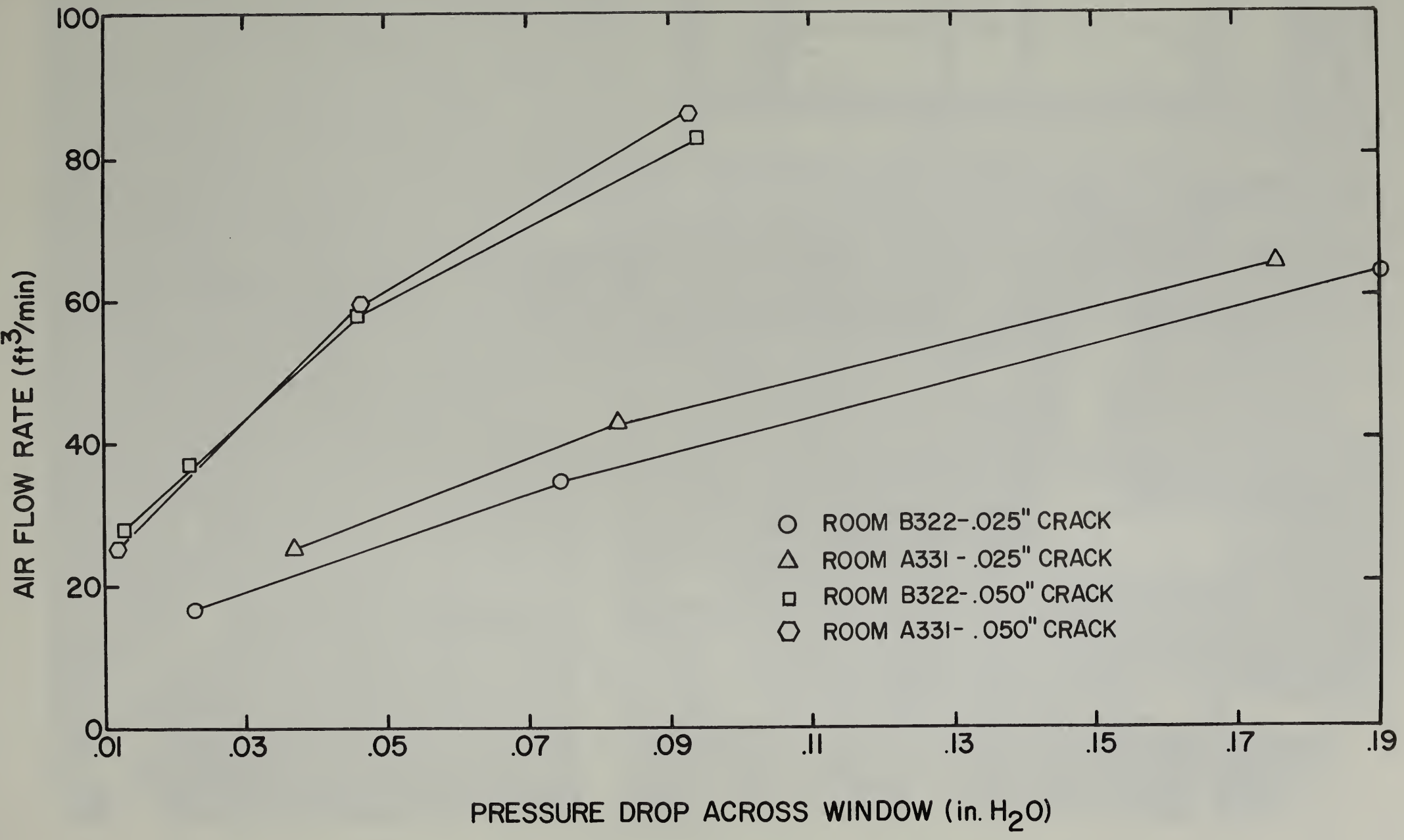
100
80
60
40
20
0
.01
.03
.05
.07
.09
.11
.13
.15
.17
.19
AIR FLOW RATE (ft3/min)
PRESSURE DROP ACROSS WINDOW (in. H2O)
ROOM B322-.025" CRACK
ROOM A331 - .025" CRACK
ROOM B322-.050" CRACK
ROOM A331- .050" CRACK

Figure 5

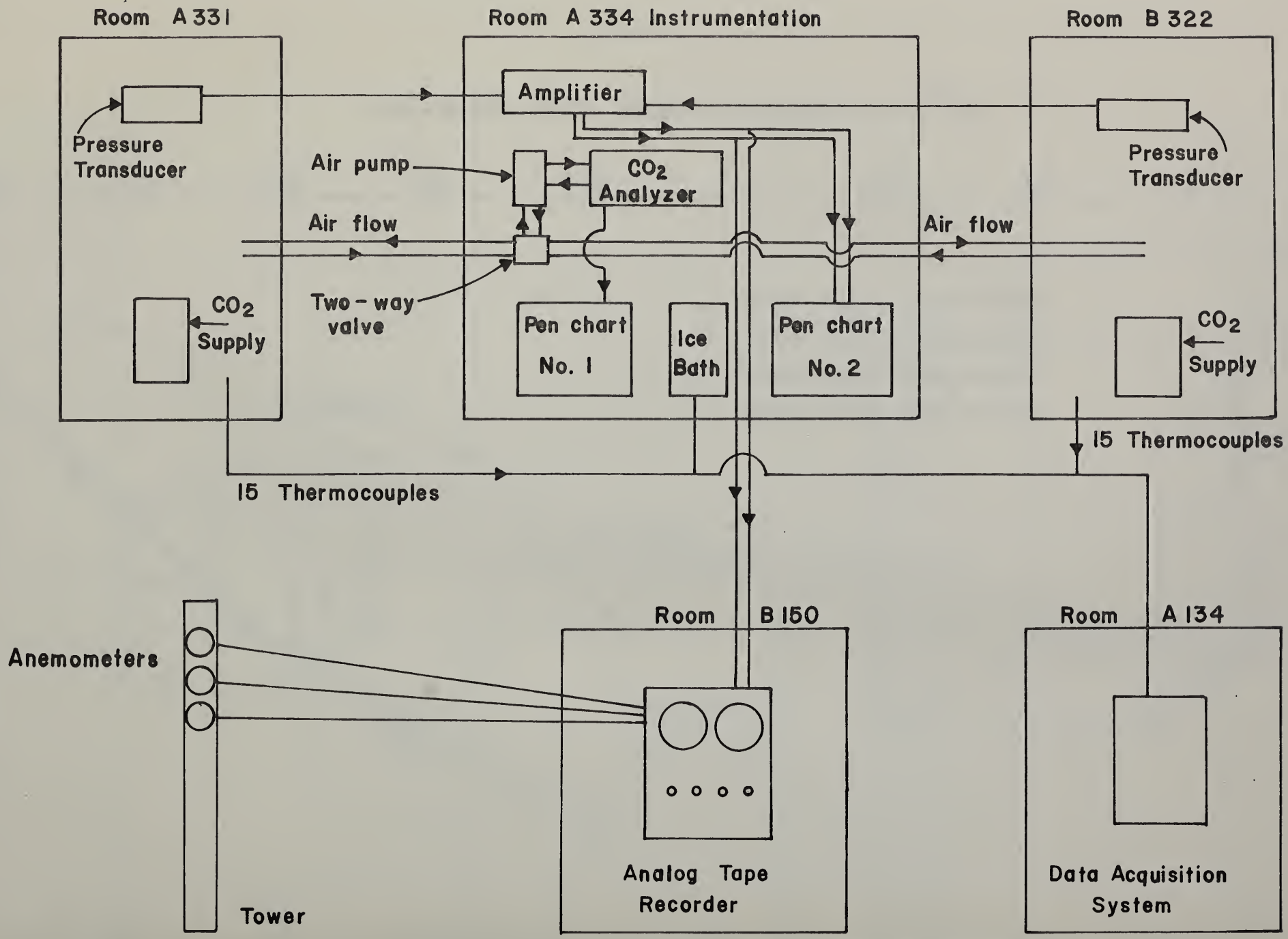
Room A 331
Room A 334 Instrumentation
Room B 322
Amplifier
Pressure Transducer
Air pump
CO_2 Analyzer
Air flow
Air flow
Pressure Transducer
Two - way valve
CO_2 Supply
Pen chart No. 1
Ice Bath
Pen chart No. 2
CO_2 Supply
15 Thermocouples
15 Thermocouples
Anemometers
Room B 150
Room A 134
Analog Tape Recorder
Data Acquisition System
Tower

Figure 6

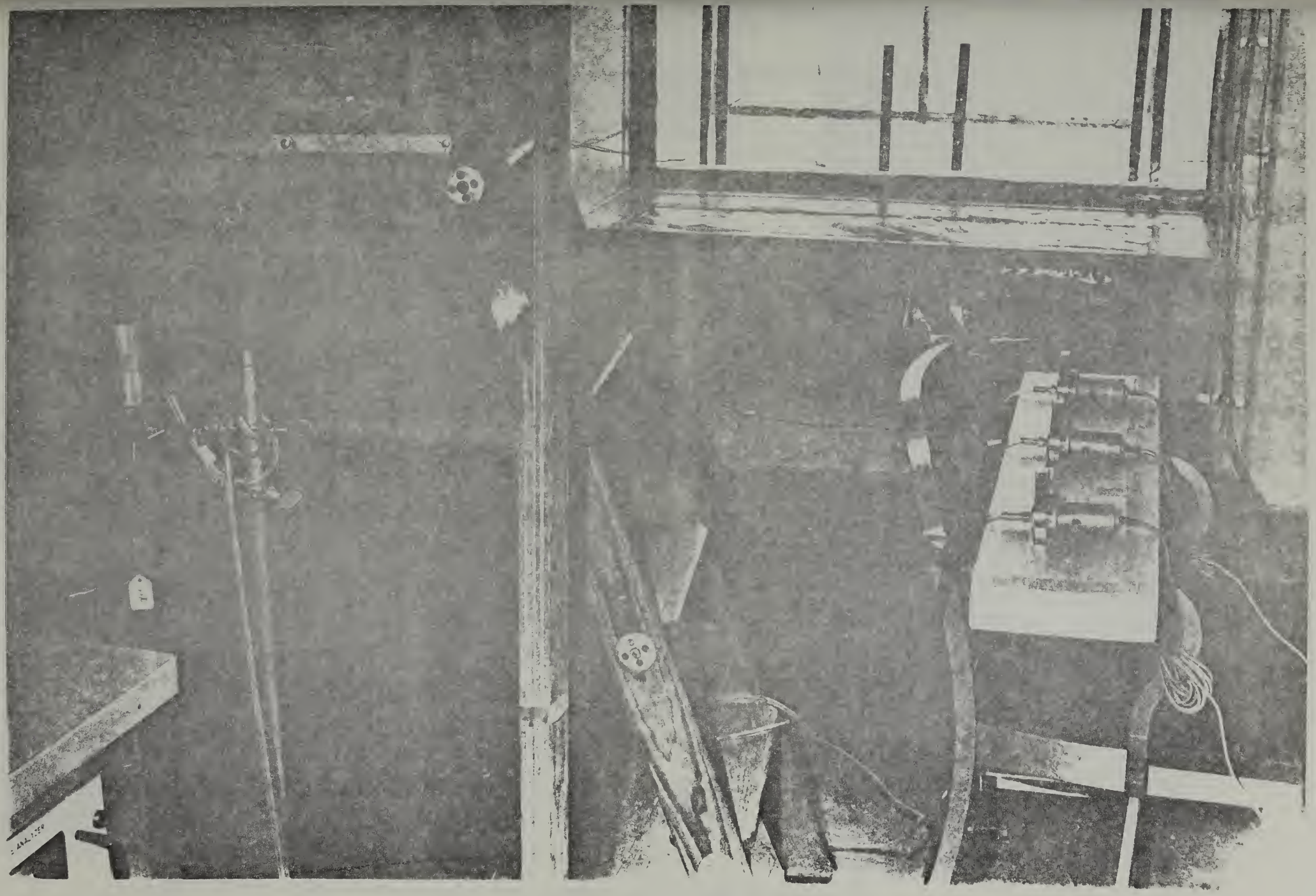

Figure 7

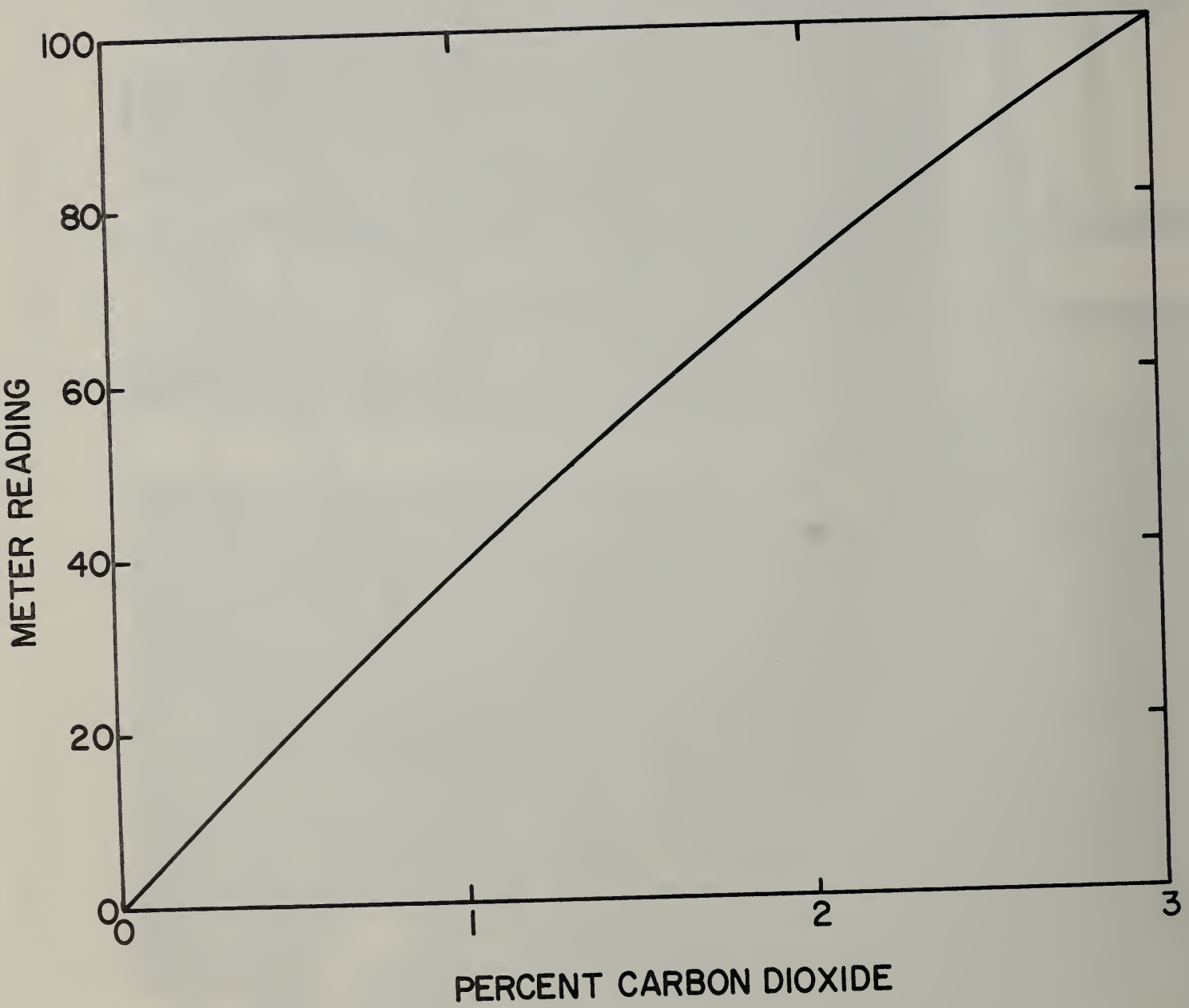

Figure 8

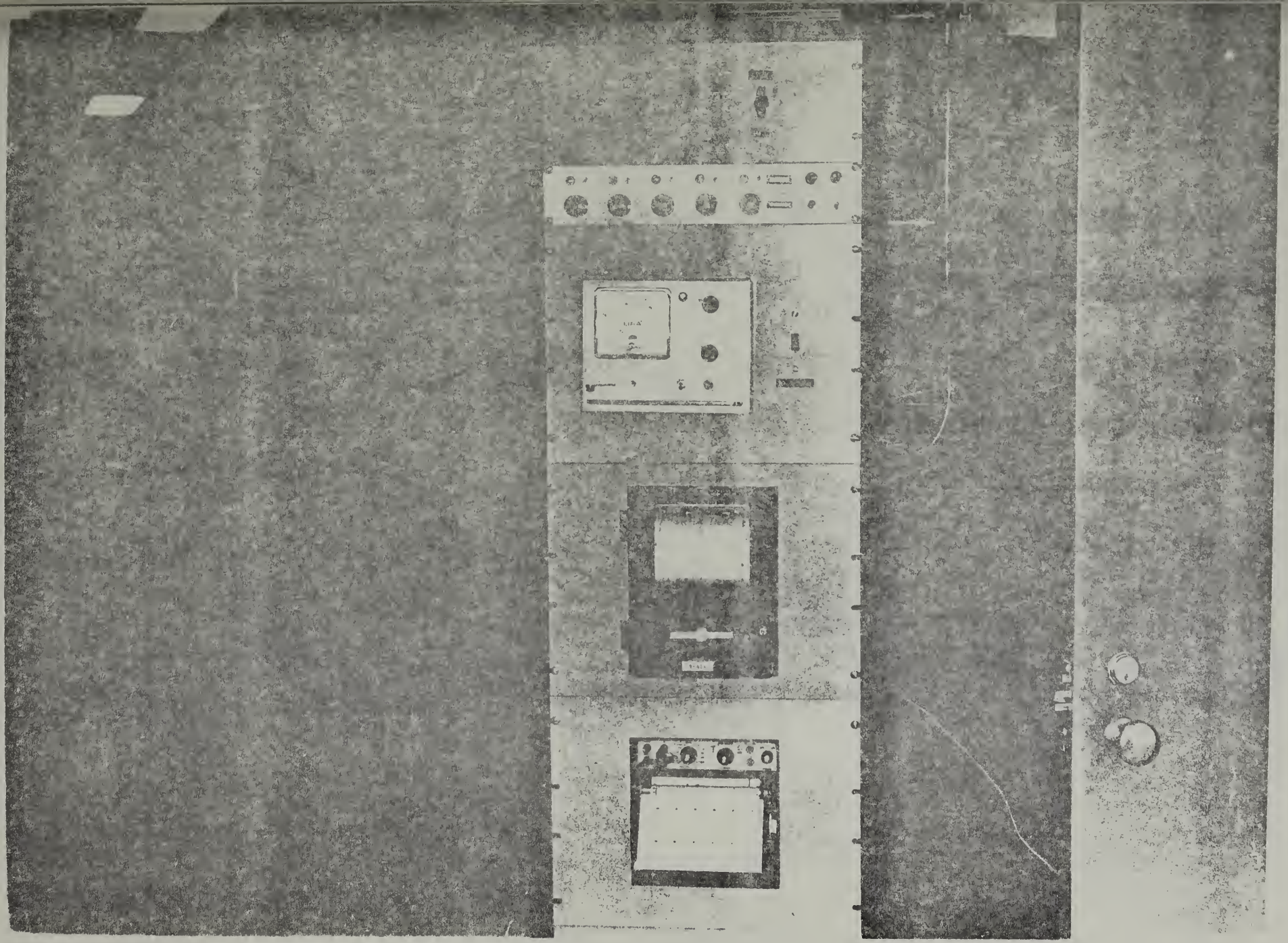

Figure 9

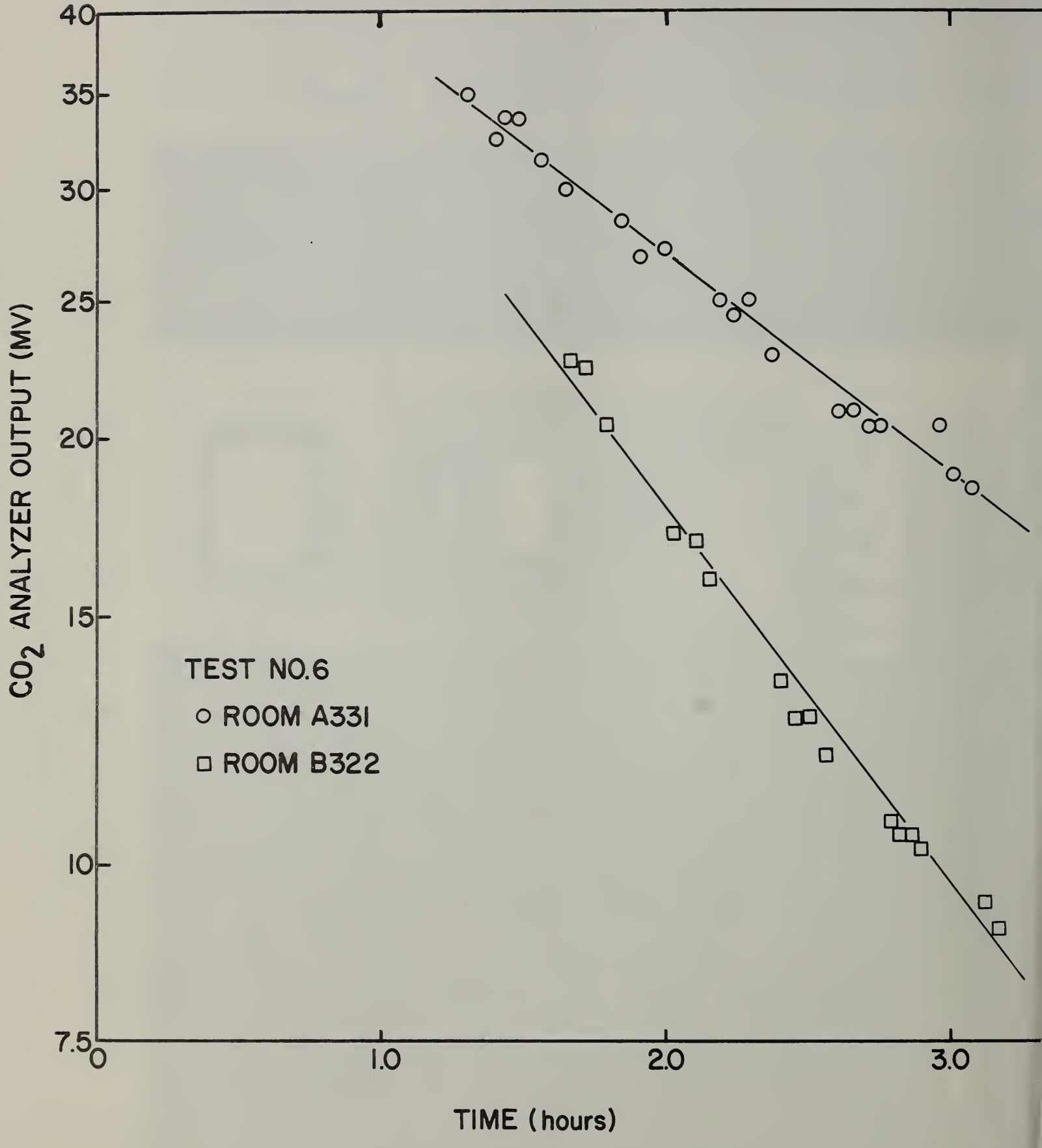
40
35
30
25
20
15
10
7.5
0
1.0
2.0
3.0
CO_2 ANALYZER OUTPUT (MV)
TIME (hours)
TEST NO.6
○ ROOM A331
□ ROOM B322

Figure 10

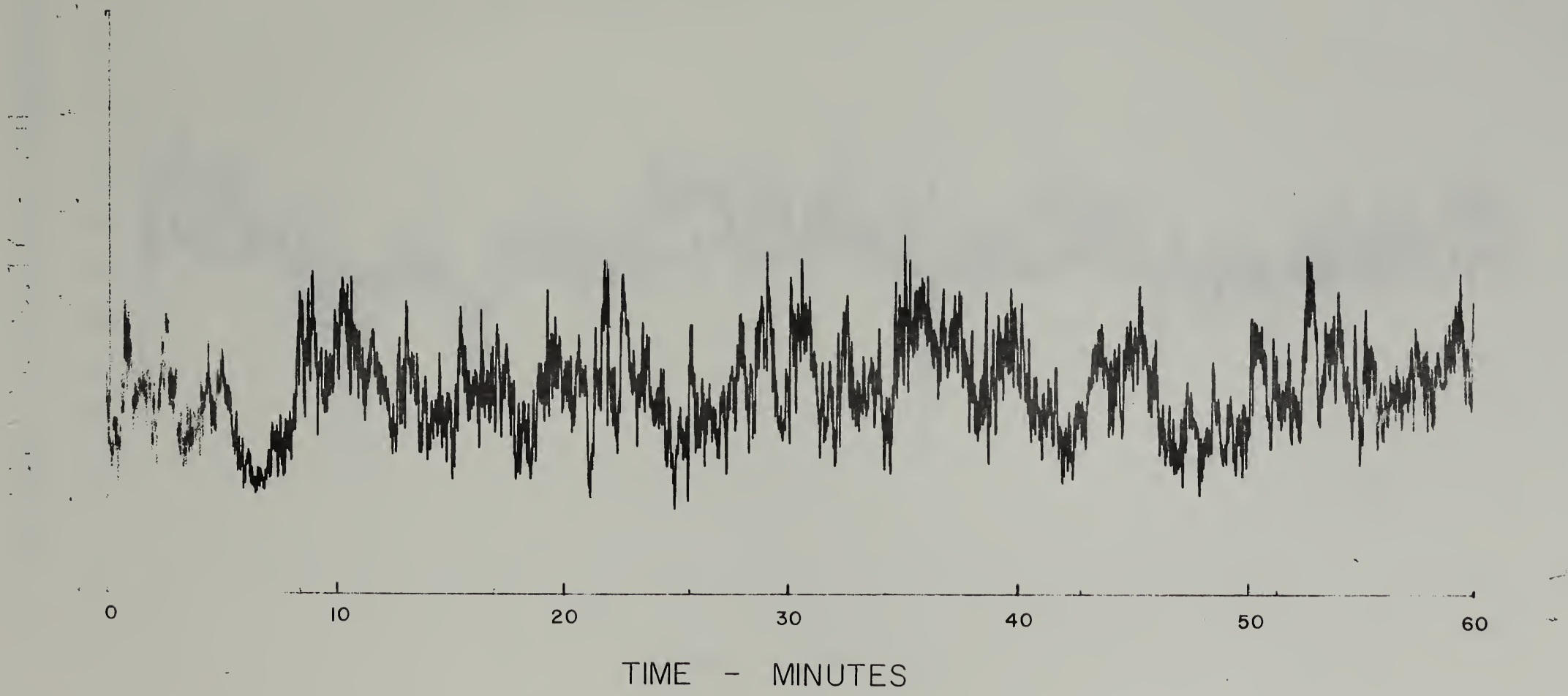

Figure 11

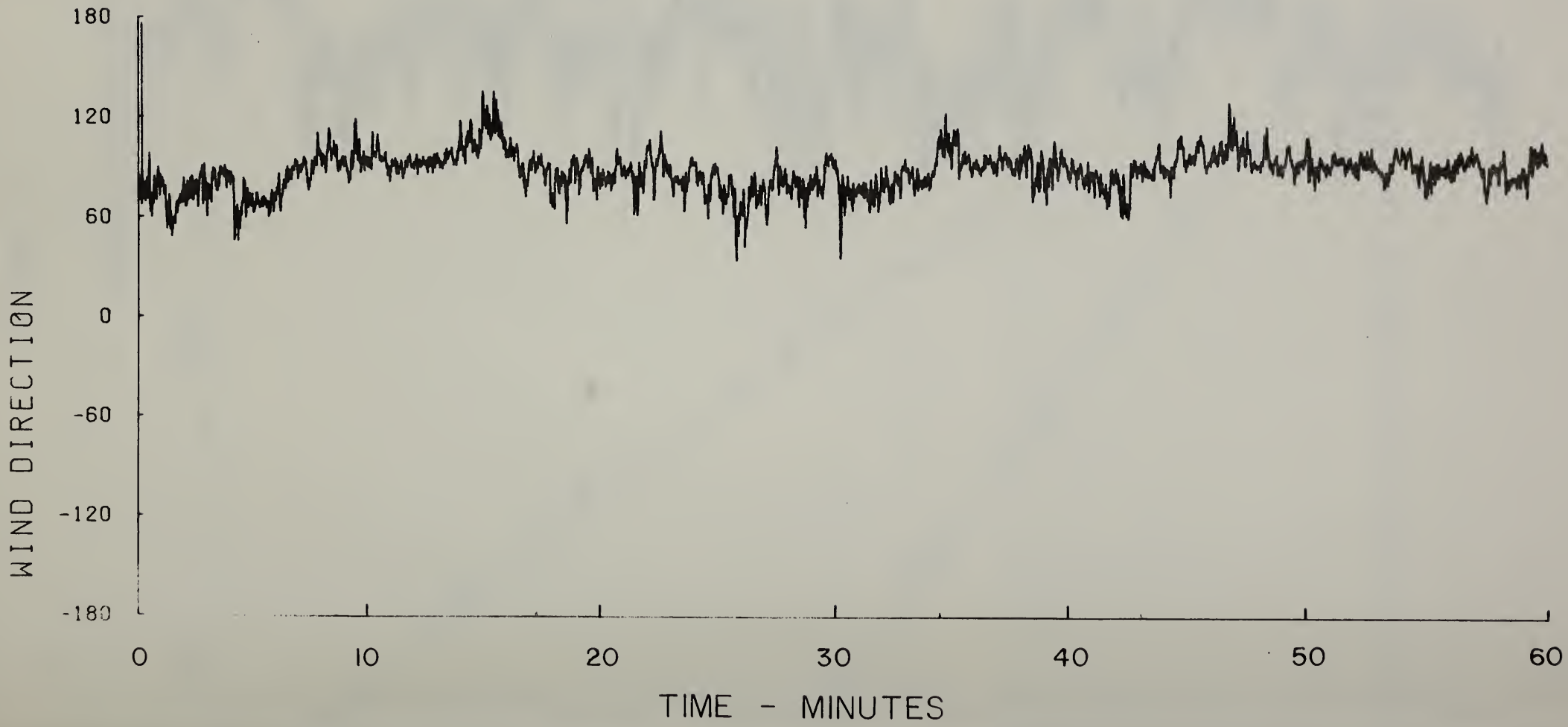
180
120
60
0
-60
-120
-180
WIND DIRECTION
0
10
20
30
40
50
60
TIME - MINUTES

Figure 12

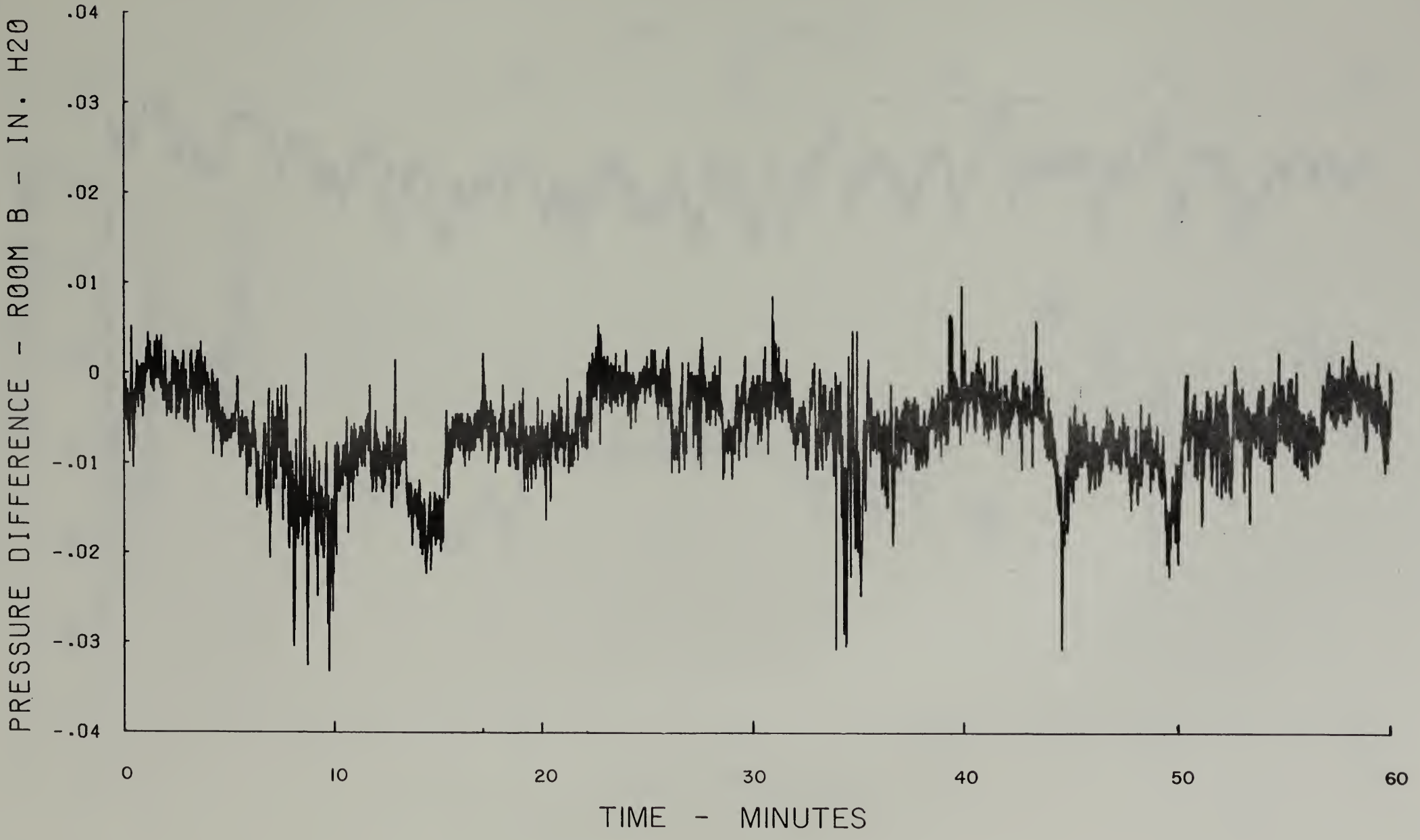
PRESSURE DIFFERENCE - ROOM B - IN. H20
.04
.03
.02
.01
0
-.01
-.02
-.03
-.04
0
10
20
30
40
50
60
TIME - MINUTES

Figure 13

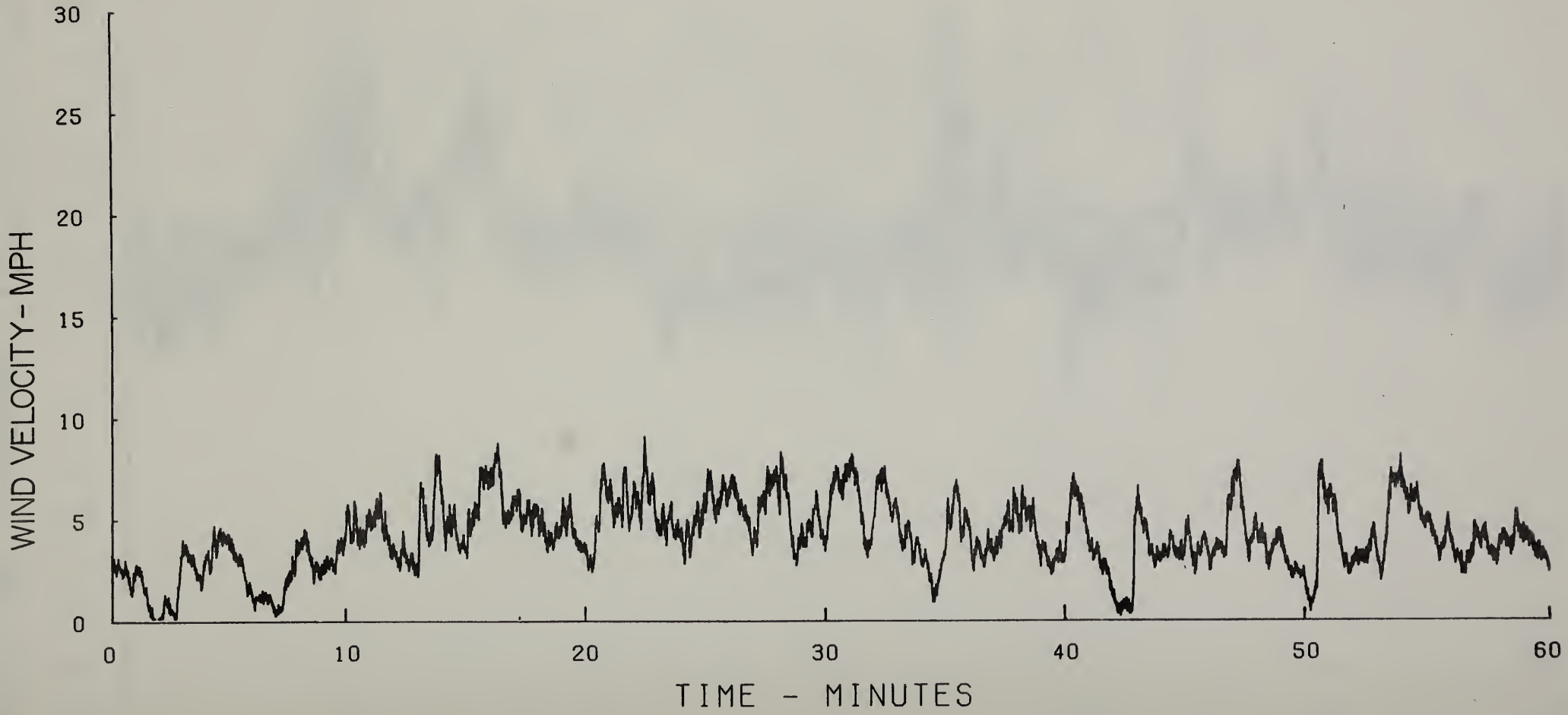
WIND VELOCITY- MPH
30
25
20
15
10
5
0
0
10
20
30
40
50
60
TIME - MINUTES

Figure 14

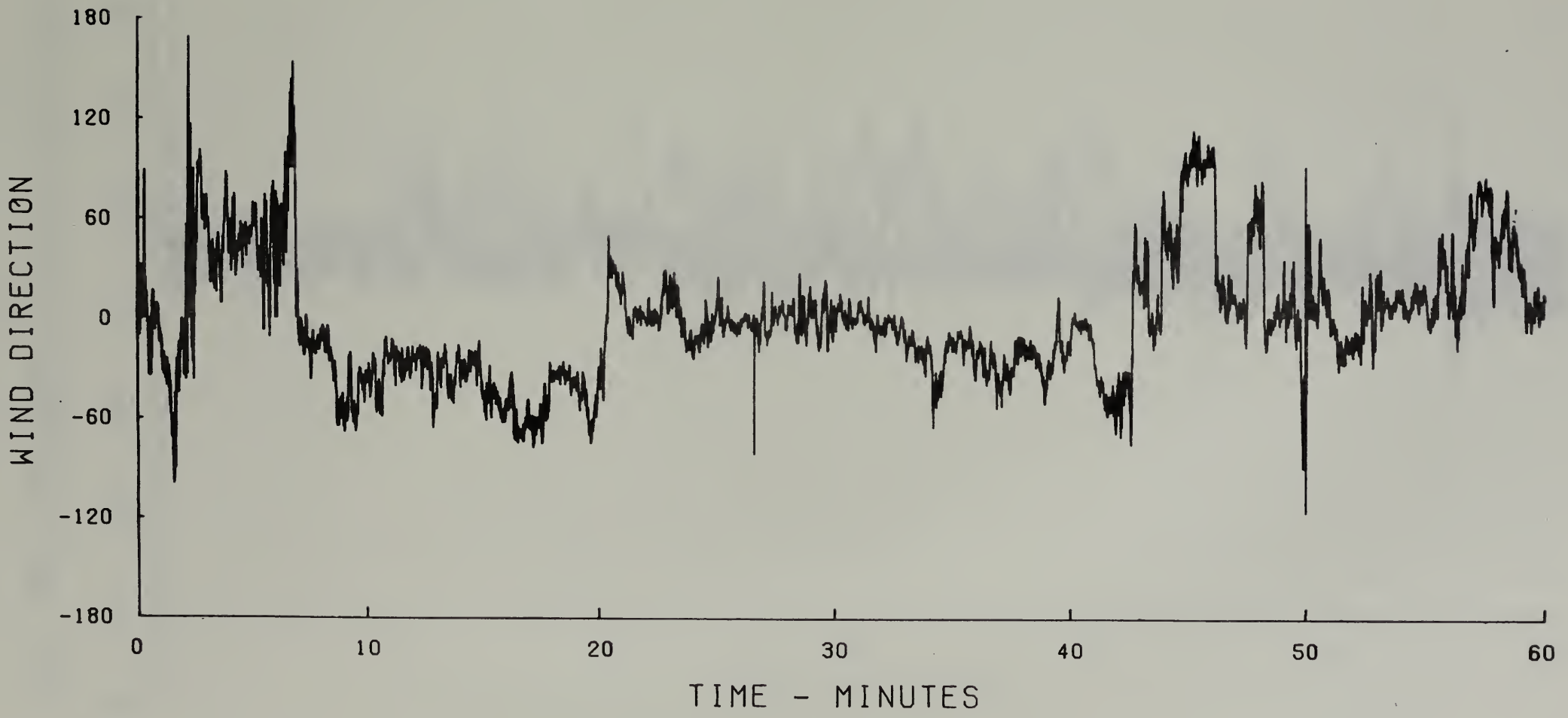
180
120
60
0
-60
-120
-180
WIND DIRECTION
0
10
20
30
40
50
60
TIME - MINUTES

Figure 15

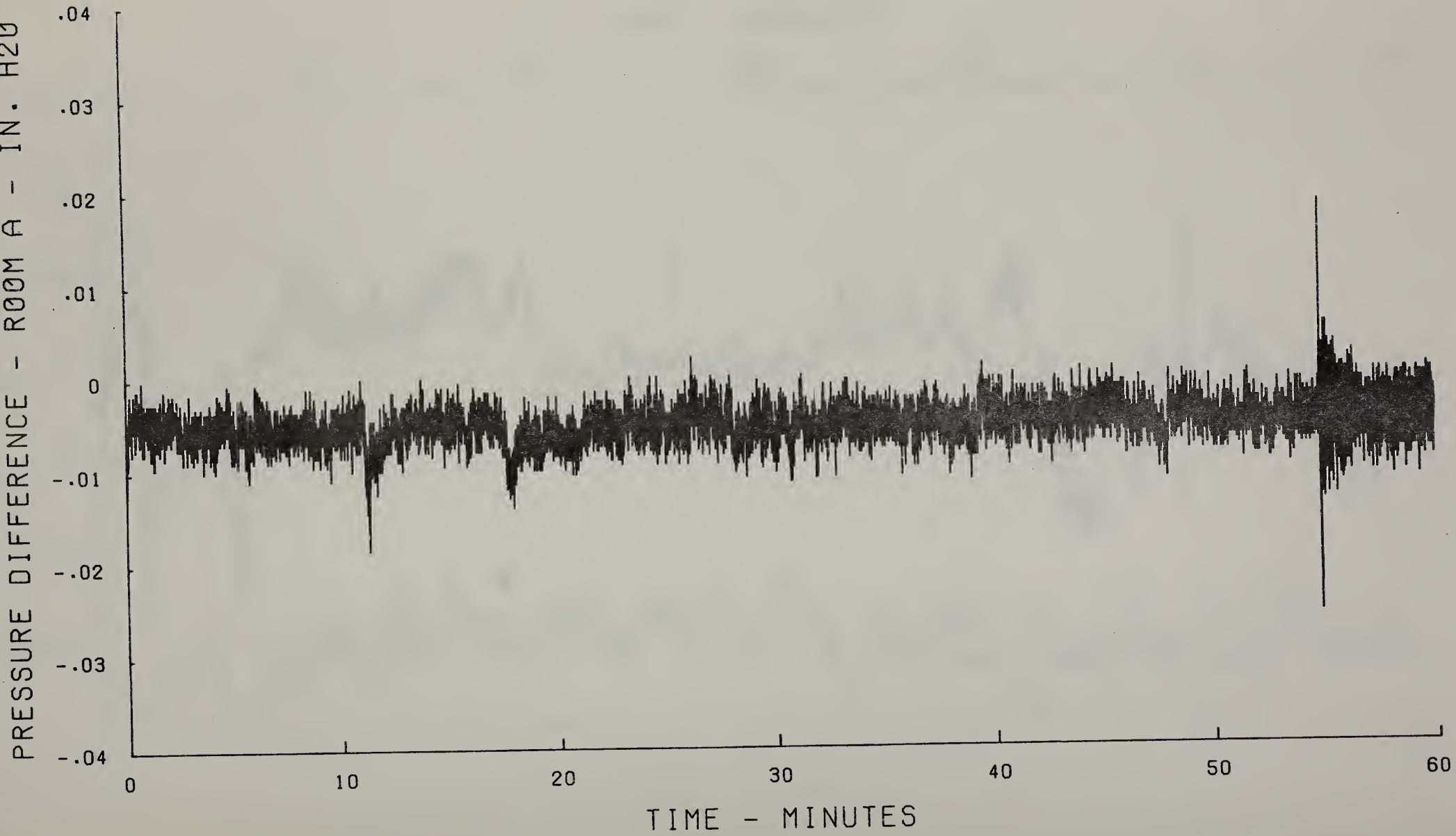
PRESSURE DIFFERENCE - ROOM A - IN. H20
.04
.03
.02
.01
0
-.01
-.02
-.03
-.04
0
10
20
30
40
50
60
TIME - MINUTES

Figure 16

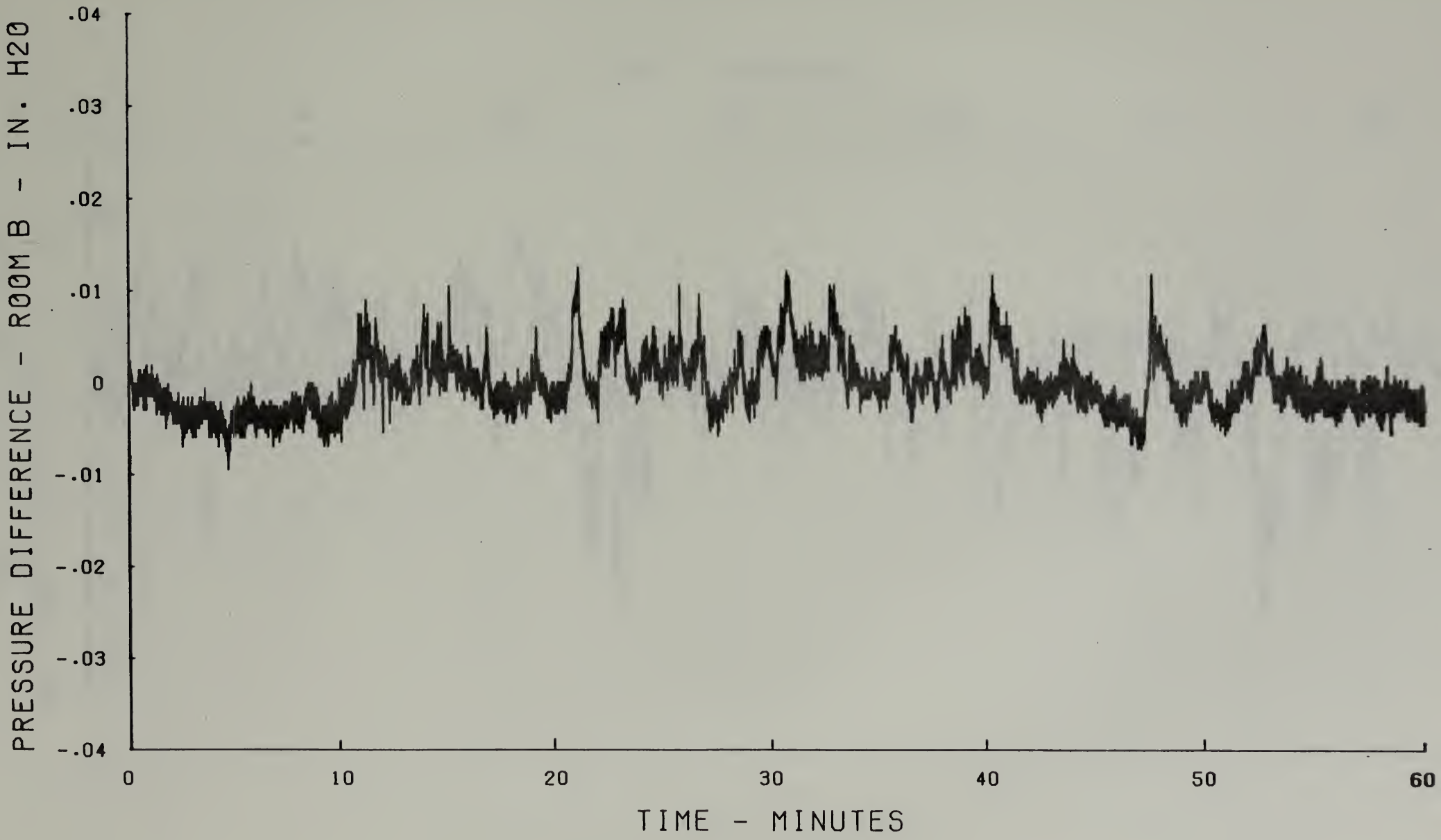
PRESSURE DIFFERENCE - ROOM B - IN. H20
.04
.03
.02
.01
0
-.01
-.02
-.03
-.04
0
10
20
30
40
50
60
TIME - MINUTES

Figure 17

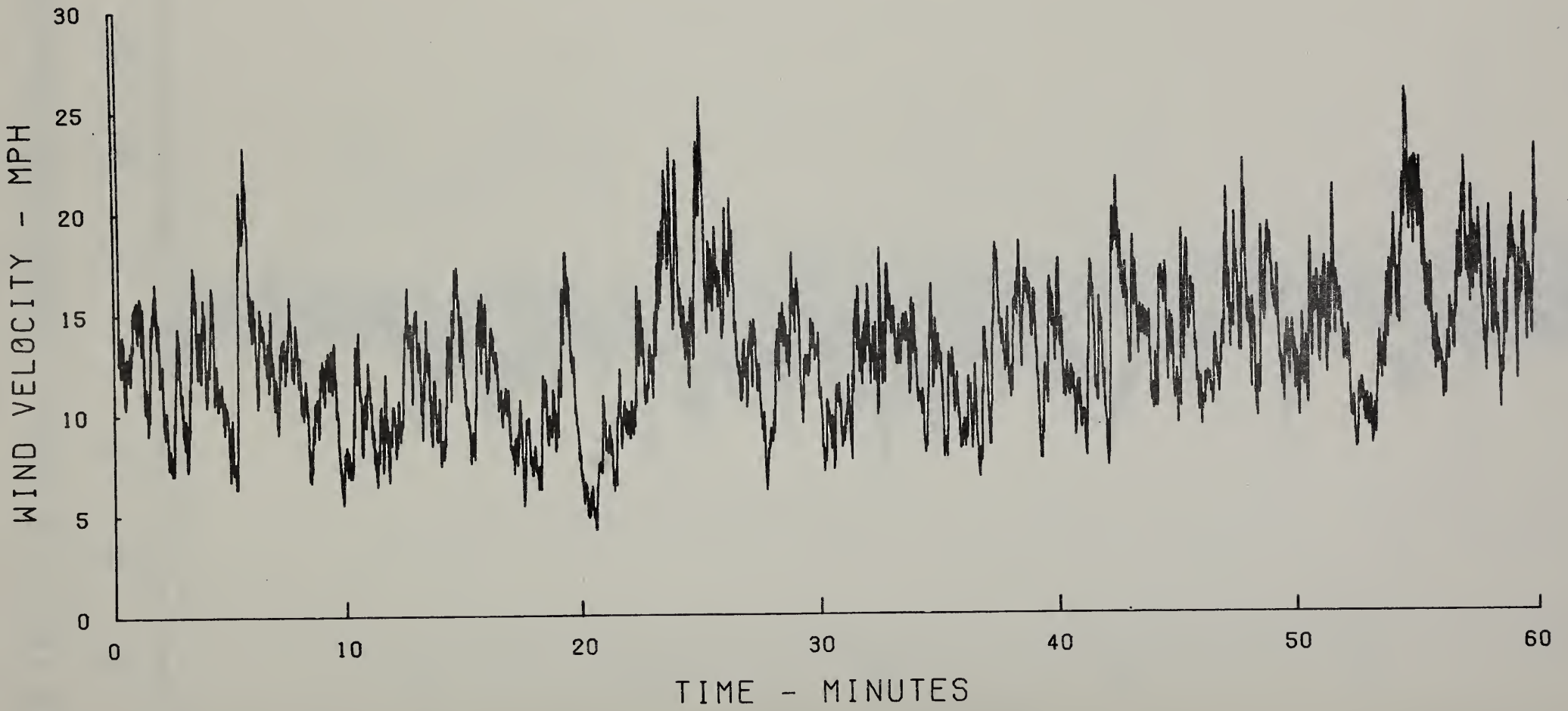
WIND VELOCITY - MPH
30
25
20
15
10
5
0
0
10
20
30
40
50
60
TIME - MINUTES

Figure 18

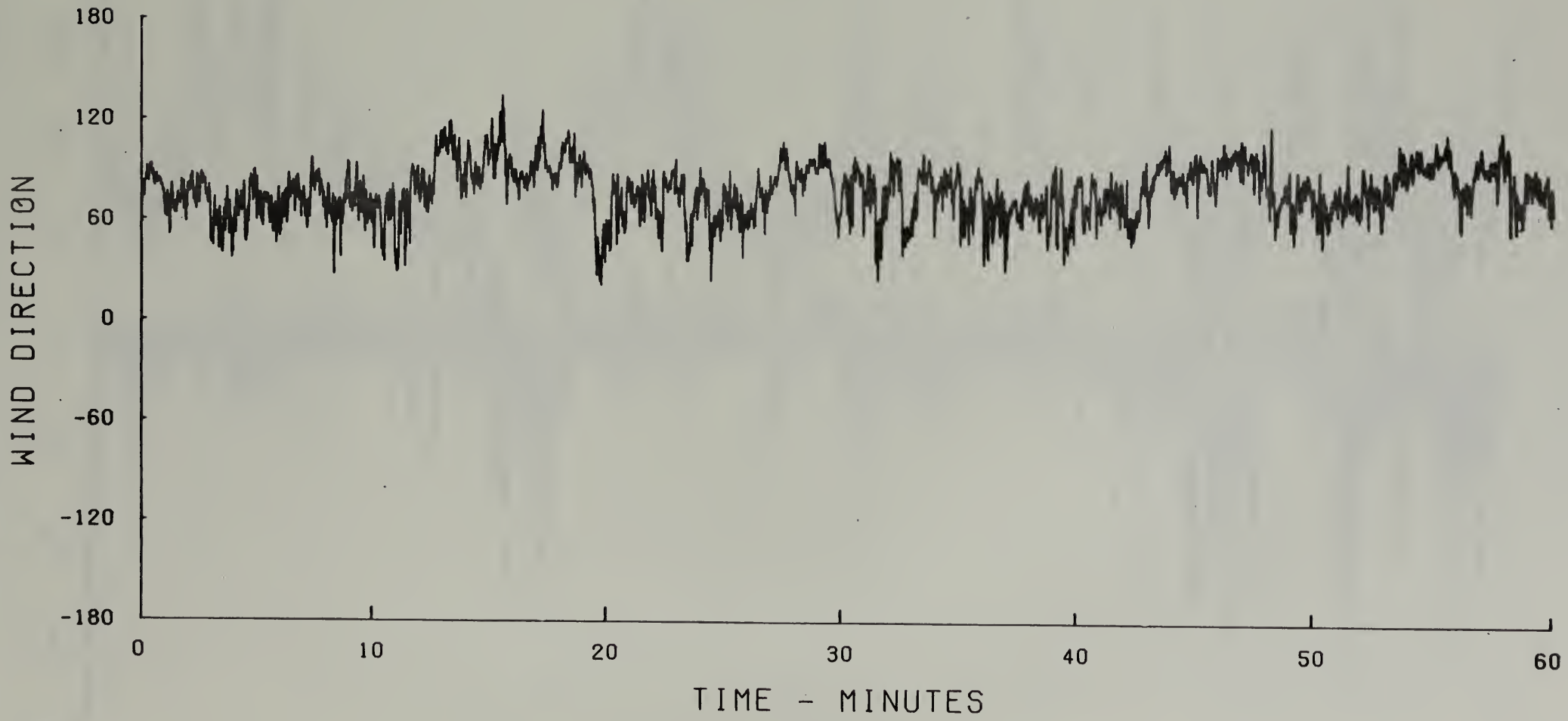
180
120
60
0
-60
-120
-180
WIND DIRECTION
0
10
20
30
40
50
60
TIME - MINUTES

Figure 19

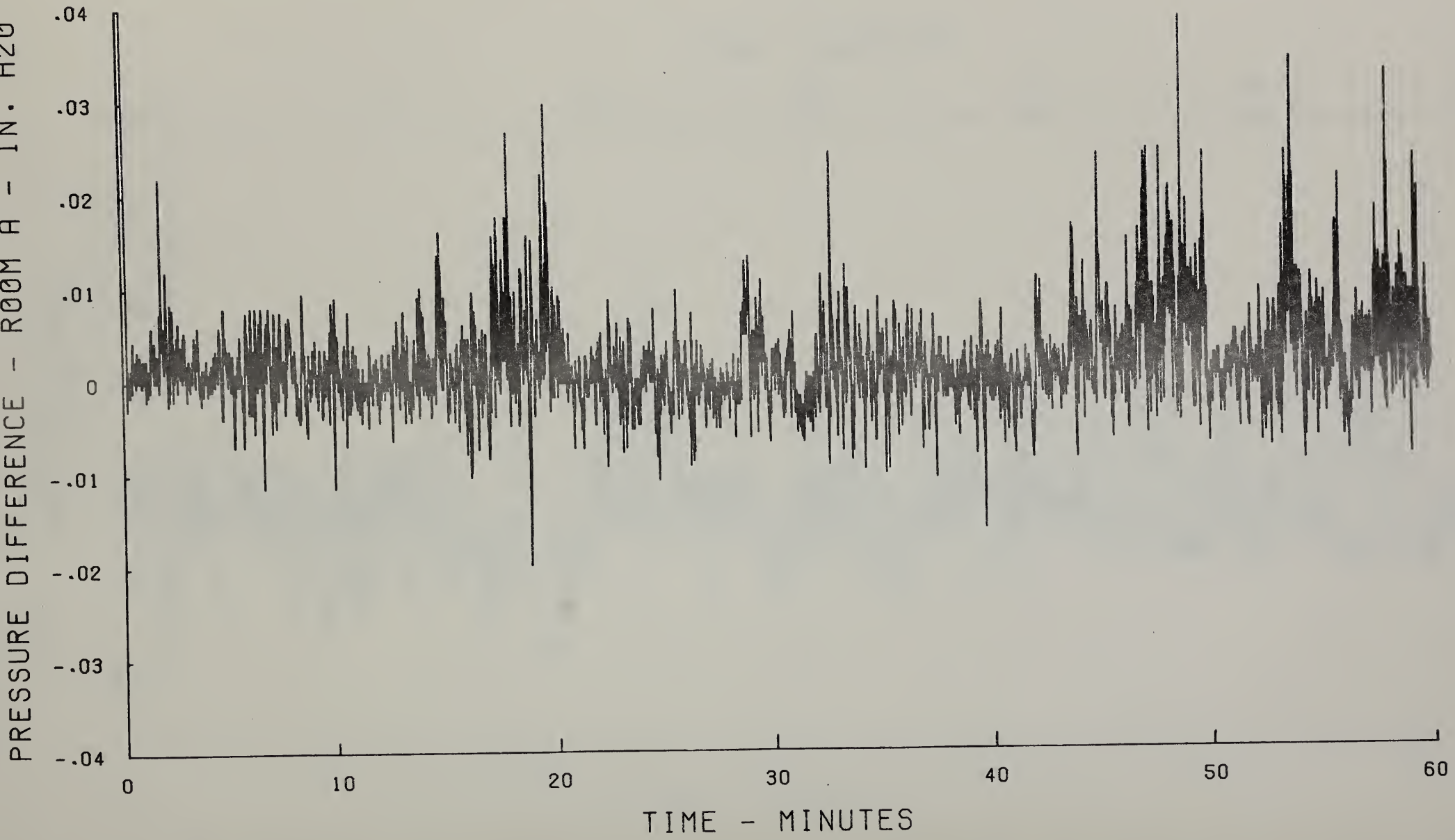
PRESSURE DIFFERENCE - ROOM A - IN. H20
.04
.03
.02
.01
0
-.01
-.02
-.03
-.04
0
10
20
30
40
50
60
TIME - MINUTES

Figure 20

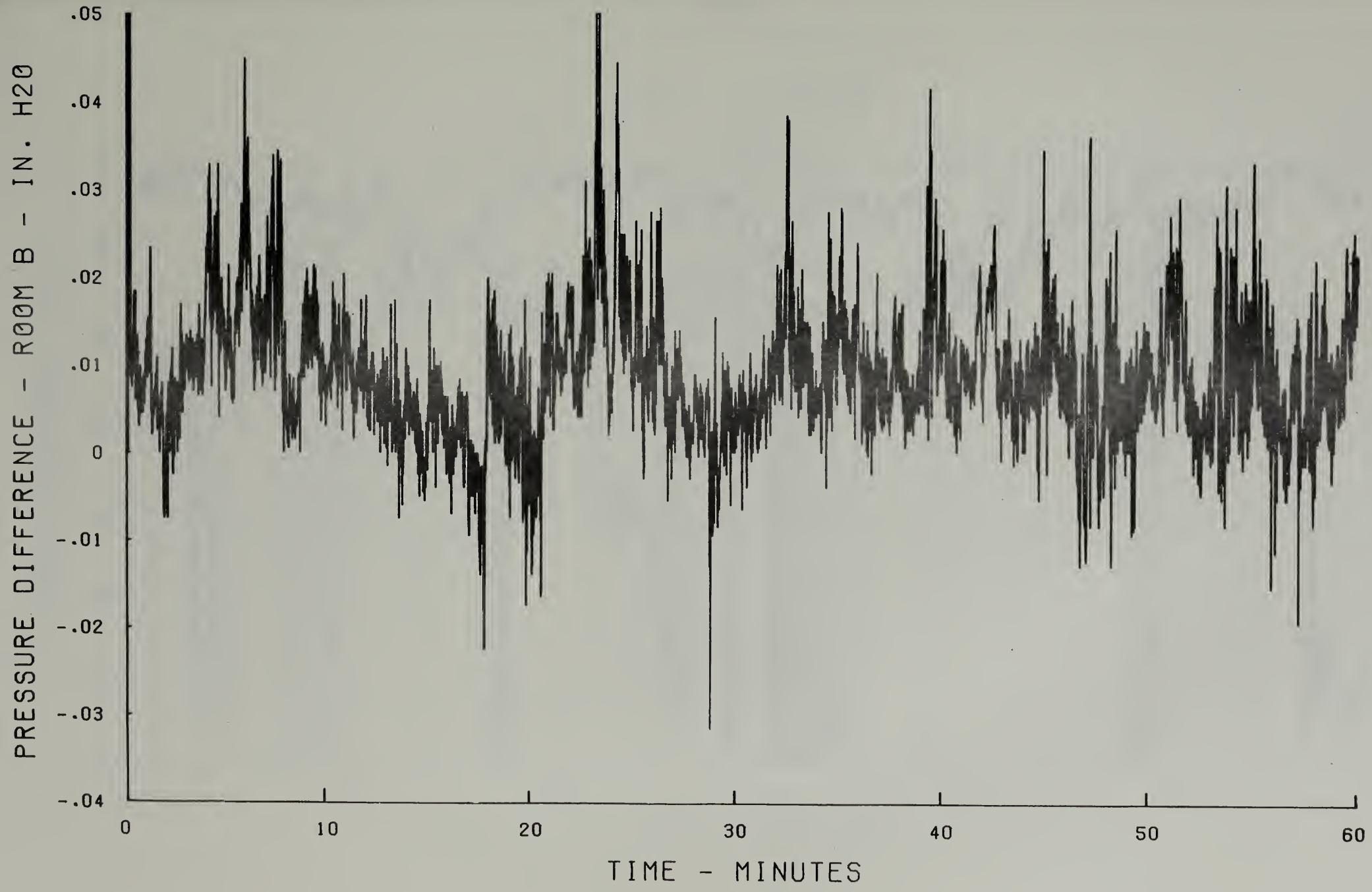
PRESSURE DIFFERENCE - ROOM B - IN. H20
.05
.04
.03
.02
.01
0
-.01
-.02
-.03
-.04
0
10
20
30
40
50
60
TIME - MINUTES

Figure 21


WIND VELOCITY - MPH
30
25
20
15
10
5
0
0
10
20
30
40
50
60
TIME - MINUTES

Figure 22

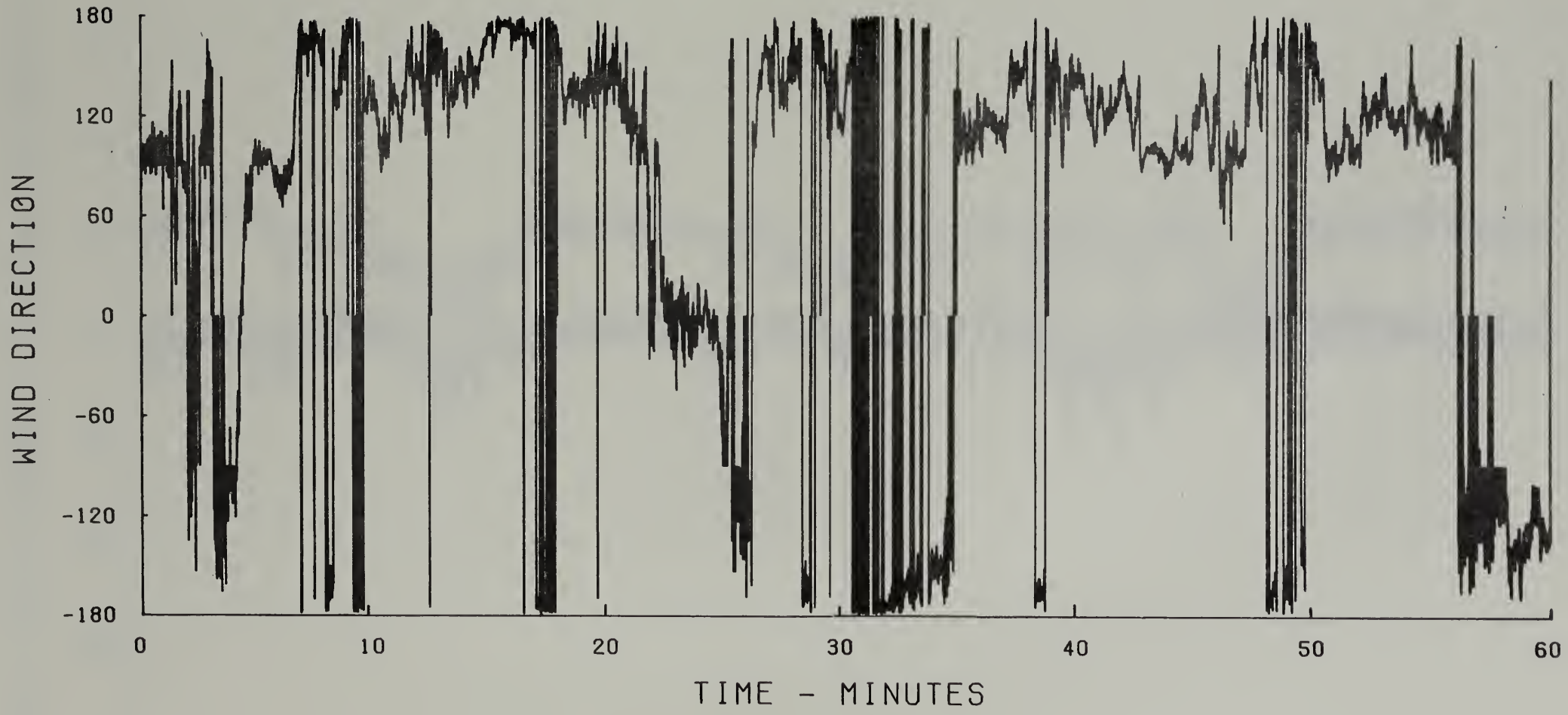
180
120
60
0
-60
-120
-180
WIND DIRECTION
0
10
20
30
40
50
60
TIME - MINUTES

Figure 23

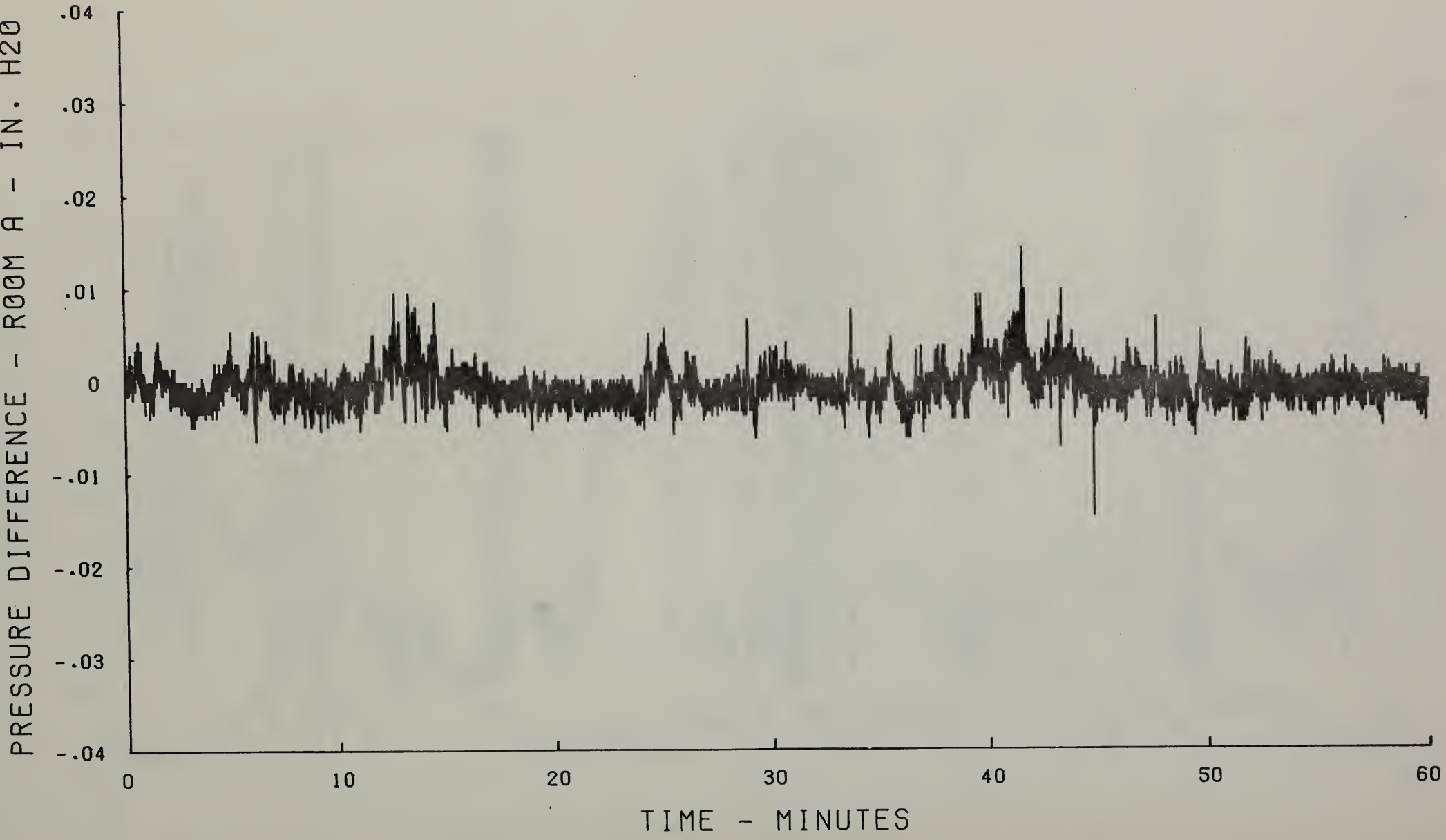
PRESSURE DIFFERENCE - ROOM A - IN. H20
.04
.03
.02
.01
0
-.01
-.02
-.03
-.04
0
10
20
30
40
50
60
TIME - MINUTES

Figure 24

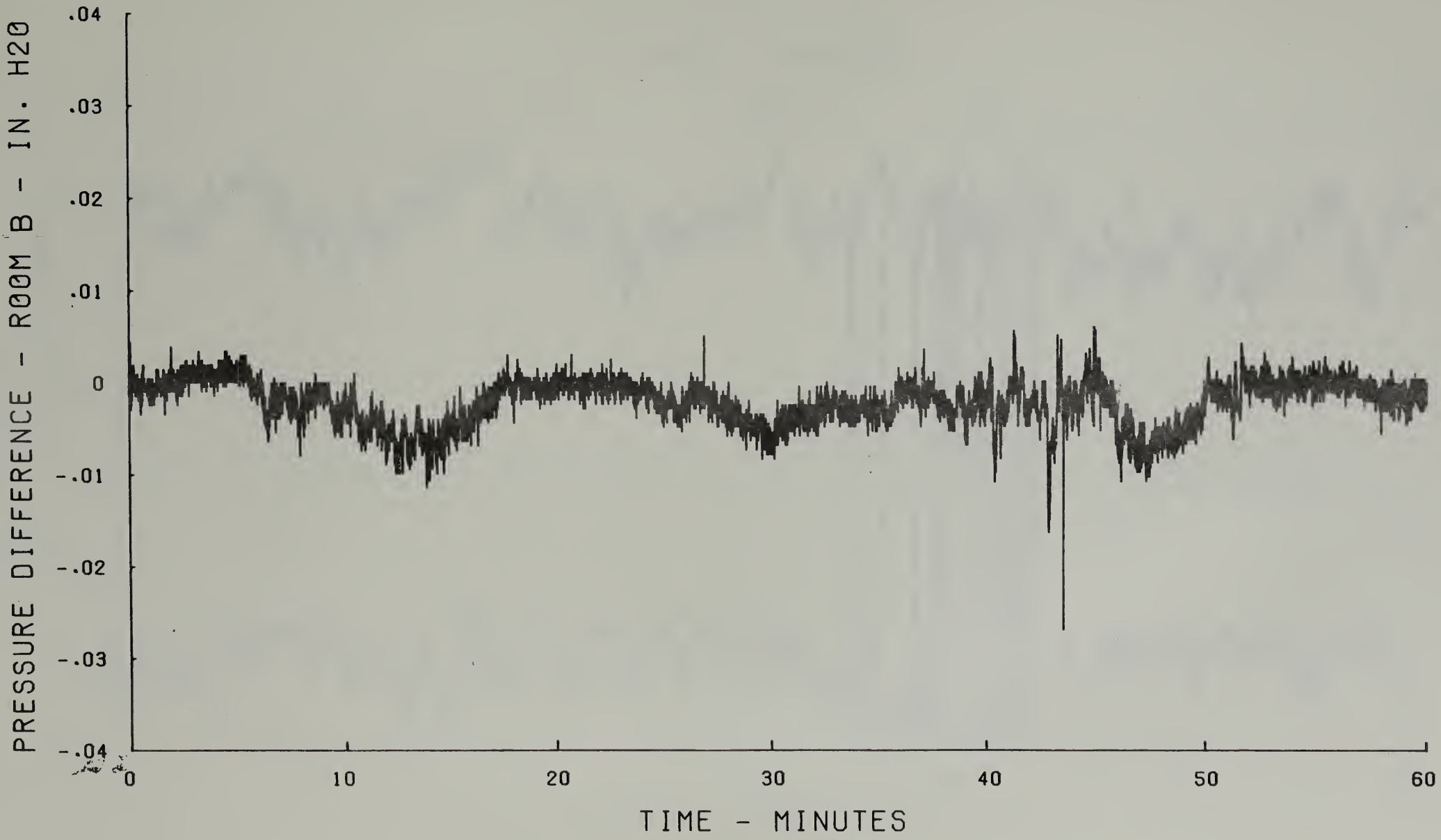
PRESSURE DIFFERENCE - ROOM B - IN. H20
.04
.03
.02
.01
0
-.01
-.02
-.03
-.04
0
10
20
30
40
50
60
TIME - MINUTES

Figure 25

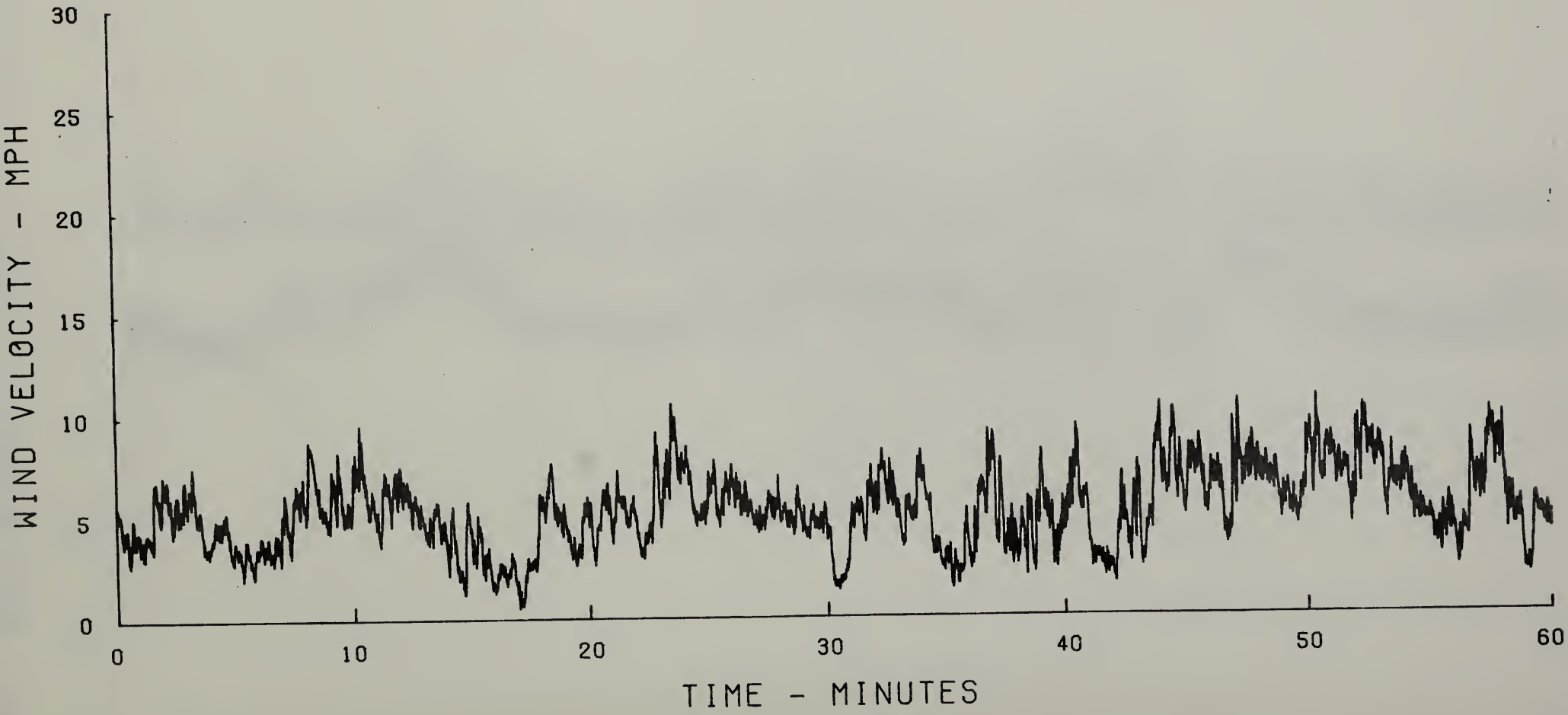
WIND VELOCITY - MPH
30
25
20
15
10
5
0
0
10
20
30
40
50
60
TIME - MINUTES

Figure 26

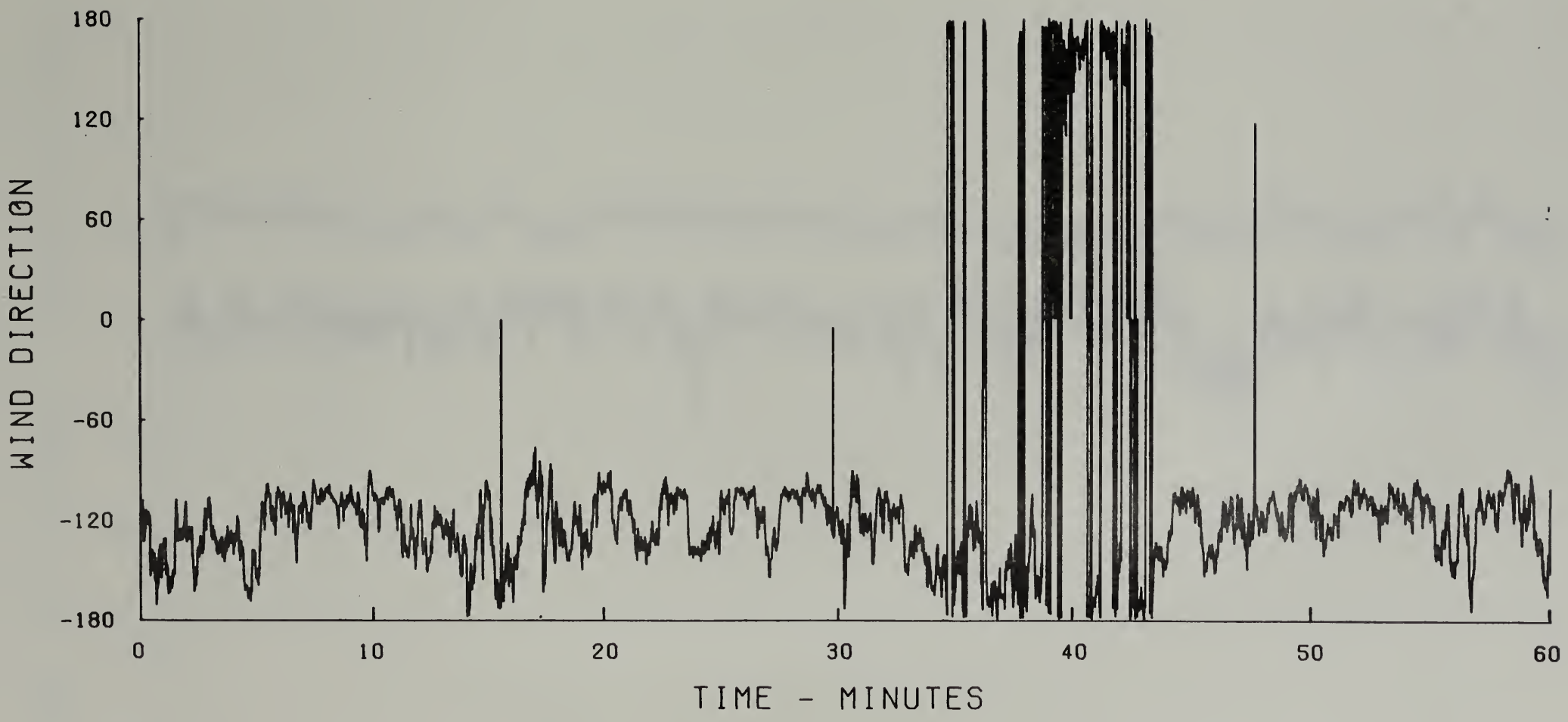
180
120
60
0
-60
-120
-180
WIND DIRECTION
0
10
20
30
40
50
60
TIME - MINUTES

Figure 27

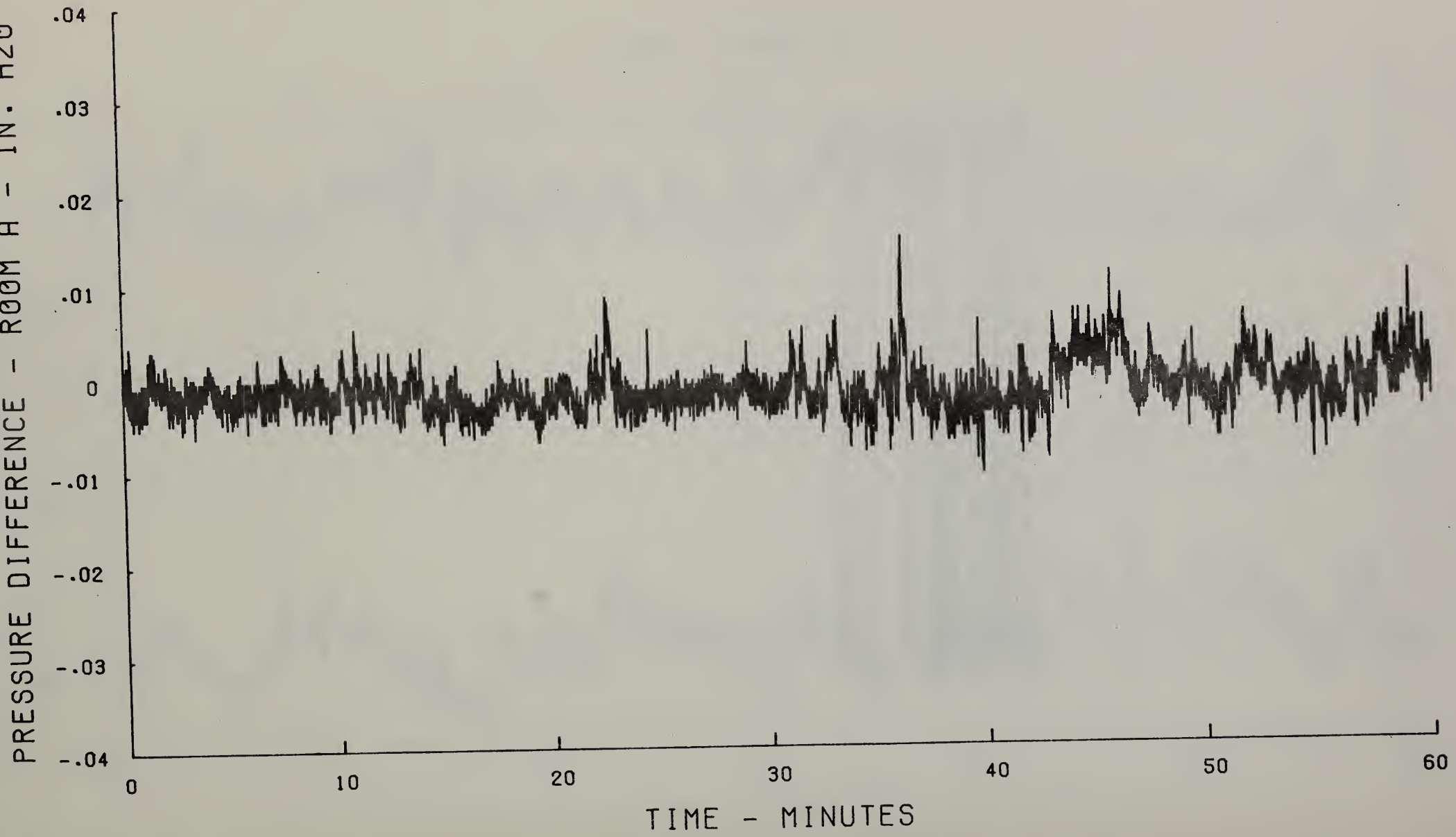
PRESSURE DIFFERENCE - ROOM A - IN. H20
.04
.03
.02
.01
0
-.01
-.02
-.03
-.04
0
10
20
30
40
50
60
TIME - MINUTES

Figure 28

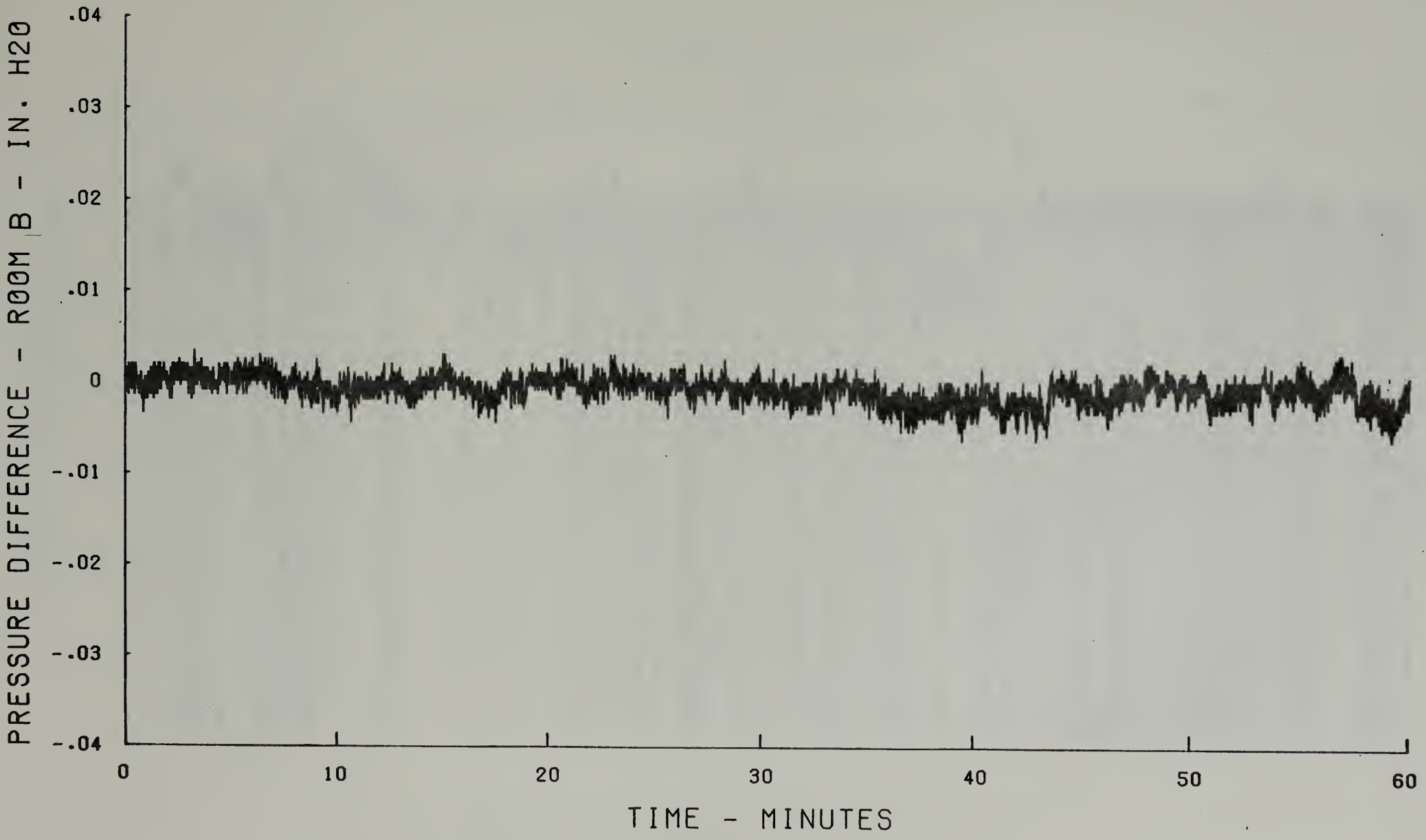
PRESSURE DIFFERENCE - ROOM B - IN. H20
.04
.03
.02
.01
0
-.01
-.02
-.03
-.04
0
10
20
30
40
50
60
TIME - MINUTES

Figure 29

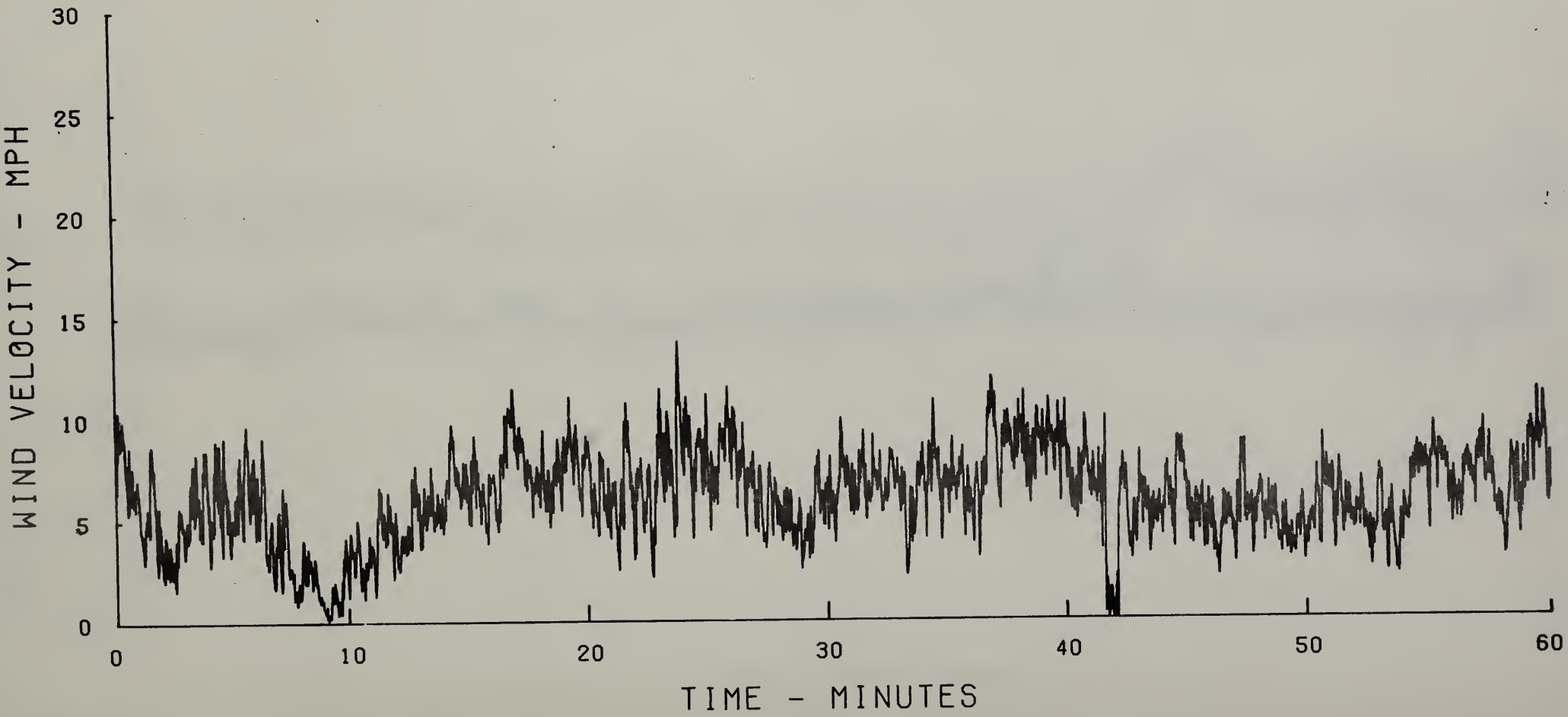
WIND VELOCITY - MPH
30
25
20
15
10
5
0
0
10
20
30
40
50
60
TIME - MINUTES

Figure 30

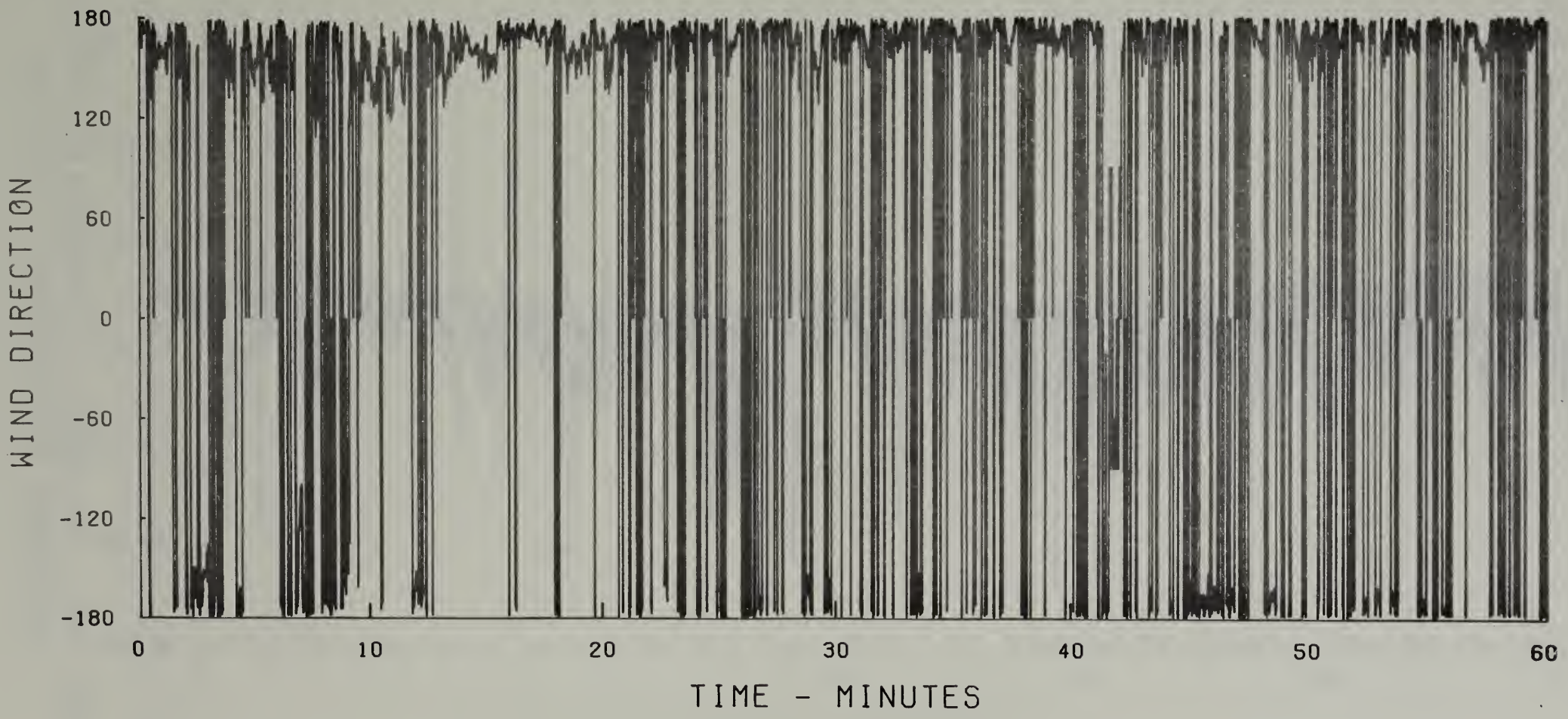
180
120
60
0
-60
-120
-180
WIND DIRECTION
0
10
20
30
40
50
60
TIME - MINUTES

Figure 31

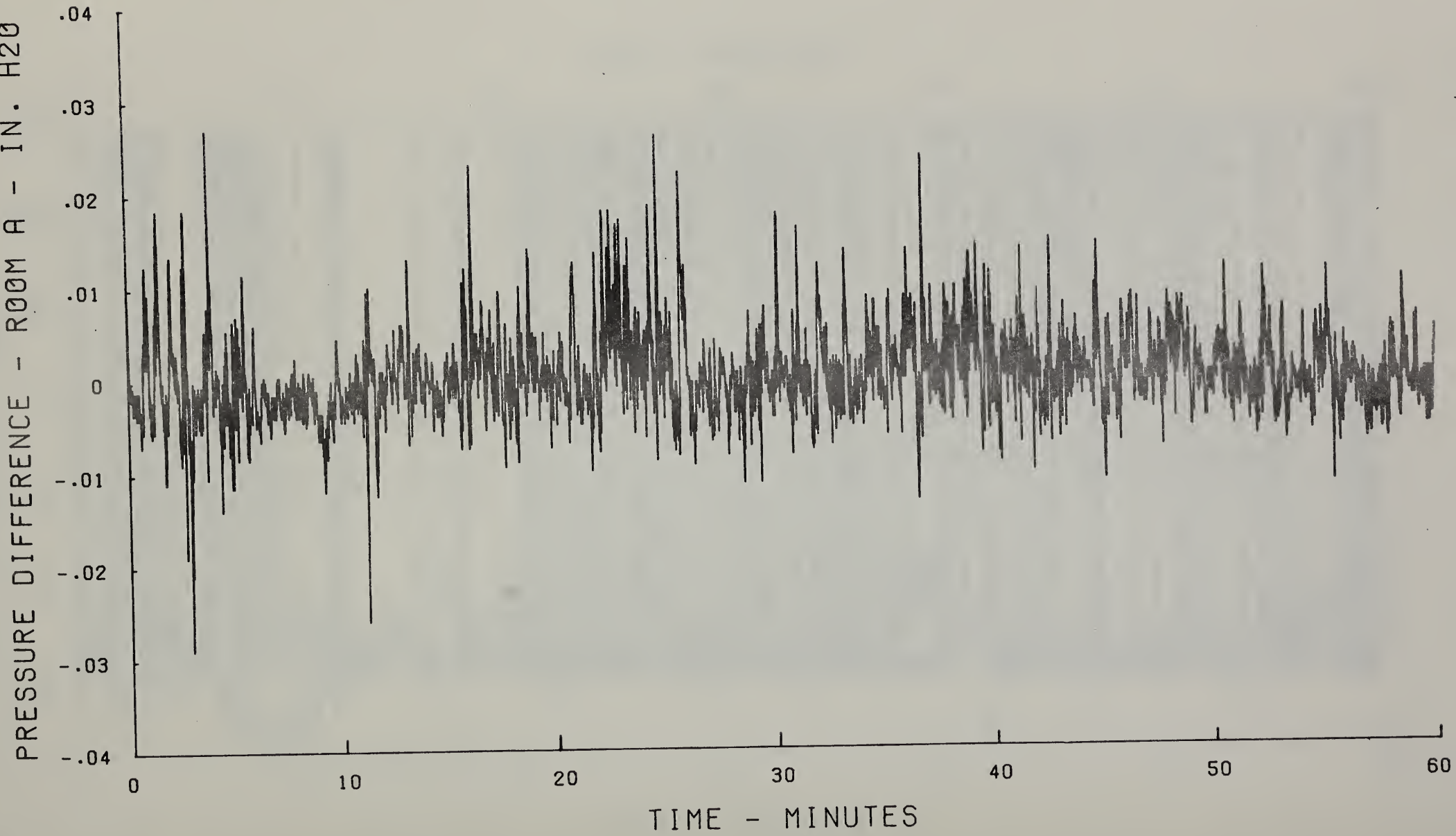
PRESSURE DIFFERENCE - R00M A - IN. H20
.04
.03
.02
.01
0
-.01
-.02
-.03
-.04
0
10
20
30
40
50
60
TIME - MINUTES

Figure 32

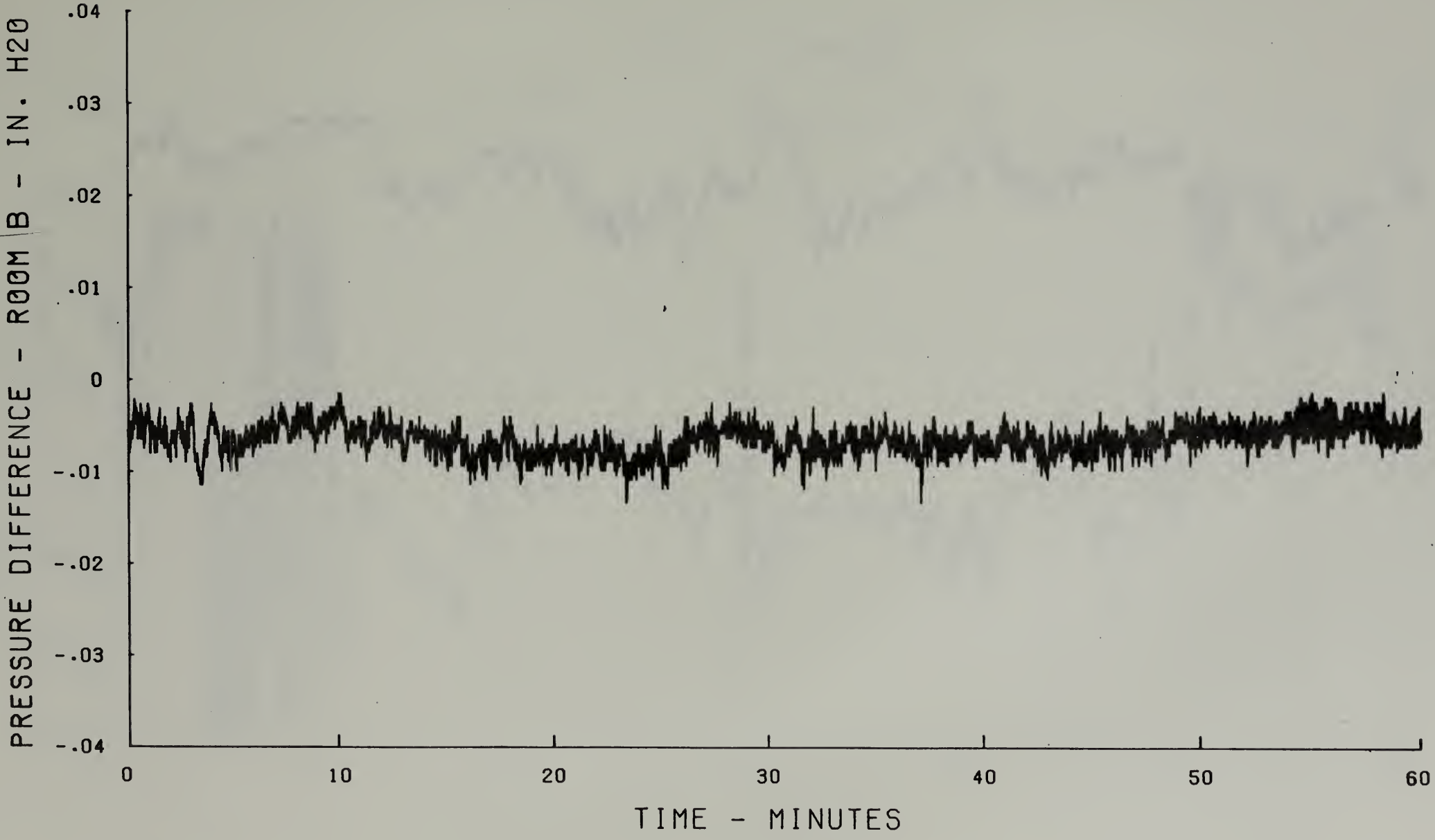
PRESSURE DIFFERENCE - ROOM B - IN. H20
.04
.03
.02
.01
0
-.01
-.02
-.03
-.04
0
10
20
30
40
50
60
TIME - MINUTES

Figure 33

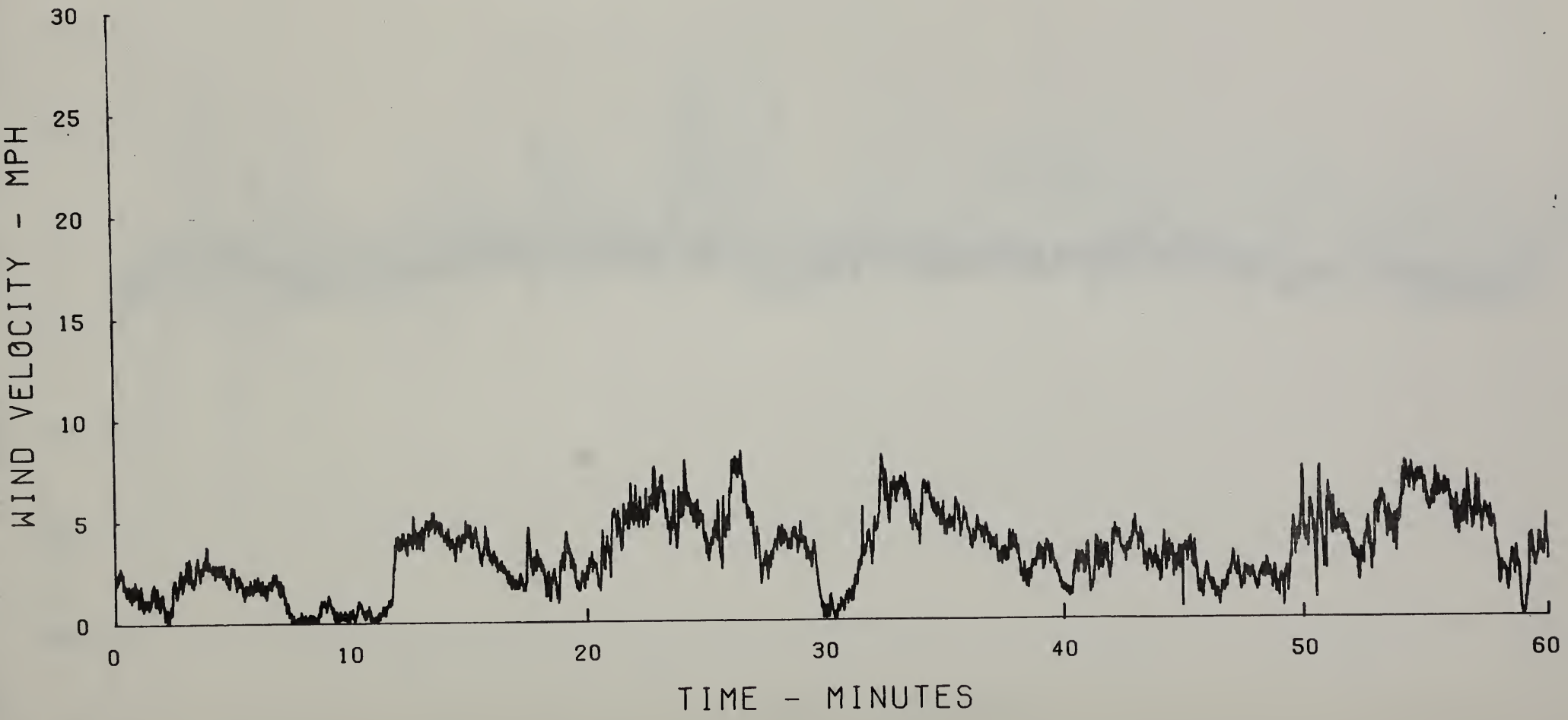
WIND VELOCITY - MPH
30
25
20
15
10
5
0
0
10
20
30
40
50
60
TIME - MINUTES

Figure 34

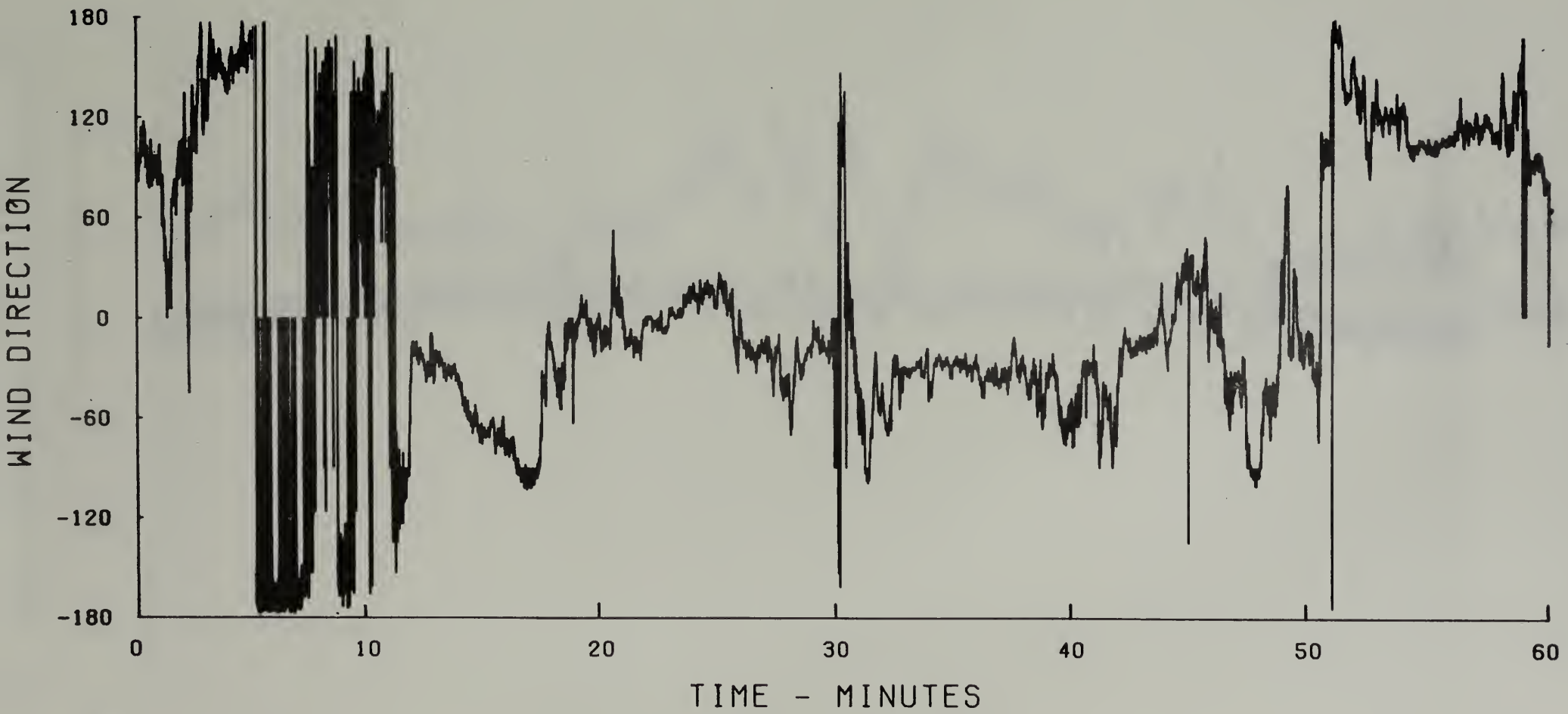
180
120
60
0
-60
-120
-180
WIND DIRECTION
0
10
20
30
40
50
60
TIME - MINUTES

Figure 35

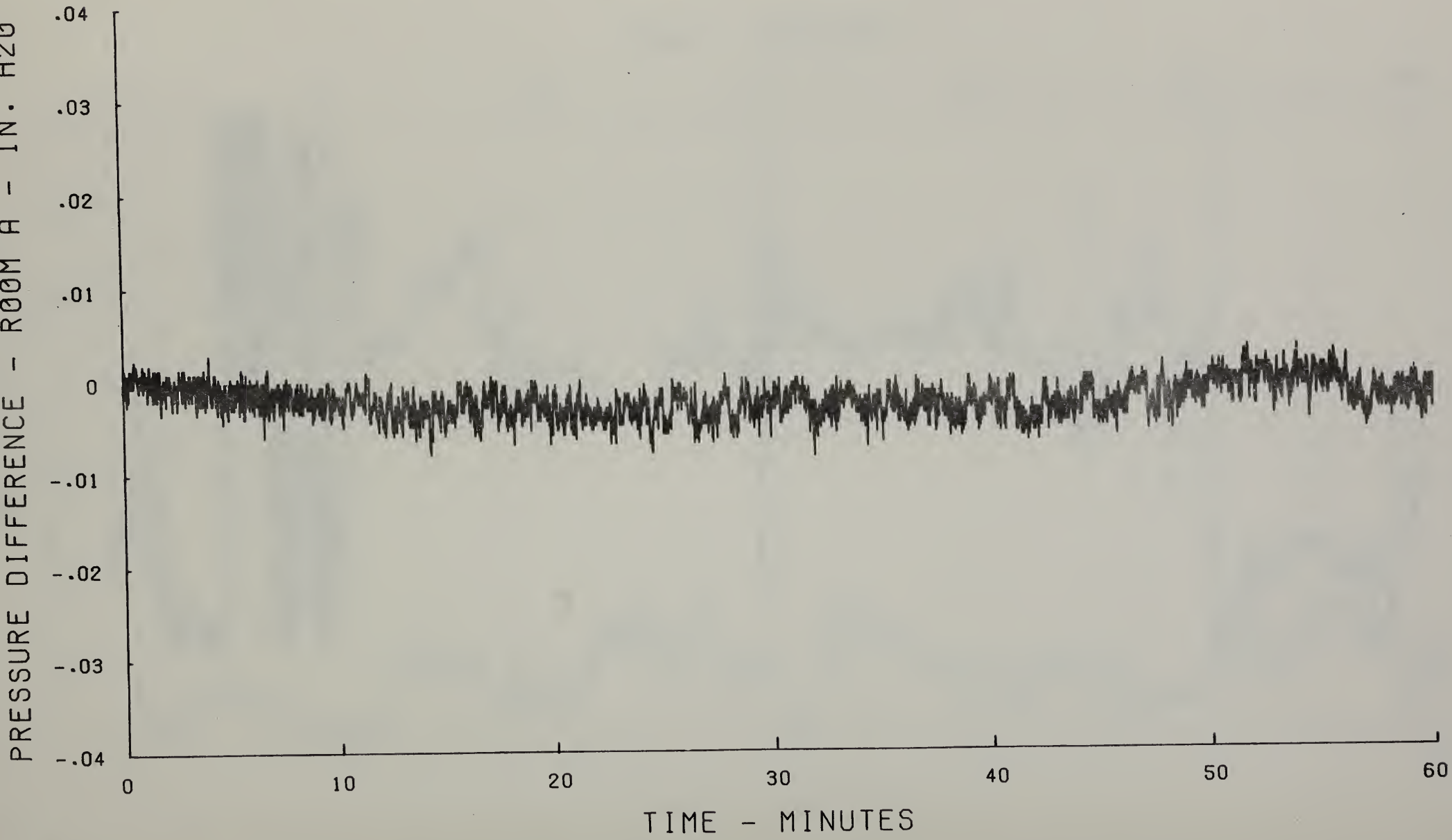
PRESSURE DIFFERENCE - ROOM A - IN. H20
.04
.03
.02
.01
0
-.01
-.02
-.03
-.04
0
10
20
30
40
50
60
TIME - MINUTES

Figure 36

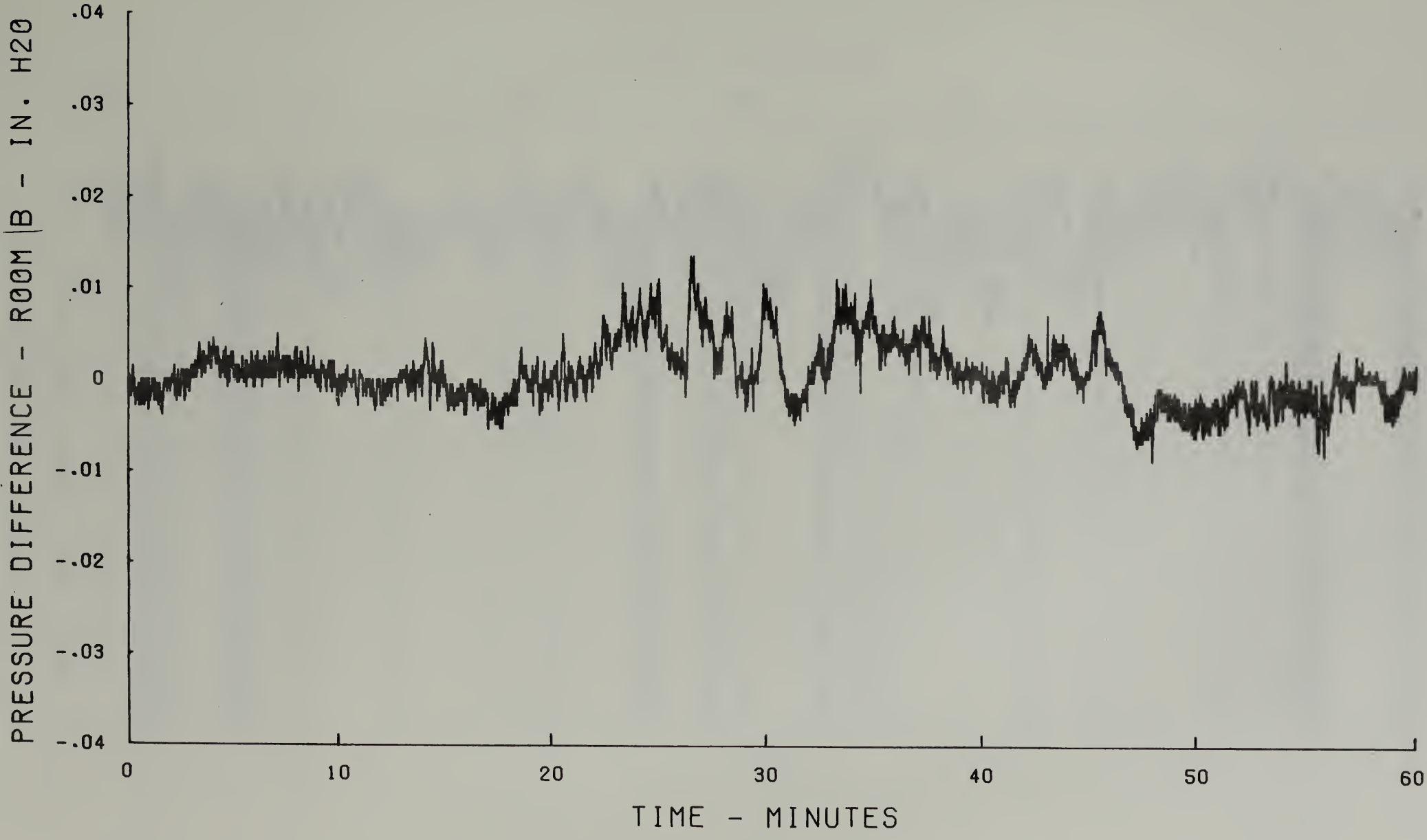
PRESSURE DIFFERENCE - ROOM B - IN. H20
.04
.03
.02
.01
0
-.01
-.02
-.03
-.04
0
10
20
30
40
50
60
TIME - MINUTES

Figure 37

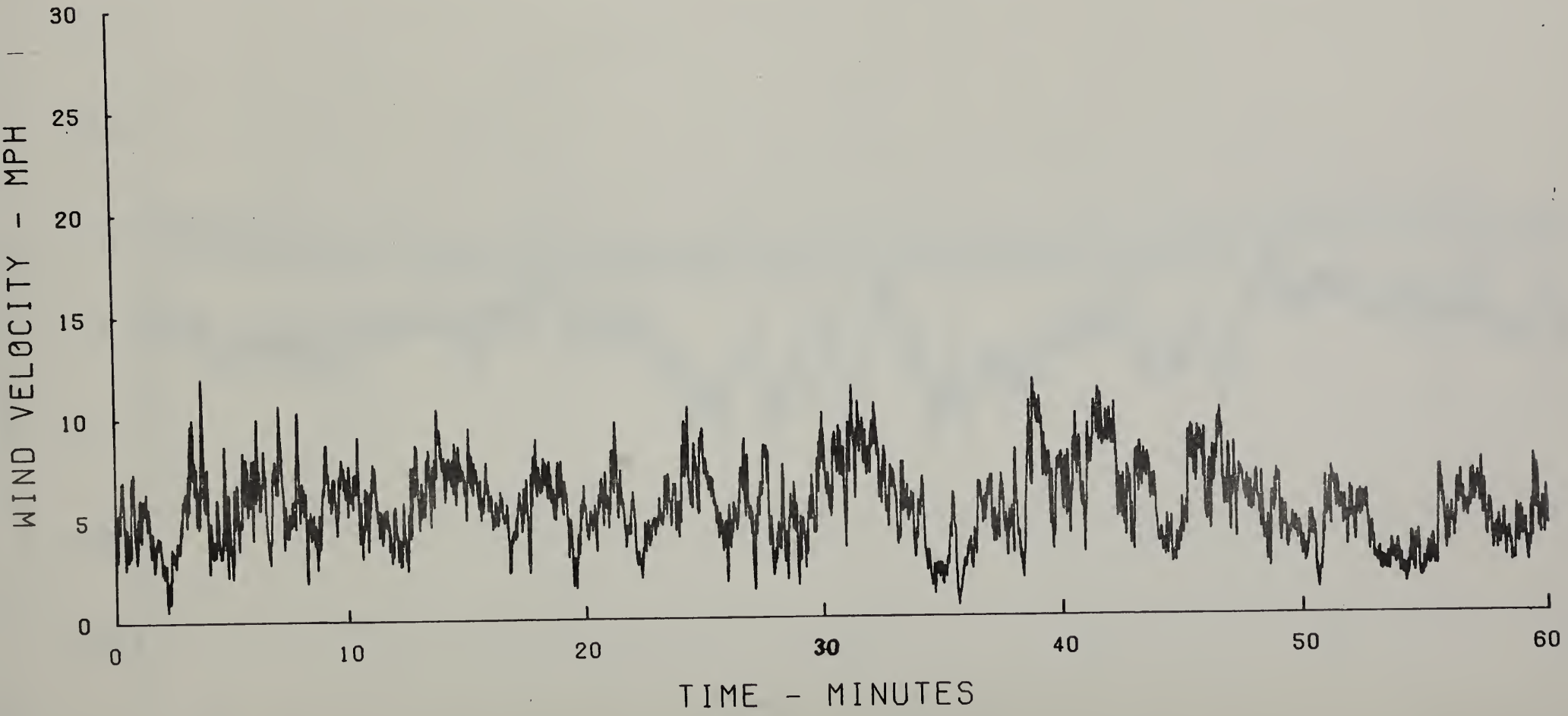
WIND VELOCITY - MPH
30
25
20
15
10
5
0
0
10
20
30
40
50
60
TIME - MINUTES

Figure 38

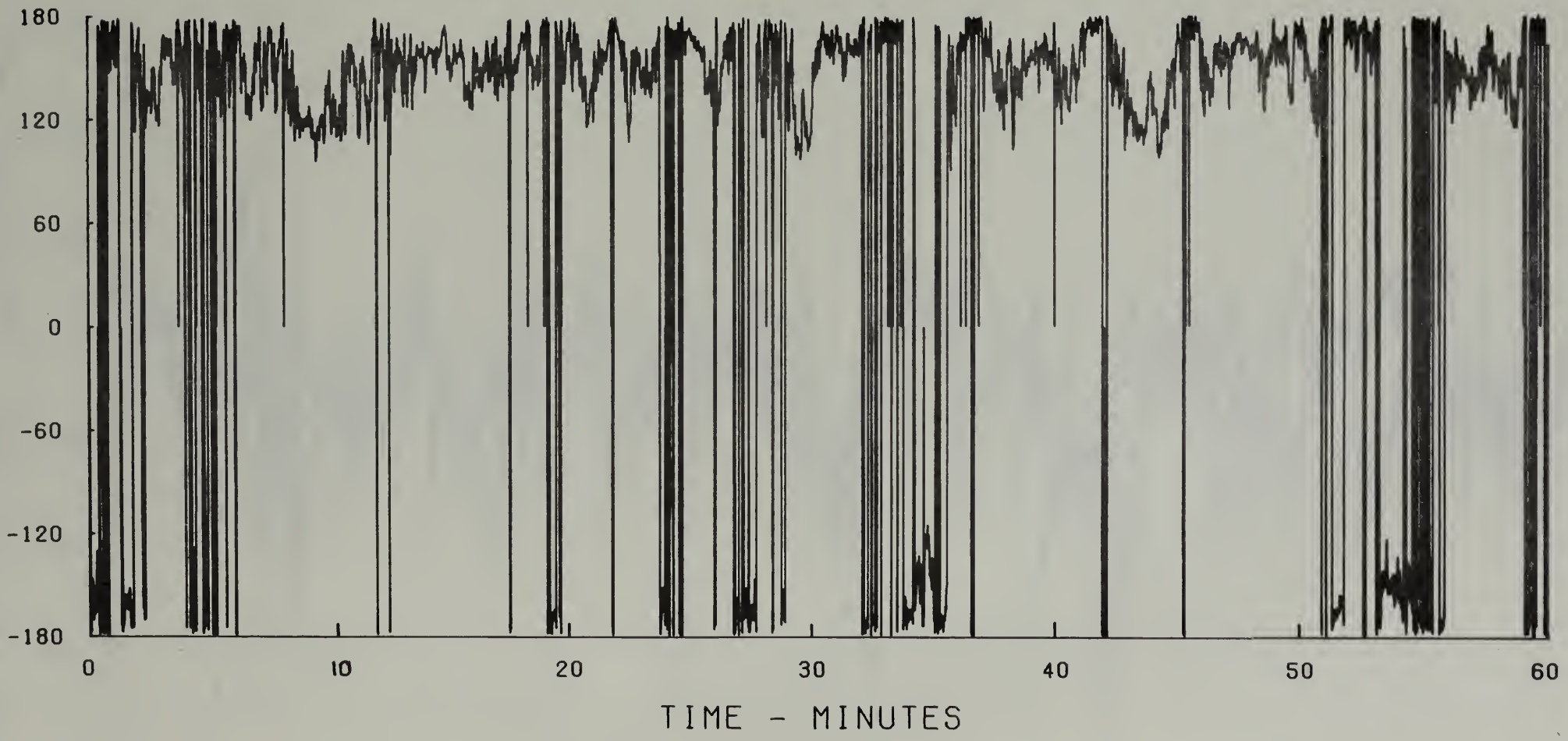
WIND DIRECTION
180
120
60
0
-60
-120
-180
0
10
20
30
40
50
60
TIME - MINUTES

Figure 39

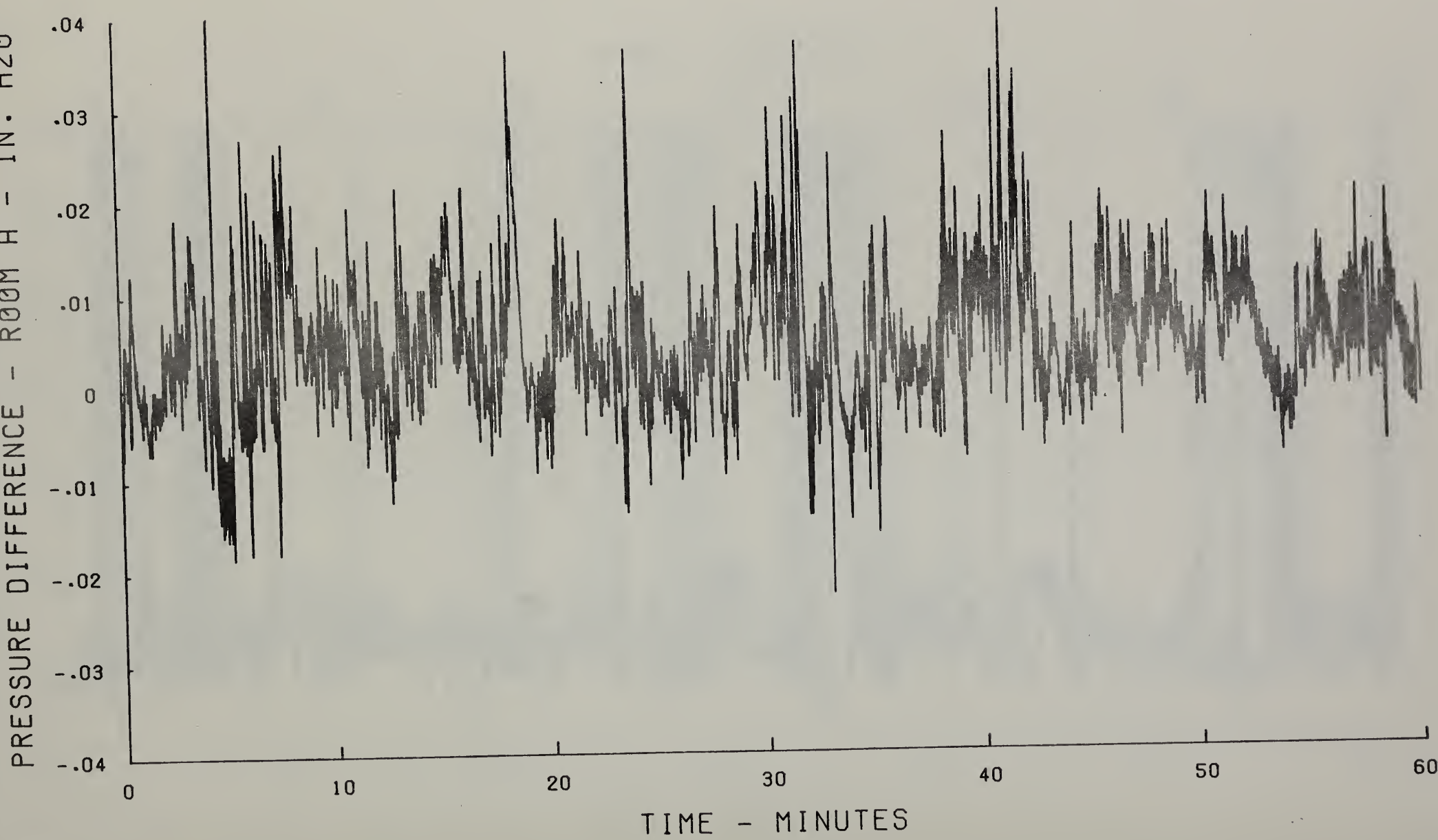
PRESSURE DIFFERENCE - ROOM A - IN. H20
.04
.03
.02
.01
0
-.01
-.02
-.03
-.04
0
10
20
30
40
50
60
TIME - MINUTES

Figure 40

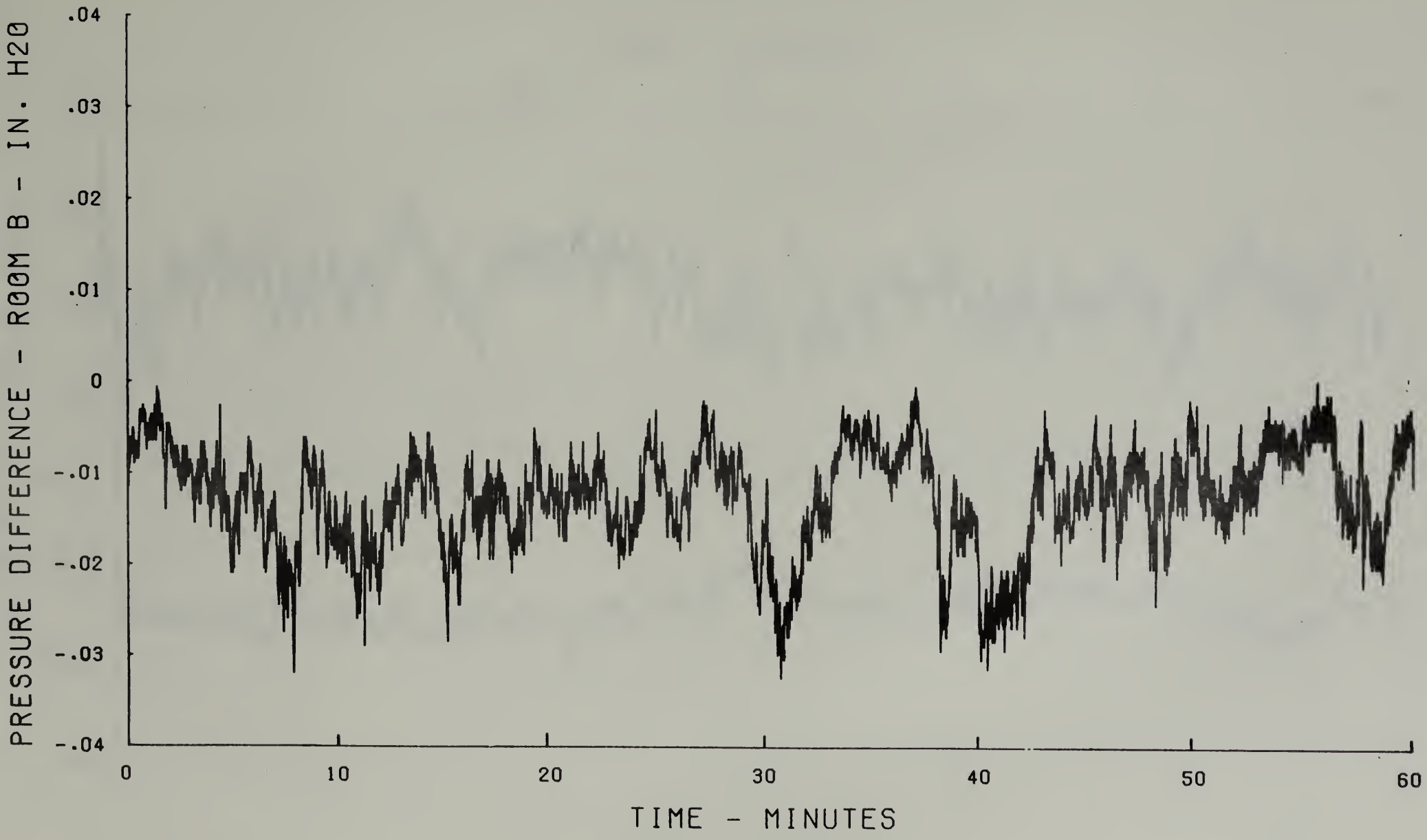
PRESSURE DIFFERENCE - ROOM B - IN. H20
.04
.03
.02
.01
0
-.01
-.02
-.03
-.04
0
10
20
30
40
50
60
TIME - MINUTES

Figure 41

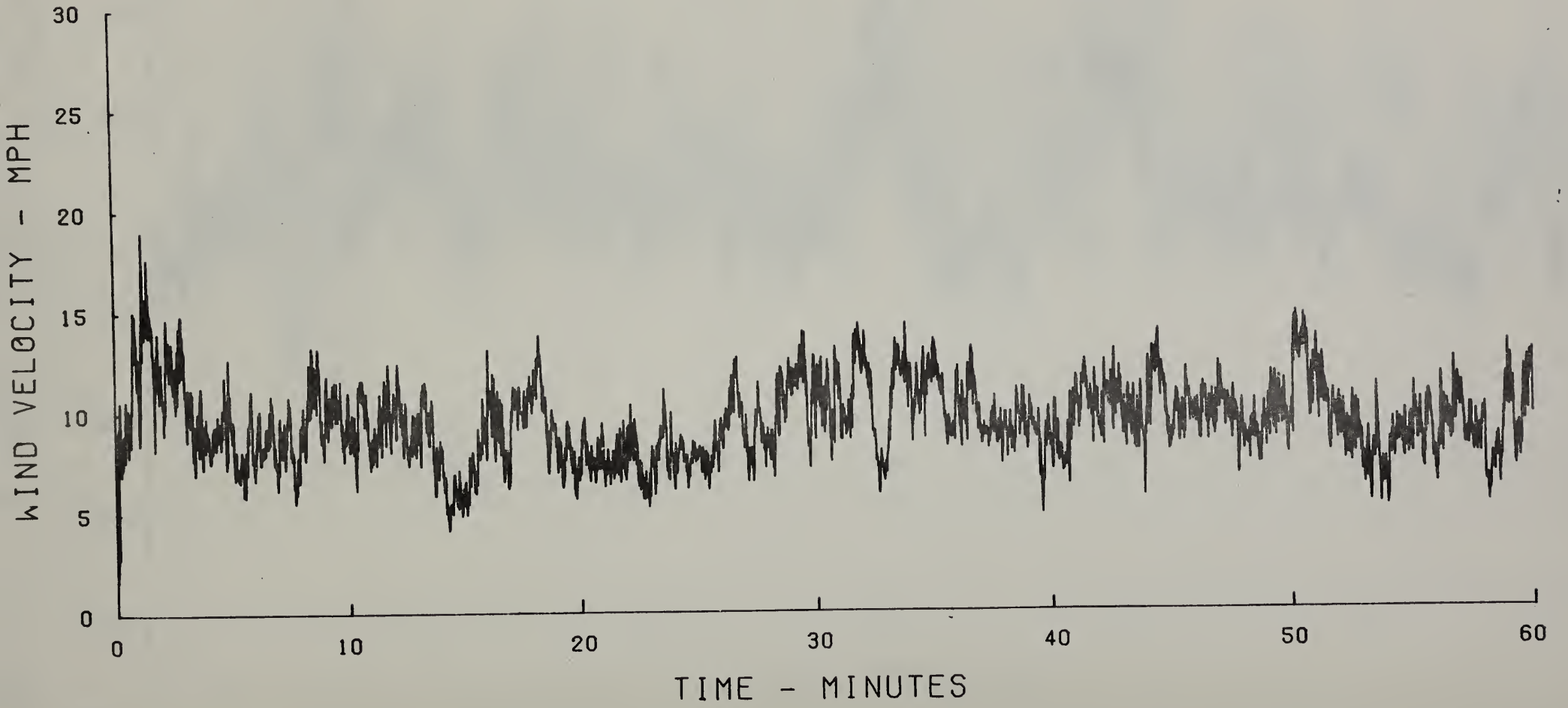
WIND VELOCITY - MPH
30
25
20
15
10
5
0
0
10
20
30
40
50
60
TIME - MINUTES

Figure 42

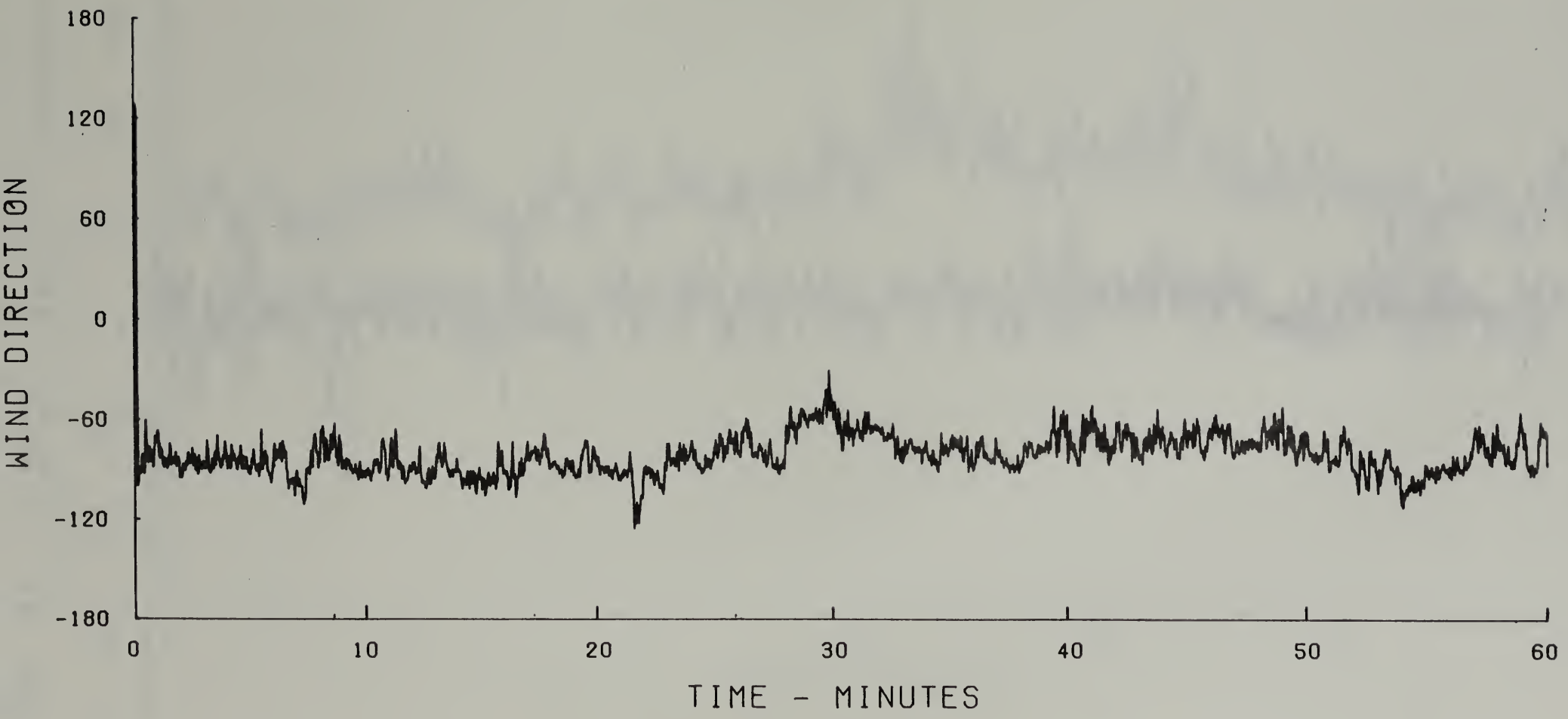
180
120
60
0
-60
-120
-180
WIND DIRECTION
0
10
20
30
40
50
60
TIME - MINUTES

Figure 43

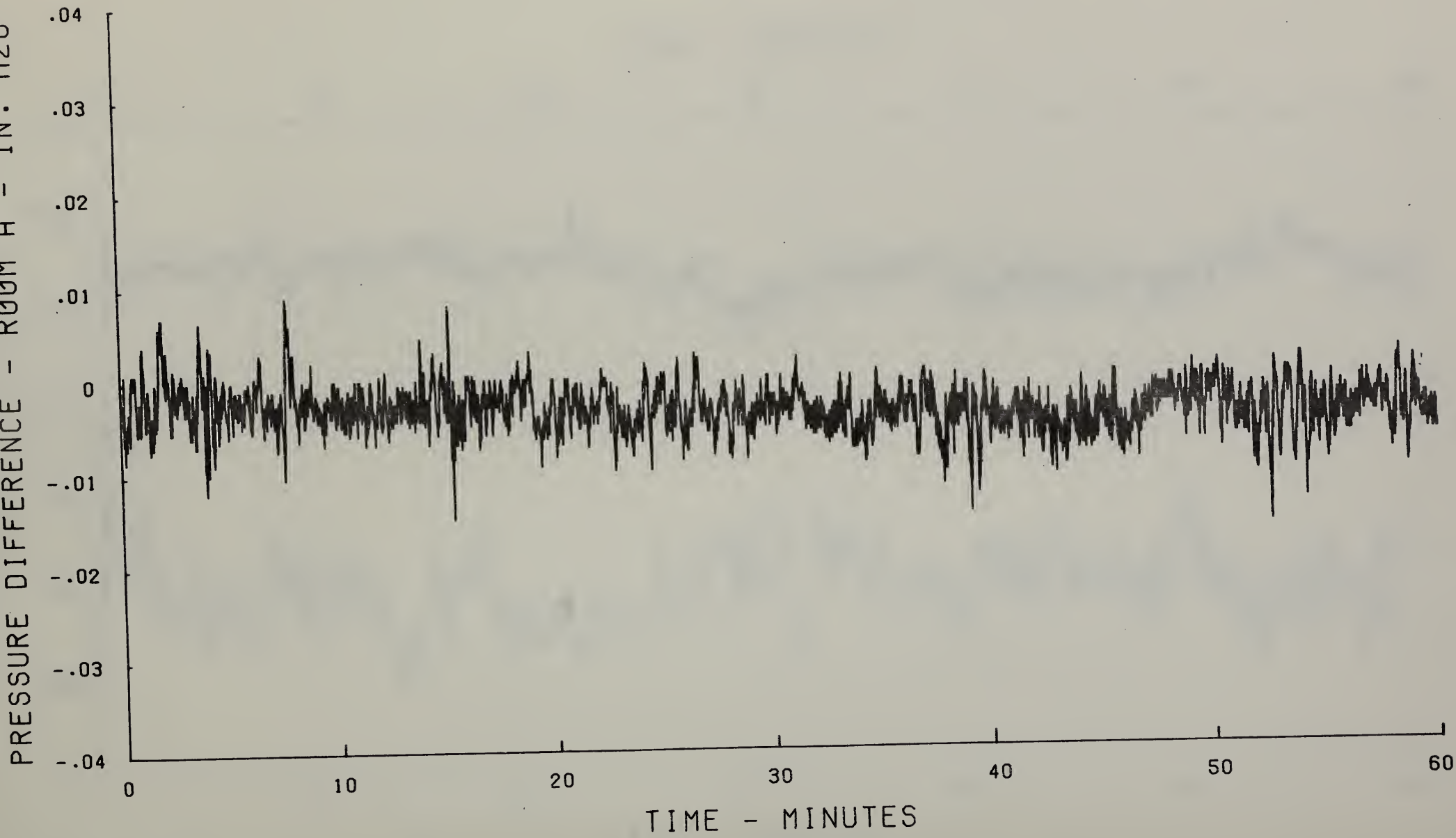
PRESSURE DIFFERENCE - ROOM A - IN. H20
.04
.03
.02
.01
0
-.01
-.02
-.03
-.04
0
10
20
30
40
50
60
TIME - MINUTES

Figure 44

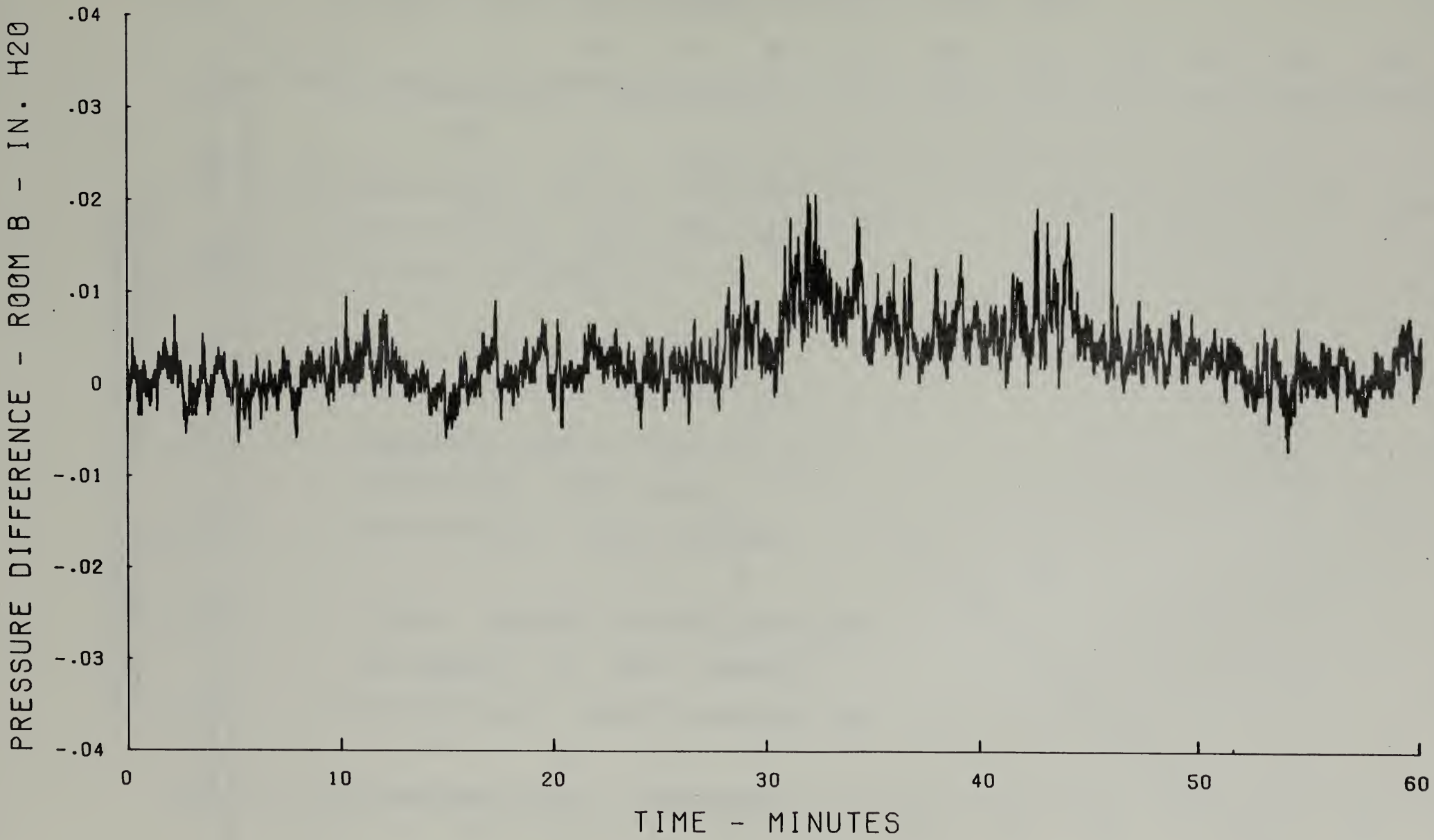
PRESSURE DIFFERENCE - ROOM B - IN. H20
.04
.03
.02
.01
0
-.01
-.02
-.03
-.04
0
10
20
30
40
50
60
TIME - MINUTES

Figure 45

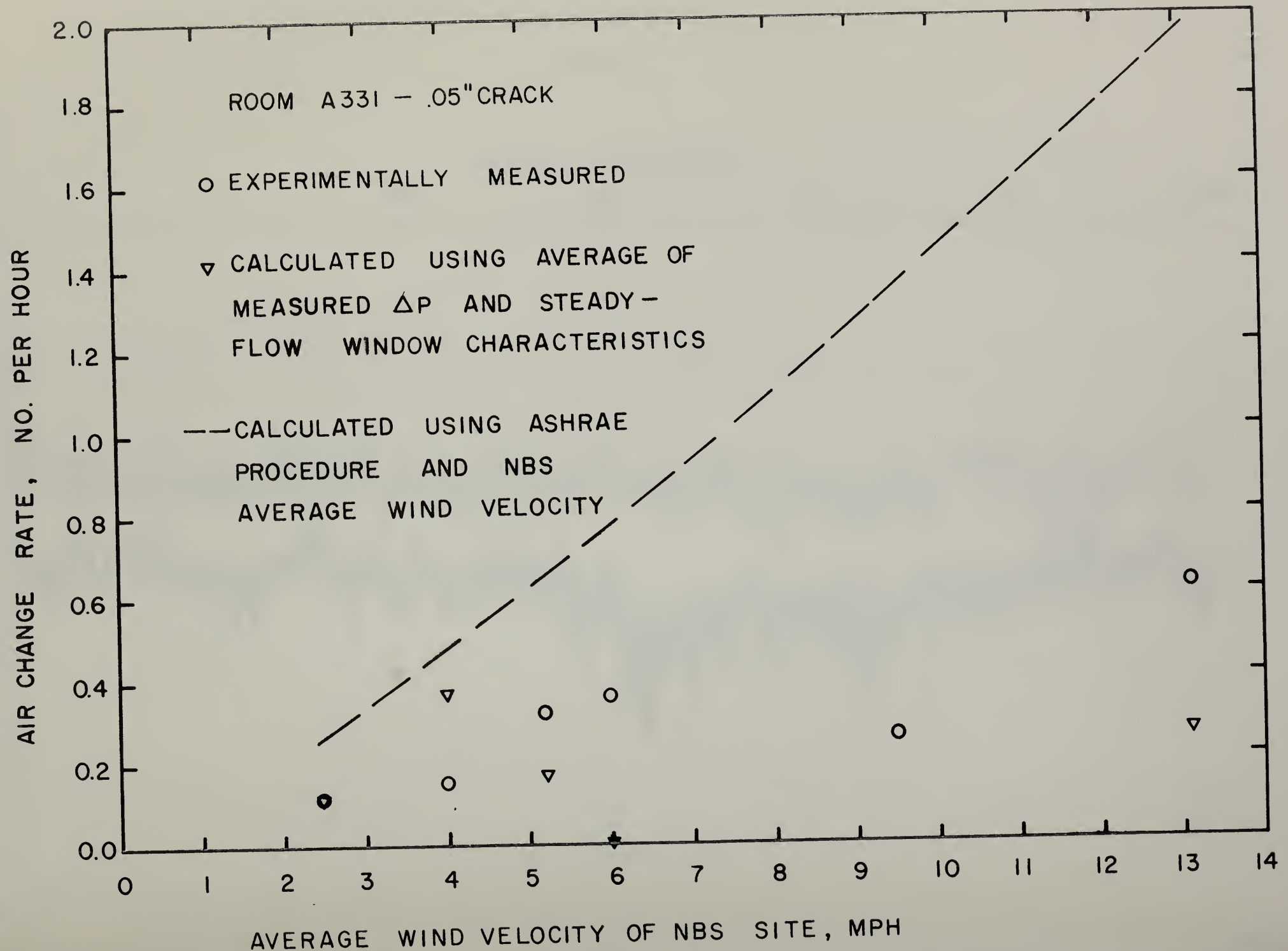
ROOM A331 – .05" CRACK
EXPERIMENTALLY MEASURED
CALCULATED USING AVERAGE OF MEASURED ΔP AND STEADY-FLOW WINDOW CHARACTERISTICS
CALCULATED USING ASHRAE PROCEDURE AND NBS AVERAGE WIND VELOCITY
AIR CHANGE RATE, NO. PER HOUR
AVERAGE WIND VELOCITY OF NBS SITE, MPH
2.0
1.8
1.6
1.4
1.2
1.0
0.8
0.6
0.4
0.2
0.0
0 1 2 3 4 5 6 7 8 9 10 11 12 13 14

Figure 46

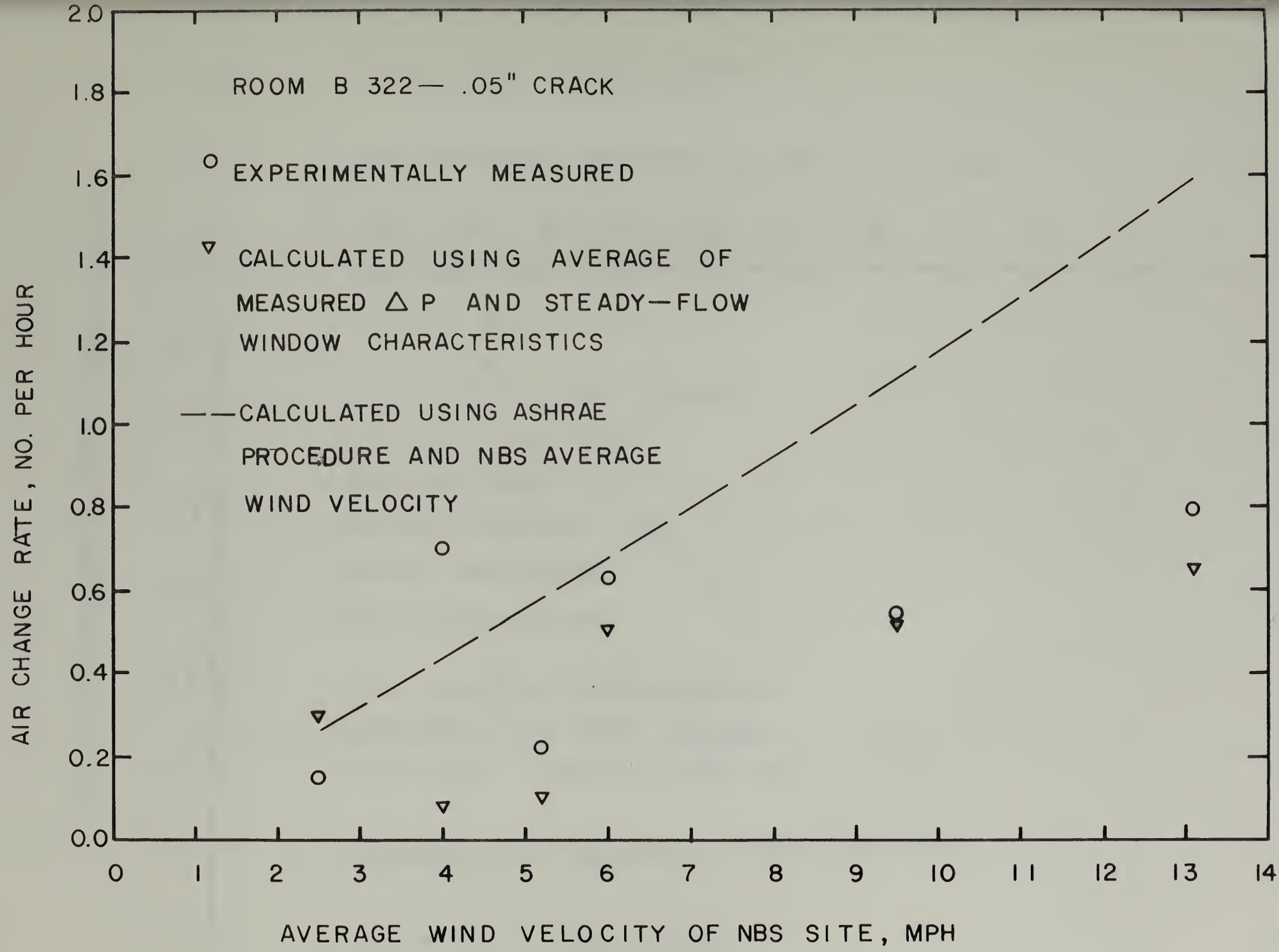
ROOM B 322— .05" CRACK
EXPERIMENTALLY MEASURED
CALCULATED USING AVERAGE OF MEASURED Δ P AND STEADY—FLOW WINDOW CHARACTERISTICS
——CALCULATED USING ASHRAE PROCEDURE AND NBS AVERAGE WIND VELOCITY
AIR CHANGE RATE, NO. PER HOUR
AVERAGE WIND VELOCITY OF NBS SITE, MPH
0.0
0.2
0.4
0.6
0.8
1.0
1.2
1.4
1.6
1.8
2.0
0
1
2
3
4
5
6
7
8
9
10
11
12
13
14

Figure 47

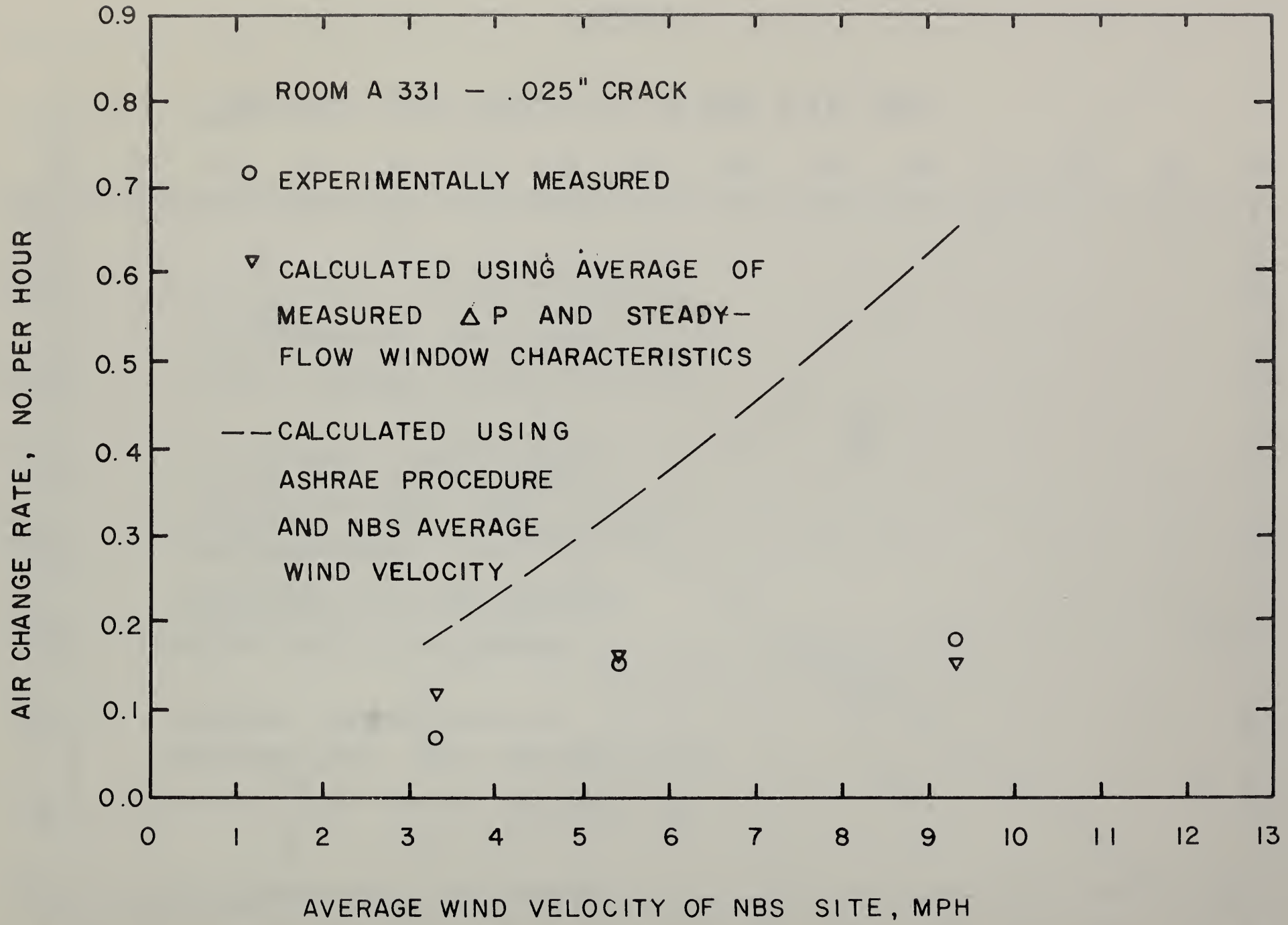
ROOM A 331 — .025" CRACK
EXPERIMENTALLY MEASURED
CALCULATED USING AVERAGE OF MEASURED ΔP AND STEADY-FLOW WINDOW CHARACTERISTICS
CALCULATED USING ASHRAE PROCEDURE AND NBS AVERAGE WIND VELOCITY
AIR CHANGE RATE, NO. PER HOUR
0.0
0.1
0.2
0.3
0.4
0.5
0.6
0.7
0.8
0.9
0
1
2
3
4
5
6
7
8
9
10
11
12
13
AVERAGE WIND VELOCITY OF NBS SITE, MPH

Figure 48

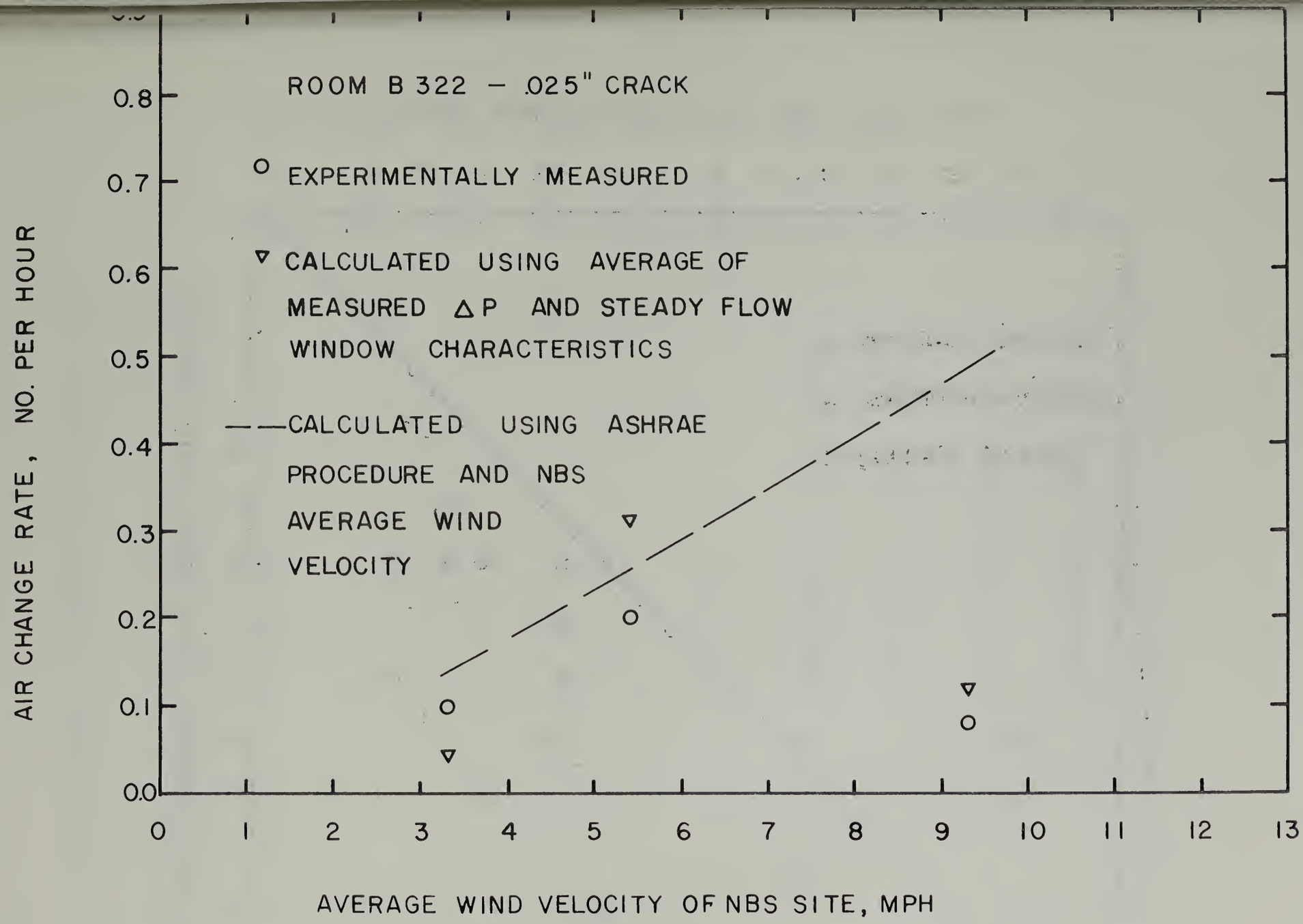
ROOM B 322 – .025" CRACK
EXPERIMENTALLY MEASURED
CALCULATED USING AVERAGE OF MEASURED ΔP AND STEADY FLOW WINDOW CHARACTERISTICS
——CALCULATED USING ASHRAE PROCEDURE AND NBS AVERAGE WIND VELOCITY
AIR CHANGE RATE, NO. PER HOUR
0.0
0.1
0.2
0.3
0.4
0.5
0.6
0.7
0.8
0
1
2
3
4
5
6
7
8
9
10
11
12
13
AVERAGE WIND VELOCITY OF NBS SITE, MPH

Figure 49

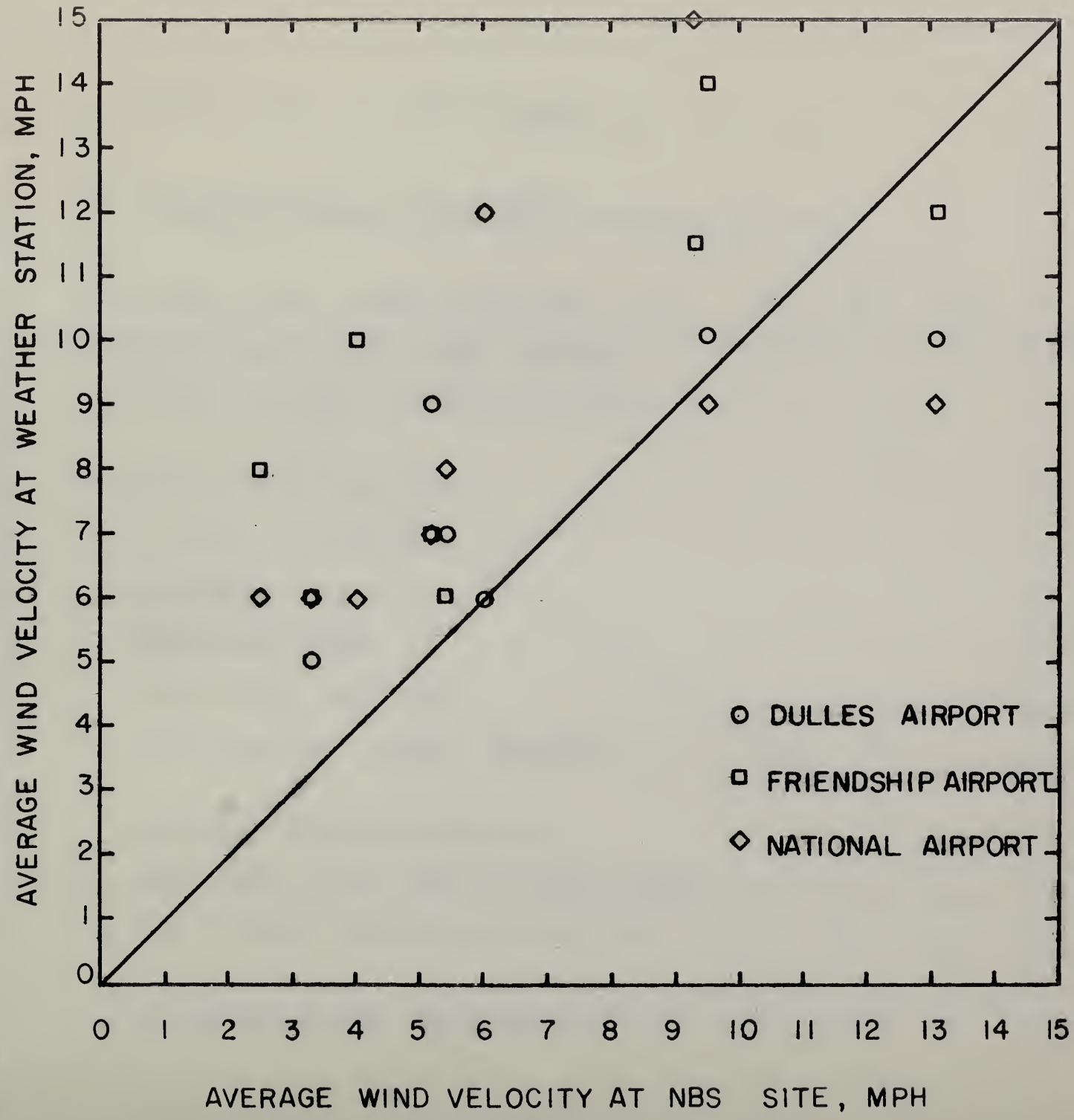
AVERAGE WIND VELOCITY AT WEATHER STATION, MPH
AVERAGE WIND VELOCITY AT NBS SITE, MPH
0 1 2 3 4 5 6 7 8 9 10 11 12 13 14 15
DULLES AIRPORT
FRIENDSHIP AIRPORT
NATIONAL AIRPORT

Figure 50

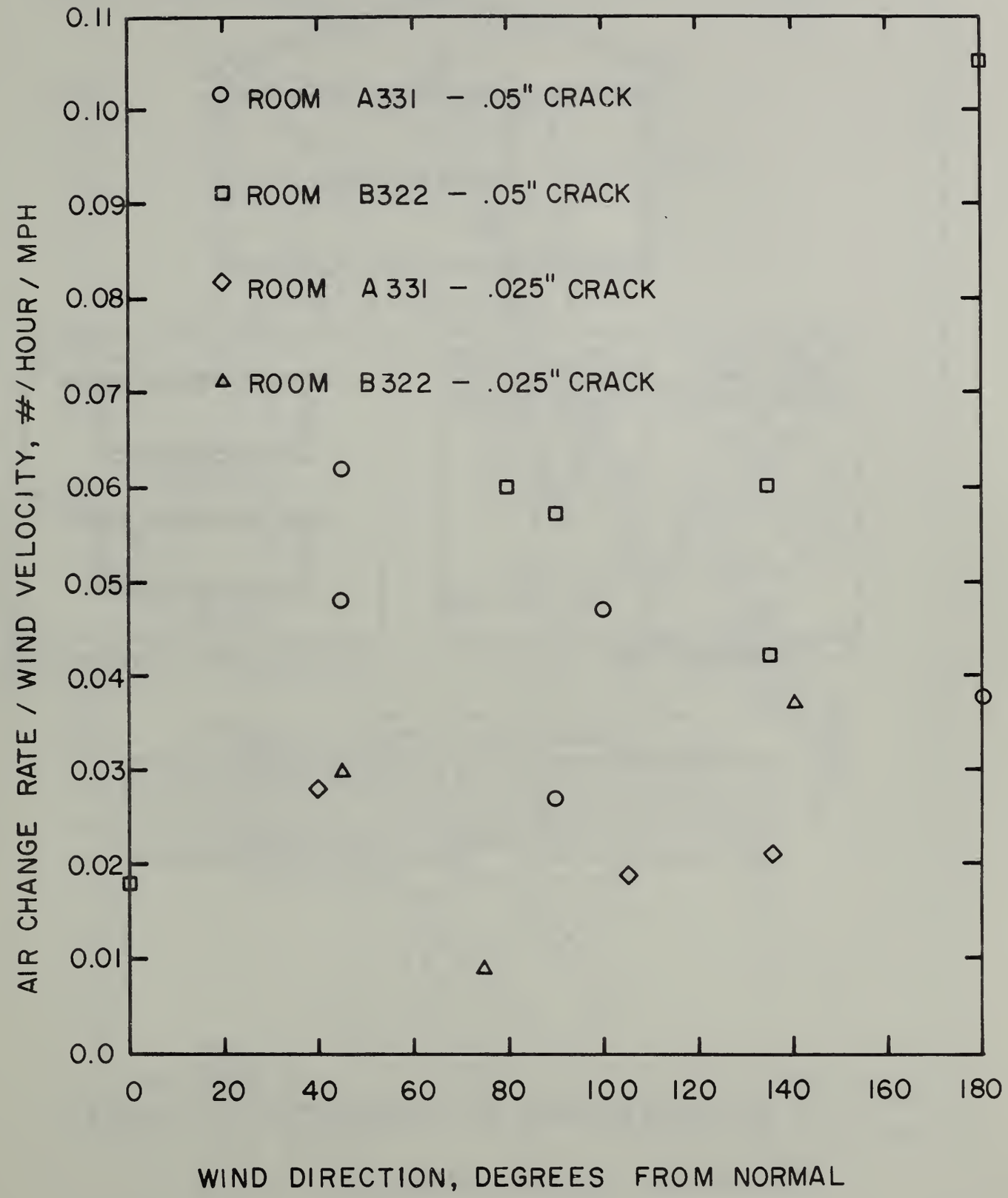
ROOM A331 – .05" CRACK
ROOM B322 – .05" CRACK
ROOM A331 – .025" CRACK
ROOM B322 – .025" CRACK
AIR CHANGE RATE / WIND VELOCITY, #/HOUR/MPH
0.11
0.10
0.09
0.08
0.07
0.06
0.05
0.04
0.03
0.02
0.01
0.0
0
20
40
60
80
100
120
140
160
180
WIND DIRECTION, DEGREES FROM NORMAL

Figure 51

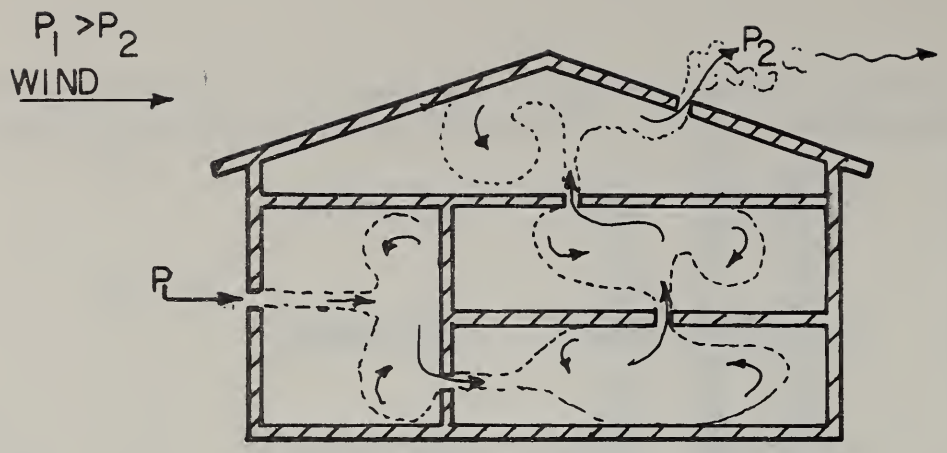

A - THROUGH FLOW $P_1 > P_2$

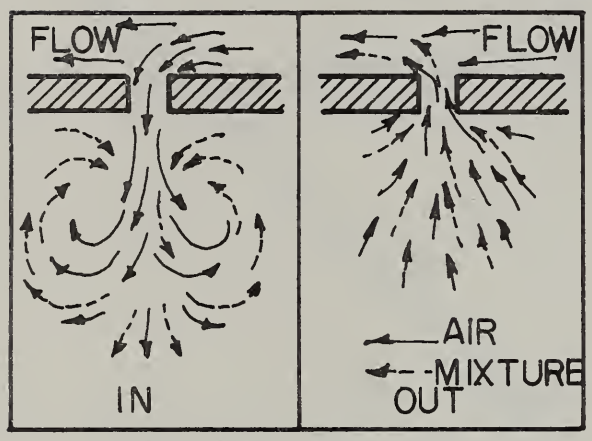

B - PULSATION. ONE HOLE

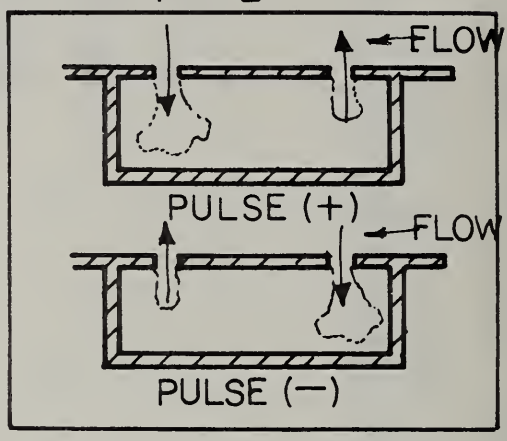

C — PULSATION. TWO HOLES

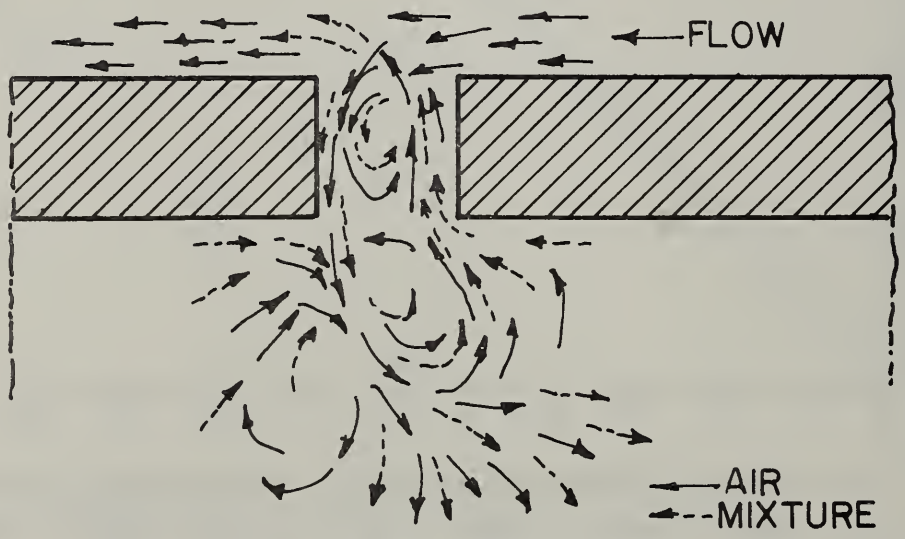

D - AIR EXCHANGE BY PENETRATION OF EDDIES

Figure 52

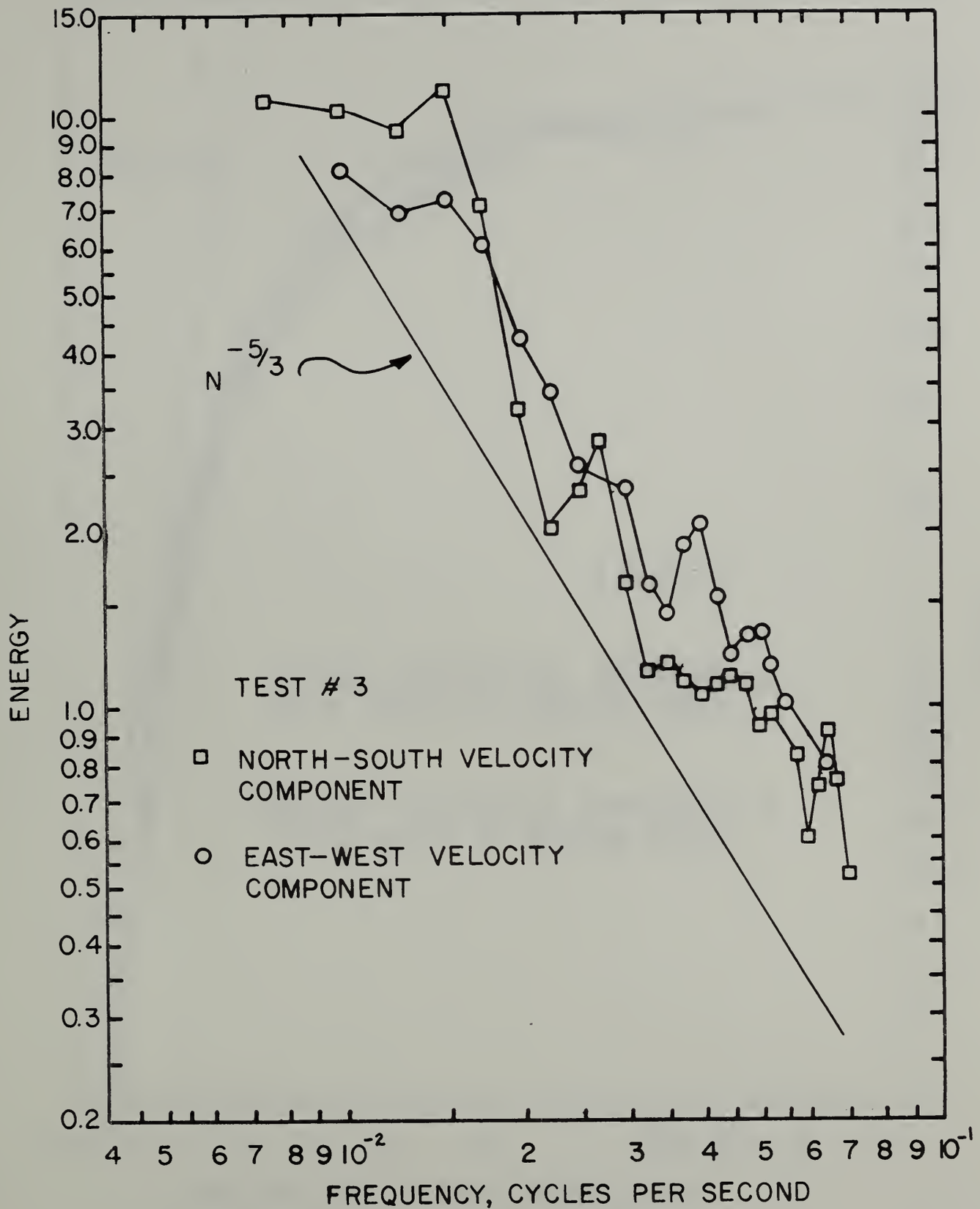
15.0
10.0
9.0
8.0
7.0
6.0
5.0
4.0
3.0
2.0
1.0
0.9
0.8
0.7
0.6
0.5
0.4
0.3
0.2
ENERGY
N^-5/3
TEST # 3
NORTH-SOUTH VELOCITY COMPONENT
EAST-WEST VELOCITY COMPONENT
4 5 6 7 8 9 10^-2 2 3 4 5 6 7 8 9 10^-1
FREQUENCY, CYCLES PER SECOND

Figure 53

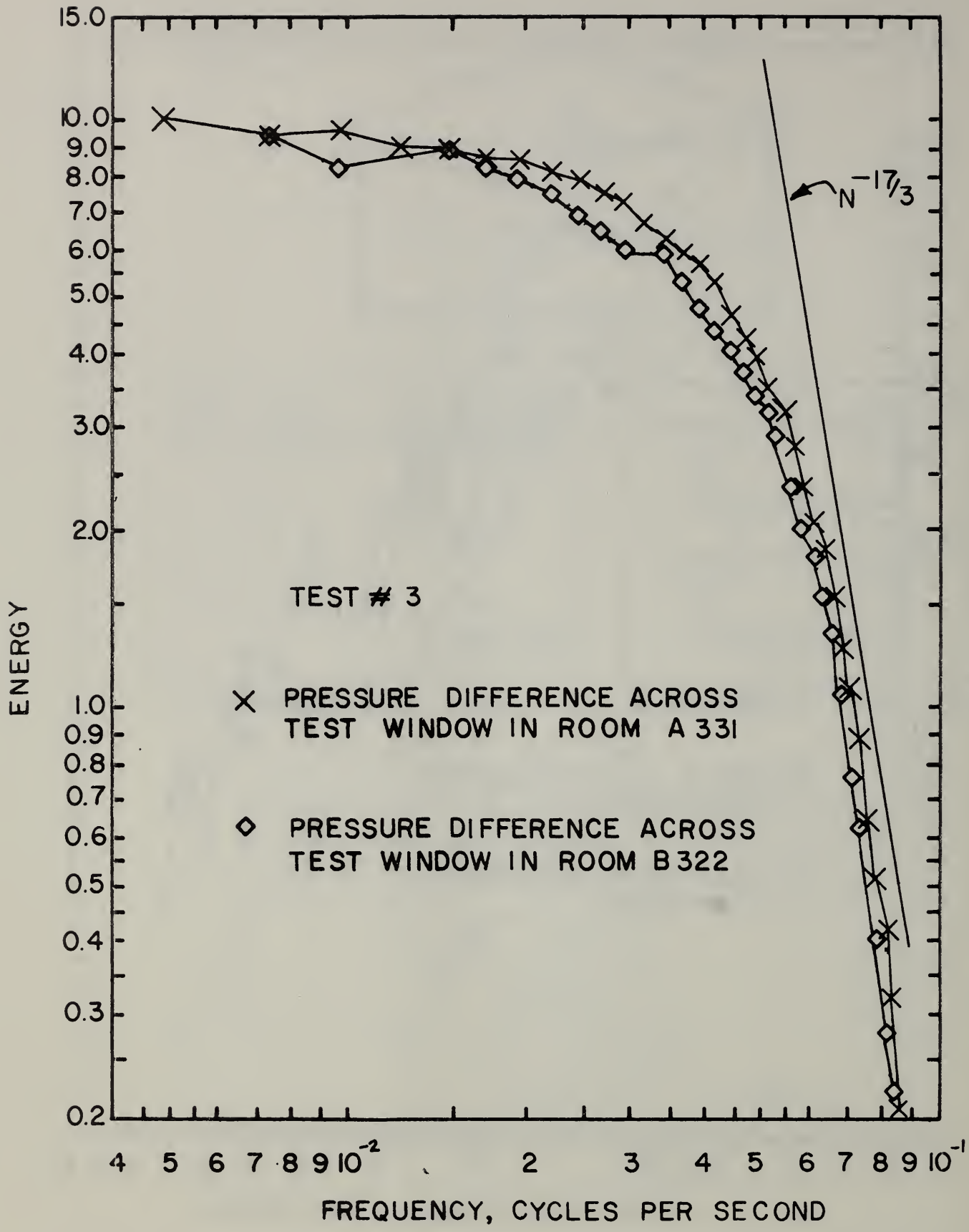
15.0
10.0
9.0
8.0
7.0
6.0
5.0
4.0
3.0
2.0
1.0
0.9
0.8
0.7
0.6
0.5
0.4
0.3
0.2
ENERGY
$N^{-17/3}$
TEST # 3
PRESSURE DIFFERENCE ACROSS TEST WINDOW IN ROOM A 331
PRESSURE DIFFERENCE ACROSS TEST WINDOW IN ROOM B 322
4 5 6 7 8 9 10^{-2} 2 3 4 5 6 7 8 9 10^{-1}
FREQUENCY, CYCLES PER SECOND

Figure 54


DEPARTMENT OF COMMERCE
NATIONAL BUREAU OF STANDARDS